UNIVERSITÄT ZU LÜBECK

From the Institute for Endocrinology and Diabetes
of the University of Lübeck
Directors: Prof. Dr. rer. nat. Jens Mittag
and Prof. Dr. med. Sebastian Meyhöfer

"The Sins of the Mother? - Role of Maternal Thyroid Hormone for Cardiovascular and Metabolic Functions in the Offspring"

Dissertation
for Fulfillment of Requirements
for the Doctoral Degree
of the University of Lübeck

From the Department of Natural Sciences

Submitted by

Mehdi Pedaran
From Teheran, Iran

Lübeck, 2022

First referee: Prof. Dr. rer. nat. Jens Mittag
Second referee: Prof. Dr. rer. nat. Henrik Oster
Date of oral examination: 16.06.2022
Approved for printing: Lübeck, 22.06.2022

EIGENSTÄNDIGKEITSERKLÄRUNG

Ich versichere, dass ich die vorliegende Dissertation ohne fremde Hilfe angefertigt und keine anderen als die angegebenen Hilfsmittel verwendet habe. Weder vorher noch gleichzeitig habe ich andernorts einen Zulassungsantrag gestellt oder diese Dissertation vorgelegt. Ich habe mich bisher keinem Promotionsverfahren unterzogen.

Lübeck, Februar 2022 ……..

(Mehdi Pedaran)

DANKSAGUNG

Ich möchte mich bei den Menschen bedanken, die mich während meiner Promotion begleitet und unterstützt haben, und ohne die diese Dissertation nicht möglich gewesen wäre.

Zuallererst möchte ich mich bei meinem Doktorvater Prof. Dr. Jens Mittag dafür bedanken, dass er mir dieses Projekt anvertraut hat und mir die Möglichkeit gegeben hat, ein Mitglied seines großartigen Teams zu sein. Vielen Dank für die hervorragende Betreuung, Unterstützung und ständige Motivation während meiner Doktorarbeit. Danke auch für deine Geduld, dein Verständnis für meine Situation und deine stets erstaunlich schnellen Korrekturen. Ich danke Dir für diese unvergesslich schöne und lehrreiche Zeit. Du bist nicht nur ein kompetenter Chef, sondern auch ein wirklich bemerkenswerter Mensch.

Mein Dank gilt auch Prof. Dr. Olaf Jöhren, dem Zweitbetreuer meiner Dissertation. Auch Dir danke ich für Deine Hilfe und Unterstützung während meiner Promotion.

Weiterhin danke ich den Mitgliedern des Prüfungsausschusses herzlich für Ihre Zeit und Bereitschaft, meine Dissertation zu lesen und mich während der Verteidigung zu prüfen.

Vielen Dank auch an alle Verantwortlichen des GRK1957 "Adipocyte-Brain Crosstalk" an der Universität zu Lübeck, die mich als assoziiertes Mitglied aufgenommen haben und mir damit die Möglichkeit gegeben haben, an sehr lehrreichen Workshops, Seminaren und den Summer Schools teilzunehmen.

Ich möchte mich bei Prof. Dr. Henriette Kirchner für die Aufnahme in den Journal Club bedanken, den sie immer engagiert organisiert hat und in dem sie u.a. sehr informativ über Literaturrecherche und den kritischen Umgang mit wissenschaftlichen Arbeiten berichtet hat. Außerdem hatte sie immer wertvolle Tipps zur Verbesserung von Präsentationen. Danke auch dafür, dass ich in Deinem Labor arbeiten durfte und Du mir Deine Geräte für meine Arbeit zur Verfügung gestellt hast. Außerdem möchte ich mich bei Cathleen für ihre große Hilfe und Unterstützung bei den epigenetischen Experimenten bedanken.

Vielen Dank auch an Prof. Dr. Lutz Schomburg und sein Team aus Berlin für die nette Zusammenarbeit bei der Erstellung meines Papers und während der Begutachtungsphase.

Ein herzlicher Dank gilt natürlich auch allen ehemaligen und derzeitigen Mitgliedern der Arbeitsgruppe, die mir während der Promotion eine große Hilfe waren und mir eine wunderschöne und unvergessliche Zeit bereitet haben. Ich werde unsere Gespräche, Diskussionen, Treffen abseits der Arbeit, sowie unsere gemeinsamen Kaffeepausen immer

in guter Erinnerung behalten. Ich bedanke mich bei Alex, Rebecca, Francesca, Kornelia, Beate, Lisbeth, Sebastian, Sogol, Ricky, Sarah, Nuria, Julia Maier und Julia Resch. Mein besonderer Dank geht auch an Carla, Isa, Jan, Natalie, Sandro, Kimberly, Christin und Shirin. Ich bin froh, dass ich Euch alle während meiner Promotion kennengelernt habe. Ihr seid alle großartig.

Bevor ich meine Promotion begonnen habe, hat mich ein großartiger Mensch überhaupt erst dazu motiviert diesen großen Schritt in meinem Leben zu wagen und hat mich auf diesem Weg unterstützt. Ein großer Dank gilt deshalb auch Dr. Andreas Weiss. Danke, dass Du mich im richtigen Moment mit den richtigen Leuten zusammengebracht hast.

Nicht zuletzt möchte ich den wichtigsten Menschen in meinem Leben meine tiefste Dankbarkeit aussprechen. Danke an Britta, meine Partnerin, für Deine Geduld und bedingungslose Unterstützung während dieser Zeit. Danke, dass du immer für mich da bist, mir den Rücken freigehalten und mich immer motiviert hast. Und natürlich danke ich Shayan, meinem wunderbaren Sohn, der mir mit seinem Lächeln immer unendlich viel Kraft und Energie gegeben hat. Danke, dass es Euch gibt.

Falls ich jemanden in meiner Danksagung vergessen haben sollte, tut mir das sehr leid. Ich hatte eine unvergessliche und sehr lehrreiche Zeit durch jeden einzelnen von Euch.

Vielen Dank Euch allen!

PUBLICATIONS

Parts of the data shown in this thesis have already published in a journal due to priority reasons:

Pedaran M, Oelkrug R, Sun Q, Resch J, Schomburg L, Mittag J. Maternal Thyroid Hormone Programs Cardiovascular Functions in the Offspring. *Thyroid*. 2021 Sep; 31(9):1424-1435. doi: 10.1089/thy.2021.0275. Epub 2021 Aug 25.

Publications that were not part of this thesis:

Oelkrug R, Harder L, **Pedaran M**, Gachkar S, Resch J, Johann K, Mittag J. Maternal Thyroid Hormone Receptor β Activation Sparks Brown Fat Thermogenesis in the Adult Offspring. *In revision*

Rudhard Y, Sengupta Ghosh A, Lippert B, Boecker A, **Pedaran M**, Kraemer J, Ngu H, Foreman O, Liu Y, Lewcock JW. Identification of 12/15-Lipoxygenase as a Regulator of Axon Degeneration through High-Content Screening. *J Neurosci*. 2015 Feb 18; 35(7):2927-41. doi: 10.1523/JNEUROSCI.2936-14.2015.

ZUSAMMENFASSUNG

Schilddrüsenhormone spielen eine wesentliche Rolle bei verschiedenen wichtigen physiologischen Prozessen wie Gehirnentwicklung und -funktion, Wachstum und Stoffwechsel, aber auch beim Herz-Kreislauf-System, insbesondere während der Schwangerschaft. Da der Embryo bis zum Ende der Schwangerschaft keine eigenen Schilddrüsenhormone produziert, ist er in dieser Zeit von denen der Mutter abhängig. Schwankungen der mütterlichen Schilddrüsenhormone haben oft schwerwiegende Auswirkungen auf die Entwicklung des Fötus und führen zu irreversiblen Störungen bei den Nachkommen, insbesondere zu neurologischen Entwicklungsproblemen wie der Aufmerksamkeitsdefizit-Hyperaktivitätsstörung. Das genaue Zeitfenster dieser entscheidenden Schilddrüsenhormonwirkung während der Schwangerschaft ist jedoch unzureichend bekannt.

In dieser Arbeit soll daher der Einfluss von Schilddrüsenhormonen auf die fötale Entwicklung in verschiedenen Phasen der Schwangerschaft und die Folgen einer veränderten Schilddrüsenhormon-Signalübertragung auf Wachstum, kardiovaskuläre Eigenschaften und Stoffwechsel bei männlichen und weiblichen adulten Nachkommen untersucht werden. Dafür wurden Mäuse verwendet, die heterozygot für einen mutierten Schilddrüsenhormonrezeptor α1 (TRα1+/m) sind und eine Resistenz gegenüber Schilddrüsenhormonen in TRα1-abhängigen Geweben wie Gehirn und Herz aufweisen, wodurch ein hypothyreotischer Phänotyp entsteht. Dieses Modell wurde mit einer Behandlung mit 3,3',5-Triiodthyronin (T3) des Muttertiers kombiniert, wodurch der mutierte TRα1-Rezeptor für bestimmte Zeiträume, entweder in der ersten oder zweiten Hälfte der Schwangerschaft, reaktiviert werden kann. Wildtyp-Geschwistertiere, die in diesen Zeiträumen erhöhten T3-Spiegeln ausgesetzt waren, dienten als Kontrollen.

Die Phänotypisierung der Nachkommen ergab bei beiden Geschlechtern und Genotypen keine Veränderung des postnatalen Wachstums nach einer T3-Behandlung des Muttertiers in beiden Hälften der Schwangerschaft. Besonders auffällig war eine signifikante Zunahme des Herzgewichts bei erwachsenen Wildtyp-Nachkommen, die während der ersten oder zweiten Hälfte der Schwangerschaft T3 über das Muttertier erhielten, während männliche TRα1-Mutanten vor diesem Effekt geschützt waren. Weiterhin wurde bei männlichen Nachkommen, die in der zweiten Hälfte der Schwangerschaft einem erhöhten mütterlichen T3-Spiegel ausgesetzt waren, unabhängig von ihrem Genotyp eine signifikante Erhöhung der Herzfrequenz festgestellt, während weibliche Nachkommen davon nicht betroffen waren. Dies lässt darauf schließen, dass das mütterliche Schilddrüsenhormon in der zweiten Hälfte

der Schwangerschaft für die Ausbildung der kardialen Eigenschaften von besonderer Bedeutung ist, wobei die spezifischen Auswirkungen von TRα1 oder dem Geschlecht abhängig sind.

Auf der Grundlage der Ergebnisse dieser Arbeit empfiehlt sich die Überwachung des Schilddrüsenhormonspiegels der Mutter während der gesamten Schwangerschaft, um Herzproblemen beim Kind vorzubeugen.

ABSTRACT

Thyroid hormones (TH) have important functions in various fundamental physiological processes such as brain development and function, growth, metabolism, but also in the cardiovascular system, especially during pregnancy. Since the embryo does not produce TH on its own until late in pregnancy, it depends on maternal TH during this period. Alterations in maternal TH often have devastating effects on fetal development leading to irreversible disorders in the offspring, especially neurodevelopmental problems such as attention deficit hyperactivity disorder. However, the precise time window of this crucial thyroid hormone action during pregnancy is poorly understood.

Therefore, the aim of the present thesis is to investigate the influence of THs on fetal development during different periods of pregnancy and the consequences of altered TH signaling on growth, cardiovascular properties, and metabolism in male and female adult offspring. For this purpose, mice heterozygous for a mutant thyroid hormone receptor α1 (TRα1+/m) were used, which exhibit resistance to THs in TRα1 dependent tissues such as brain and heart, which display a hypothyroid phenotype. This model was combined with maternal 3,3',5-triiodothyronine (T3) treatments, which can reactivate the mutant receptor for defined periods, either in the first or second half of pregnancy. Wildtype littermates that were exposed to elevated T3 levels in these periods were used as controls.

Phenotyping of the offspring revealed no alteration in postnatal growth after maternal T3 treatment in either half of pregnancy in both genders and genotypes. Most notably, however, there was a significant increase in heart weight in adult wildtype offspring born to dams that received T3 during the first or second half of pregnancy, whereas TRα1 mutant males were protected from this effect. Moreover, a significant increase in heart rate was detected selectively in male mice exposed to elevated maternal T3 during the second half of pregnancy regardless of their genotype, whereas female mice were not affected. This indicates that maternal TH is of particular relevance in the second half of pregnancy for establishing cardiac properties, with specific effects depending on TRα1 or gender.

The data in this study therefore advocate monitoring of maternal TH levels during pregnancy to avoid cardiac problems in the offspring.

TABLE OF CONTENTS

1. INTRODUCTION

Thyroid hormones (THs) are crucial for fetal development but also for adult life (Cheng et al., 2010; Yen, 2001). They regulate tissue differentiation and tissue development as well as metabolic function throughout the body (Pascual & Aranda, 2013). Although as early as 1500 BC, efforts were made to treat goiter with iodine-containing food, the actual importance of thyroid secretions for human health was not scientifically recognized until the late 19th century (Stepien & Huttner, 2019), when thyroid deficiency was directly linked to cretinism. At the end of the 19th century, the first successful treatment by injection of thyroid extracts was published (Slater, 2011) and THs were identified as active components, chemically characterized and ultimately synthesized in the early 20th century (Charles et al., 1927).

With the systematic observation of neurological cretinism prevalent in iodine deficient regions, specific functions of TH signaling in brain development were recognized (Lamberg, 1991). Today, more than 30% of the German population develop a thyroid condition from mild to moderate iodine deficiency during their lifetime, leading to goiter and other forms of iodine deficiency diseases (Schaffner et al., 2021). Taken together, these findings underline the importance of proper TH metabolism for our health even today.

1.1 The Endocrine System

For all functions in the body to work smoothly, as well as to maintain homeostasis, the various parts of the body and organs must communicate with each other. This communication is made possible primarily by the nervous system and the endocrine (hormonal) system. The first mentioned system (i.e. the nervous system) enables rapid transmission of information between the different parts of the body, while the endocrine system provides longer-lasting regulatory actions. Thus, the nervous system and the endocrine system complement each other for effective communication between organs (Licinio & Frost, 2000; ThyagaRajan & Priyanka, 2012).

The stimuli of the nervous system influence the release of particular hormones and the other way around. Generally, hormones as TH regulate metabolism, growth and development, emotions and mood, fertility, sleep, and notably cardiovascular system (Malcomson & Nagy, 2015).

1.2 Thyroid Gland Development

In mammals, the mature thyroid gland is located in the neck region and produces THs including triiodothyronine, thyroxine and calcitonin.

During embryonic development in humans, the thyroglossal duct develops at the base of the tongue and then atrophies into thyroid tissue to form two thyroid lobes around day 20 after fertilization (D20). These develop from a midline outpouching of the endoderm in the floor of the primitive oral cavity (D20 – D22). The lateral ultimobranchial anlagen originate from the fourth pharyngeal pouch and produce parafollicular cells, also known as C cells. These cells secrete calcitonin, a hormone that plays an essential role in calcium homeostasis (Fagman & Nilsson, 2011; Trueba et al., 2005).

The thyroid gland appears as a flask-like structure with a narrow neck attached to the oral cavity. The structure gradually enlarges and becomes bilobed; the stalk ruptures and the gland changes to a solid mass of laterally expanding tissue (D24 – D28). Between the sixth and seventh week after fertilization, the thyroid has reached its final shape and position in the anterior lower neck and weighs 1-2 mg (Kratzsch & Pulzer, 2008; Lydiatt & Bucher, 2011).

The structural differentiation of the thyroid gland can be summarized into three stages: Pre-colloid, initial colloid, and follicular growth phase. During the last phase of follicular organization (D70 – D84), iodide concentrations and TH synthesis can be detected (Fisher & Polk, 1989; Sterrett, 2019). As the fetal thyroid gland in humans cannot produce thyroid hormones until late within pregnancy (Nilsson & Fagman, 2017), the embryo's or fetus's need for thyroid hormones must be met by the maternal thyroid gland (De Escobar et al., 2007; Visser & Peeters, 2020).

In adult humans, the thyroid gland consists of two lateral lobes (left and right) connected by the isthmus that crosses the midline at the level of the first or second tracheal cartilage ring. Each lobe consists of numerous thyroid follicles, the functional unit of the gland. The thyroid follicles vary in size and shape and are composed primarily of thyroid epithelial cells, also known as thyrocytes or thyroid follicular cells, and a small number of C cells. The thyrocytes form a single-layered epithelium enclosing a central lumen filled with colloid. The colloid material serves as a reservoir for TH production. When stimulated, thyrocytes transport activated THs from the colloid-filled inner cavity into the bloodstream for rapid distribution to the respective target tissues (Maenhaut et al., 2000; Nilsson & Fagman, 2017).

What we know about thyroid gland morphogenesis is largely due to studies in mouse models, although the developmental processes proceed in mice more rapidly than in humans. The development of the thyroid gland begins in mice at embryonic day 8.5 (E8.5). At this time, the floor of the primitive pharynx thickens and expression of transcription factors such as *Nkx2.1*, *Nkx2.5*, *Pax8*, *Foxe1*, and *Hhex* starts (E8.5 – E9.5). This is followed by outgrowth and budding of the thyroid primordium and caudal migration towards its final position. By E9.5 – E10, the median thyroid primordium appears as two lobes connected to the primitive pharynx by a narrow channel, the thyroglossal duct, which disappears by E11.5. At E12.5 – E13.5, the median thyroid primordium consists of two lobes, an isthmus, and a remnant pedicle. Finally, by E15 – E16, the thyroid gland reaches its final position and shape, and follicle formation begins, giving rise to functional TH follicles by E16.5 (De Felice & Di Lauro, 2004; Fagman et al., 2006; Fernández et al., 2015; Löf et al., 2018; Richard & Flamant, 2018; Van Vliet, 2003; Westerlund et al., 2008).

Table 1 and figure 1 display the differences in thyroid gland development in mouse and human.

Table 1: Differences in the developmental stages of the thyroid gland in mouse and human.

Stages:	**I.**	**II.**	**III.**	**IV.**	**V.**
	Thickening of the floor of the primitive pharynx	Specification and budding of thyroid gland anlagen	Expansion of thyroid primordium, proliferation of thyroid precursor cells	Folliculogenesis	Matured thyroid gland
Mouse (E)	E8.5 – E9.5	E9.5 – E10	E11.5 – E15	E15 – E16	E15.5 – E16.5
Human (D)	D20 – D22	D24 – D28	D30 – D35	D48 – D60	D70 – D84

Abbreviations: **E**: embryonic day; **D**: day after fertilization.

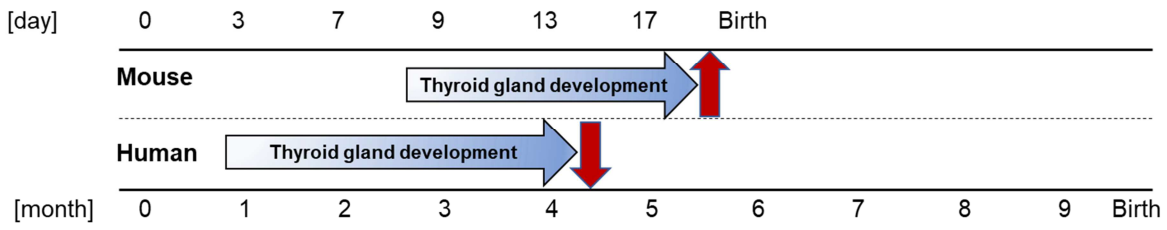

Figure 1: Timeline of thyroid gland development in mouse and human. In mouse, thyroid gland development begins on embryonic day 8.5 to 9.5 and TH production on embryonic day 17.5, whereas in human, thyroid gland development begins on day 20 to 22 after fertilization and TH production starts around day 130. The red arrows show the onset of thyroid hormone production in mouse and human.

1.3 Thyroid Hormone Synthesis

THs belong to the non-peptide hormones and are required for optimal health and function of nearly all tissues throughout the body. They play a critical role in both embryonic and postnatal development and homeostasis in vertebrates (Josef Köhrle, 2018; van der Spek et al., 2017).

TH synthesis and secretion are regulated by a complex interplay between the components of the hypothalamic-pituitary-thyroid (HPT) axis. This belongs to the neuroendocrine systems and, as the name suggests, leads from the hypothalamus to the pituitary gland further to the thyroid gland and subsequently to peripheral target organs (Fekete & Lechan, 2014; Wondisford, 2018). In humans, formation and maturation of the neonatal HPT axis begins in utero early in pregnancy with fetal dependence on maternal THs (Eerdekens et al., 2020; Eng & Lam, 2020). In mice, the HPT axis is fully matured in postnatal life around day 15 (Friedrichsen et al., 2003; Wondisford, 2018).

Located at the base of the brain, the hypothalamus is connected to the pituitary gland by the stalk-like infundibulum, also known as the pituitary stalk. This carries blood vessels as well as nerve fibers that enable the transport of stimulating and inhibiting hormones and other signaling molecules (Feldt-Rasmussen et al., 2021; Fliers et al., 2014).

1.4 Regulation of Hypothalamus-Pituitary-Thyroid (HPT) Axis

The secretion of the thyroid hormones T3 (3,3',5- triiodothyronine) and T4 (3,3',5,5'-tetraiodothyronine or thyroxine) is regulated by the hypothalamic-pituitary-thyroid (HPT) axis.

In the paraventricular nucleus of the hypothalamus, thyrotropin-releasing hormone (TRH) is produced by hypophysiotropic neurons. Via the hypophyseal portal system, this hormone is transported from the hypothalamus to the anterior pituitary, where TRH subsequently stimulates the secretion of thyroid-stimulating hormone (TSH) by thyrotropic cells. TSH, in turn, stimulates the thyroid follicular cells (thyrocytes) in the thyroid gland to transport the thyroid hormones T4 and T3 into the cell lumen. Then T4 (biologically less active form) and T3 (active form) are transported by specific transporters across the cell membrane into the blood (Figure 2) (Groeneweg et al., 2019; Porst et al., 2021).

In human blood, most T4 and T3 is bound by transport proteins, such as thyroxine-binding globulin (TBG), thyroid-binding prealbumin (TBPA), and albumin, whereas only 0.03% of T4

and 0.3% of T3 are free in blood. However, in mice, T4 and T3 bind to the transport protein albumin (Jahnke et al., 2004).

In the thyroid gland is mainly the prohormone T4 secreted, which in humans has a half-life of seven days compared to the much shorter half-life of T3 of one day (Bianco et al., 2014; Schussler, 2000). Compared to human, the half-life in mice is much shorter: eight hours for T4 and two hours for T3 (Gereben et al., 2008).

The HPT axis is predominantly responsible for maintaining normal circulating thyroid hormone levels through a self-regulating negative feedback system. Because elevated free TH levels inhibit further release of TRH and TSH, which in turn results in lower T3 and T4 secretion. In more detail, circulating concentrations of TH feed back to the hypothalamus and the pituitary, thereby causing a reduction in biosynthesis and secretion of TRH and TSH, respectively, and ultimately fine regulation of peripheral TH concentrations is enabled (Fekete & Lechan, 2014; Picou et al., 2014; Prummel et al., 2004; Yen et al., 2006).

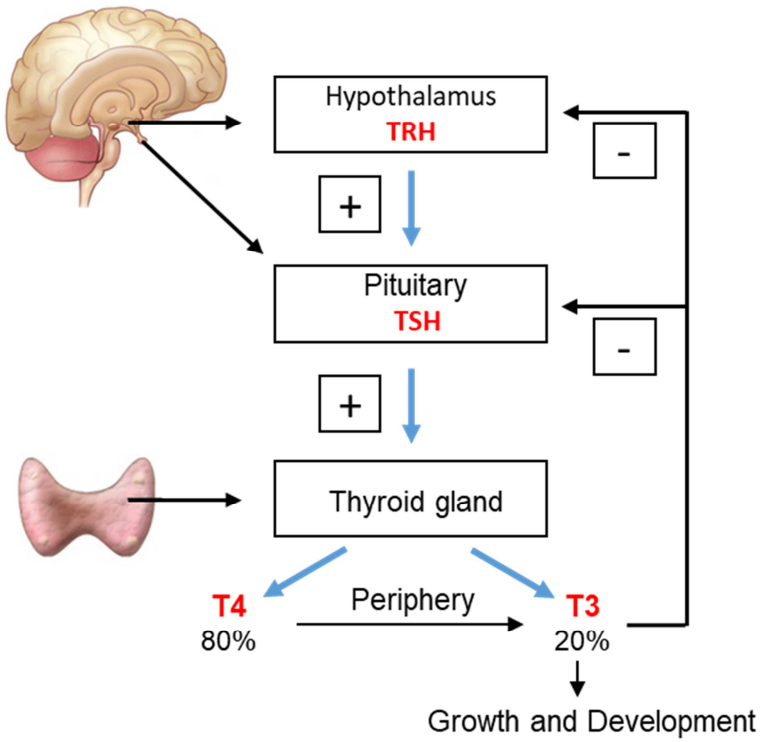

Figure 2: Schematic illustration of the hypothalamic-pituitary-thyroid (HPT) axis in mammals. The paraventricular nucleus of the hypothalamus synthesizes thyrotropin-releasing hormone (TRH). TRH is transported to the anterior pituitary and causes the secretion of thyroid-stimulating hormone (TSH). TSH stimulates follicular cells in the thyroid gland to produce THs (T4 and T3). Subsequent increases in peripheral TH concentrations are sensed by both TRH- and TSH-secreting cells and cause a reduction in TRH- and TSH-release and production in a negative feedback loop.

1.5 Thyroid Hormone Metabolism and Action

As mentioned above, most of T4 and T3 secreted by the thyroid gland are bound to serum proteins. Only a minority of THs remain unbound and distribute via the blood stream as free T4 (fT4: 0.03%) and T3 (fT3: 0.3%). The free thyroid hormones can enter the cells (Pirahanchi et al., 2021).

Both forms of bound and unbound T4 and T3 are referred to as total T4 (tT4) and total T3 (tT3), respectively. The TH storage form tT4 occurs in approx. 40-fold higher concentration than tT3.

To reach sufficient T3 concentration in target tissues, although only a minority of THs are present in the biologically active form (T3), and a mechanism to convert the T4 to T3 in target tissues is often required to fulfill signaling activity (Dentice & Salvatore, 2011; Pilo et al., 1990; St Germain et al., 2009).

The deiodination of T4 to T3 is catalyzed by a family of selenium-containing enzymes called iodothyronine deiodinases type 1-3 (DIO 1-3) (J. Köhrle, 1994; Schomburg, 2010).

These deiodinases regulate T3 availability in cells in response to TH levels in a tissue- and spatial-dependent manner. They either activate T4 by removing iodine from the outer ring to produce T3 (DIO1, DIO2) or inactivate T4 by facilitating inner ring deiodination (DIO1, DIO3) to produce reverse T3 (rT3). In addition, T3 and reverse T3 (rT3) can be further inactivated by DIO1 or DIO3 generating 3,5-diiodo-L-thyronamine (3,5-T2), 3,3'-diiodo-L-thyronamine (3,3'-T2) and 3',5'-triiodothyronine (3',5'-T2), respectively (Figure 3) (Bianco & Kim, 2006; Galton et al., 2021; Moreno et al., 2017).

DIO1 with the ability to deiodinate both rings is mainly expressed in liver, kidney, thyroid and pituitary. In the central nervous system, including the hypothalamus, pituitary and cortex, DIO2 converts T4 to T3. Lastly, DIO3 is expressed primarily during the late developmental and early postnatal stages in the placenta and uterus. So, this deiodinase plays a crucial role in protecting fetal tissues by producing the inactive iodothyronines, especially during critical developmental stages (de Escobar et al., 2004; Hernandez & Stohn, 2018; Huang, 2005).

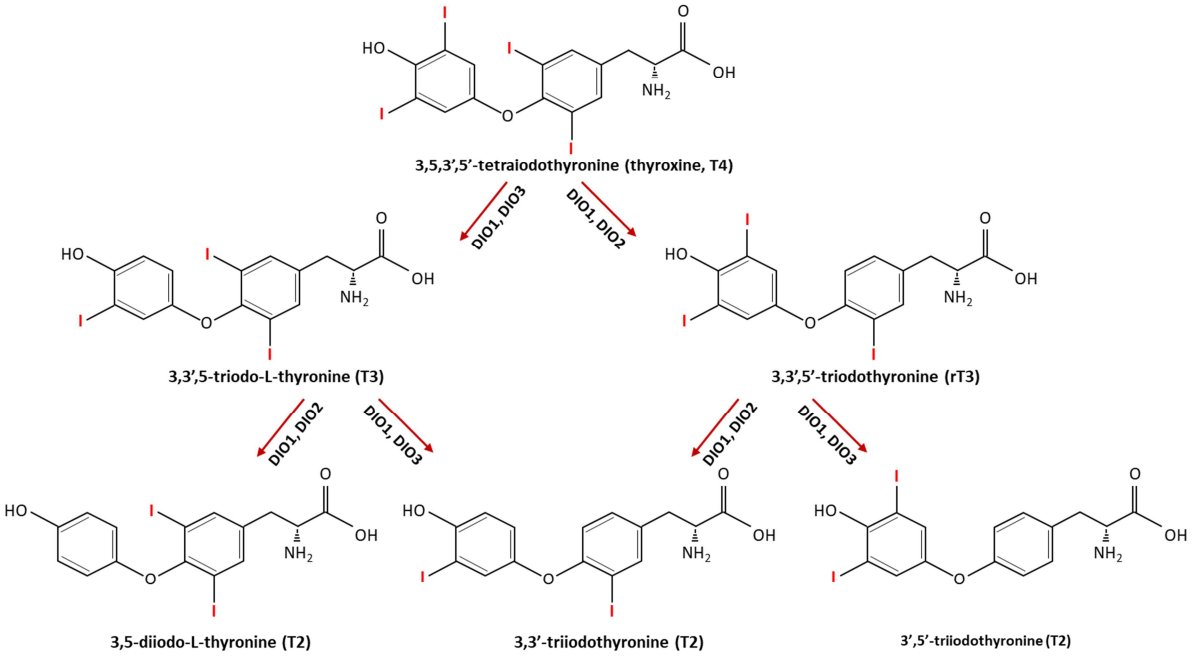

Figure 3: Structure of T4, T3, reverse T3 (rT3) and T2 with the corresponding deiodinases that catalyze the activation or inactivation of the hormones.

1.6 Thyroid Hormone Receptor

Following thyroid gland production of T4 and T3, these hormones are transported to the cytoplasm of target cells by the adenosine triphosphate (ATP)-dependent monocarboxylate transporters (MCT8 or MCT10) or organic anion transporter proteins (OATPs) (Anyetei-Anum et al., 2018; Davis et al., 2008; Visser et al., 2011). The amount of converted T3 available for binding to nuclear receptors is further regulated by the cell-specific expression of selenoenzymes deiodinases. In mammals, T3 exerts its function through binding to specific thyroid hormone receptors (TRs) α and β located in the nucleus. The TRs are encoded by different genes: in humans, *THRA* is located on chromosome 17 and *THRB* on chromosome 3; in mice, however, *Thra* is located on chromosome 11 and *Thrb* on chromosome 14 (Lin & Koenig, 1999; Sap et al., 1986).

Two mRNA species are transcribed from the *THRA* gene. While the truncated *THRA* gene product TRα2 lacks the ability to bind the hormone T3, TRα1 can bind T3 as well as form dimers with TRα2 (Paisdzior et al., 2021; Tagami et al., 1998). TRα2 differs from TRα1 not only in length but also in amino acid composition in the C-terminal region.

Two T3-binding isoforms of THRβ, i.e. TRβ1 or TRβ2, are expressed in human and mice. A third isoform, TRβ3, is found only in rats (Aranda & Pascual, 2001; Ruiz-Llorente et al., 2014).

TRα1 is the major isoform for postnatal development, gastrointestinal tract and cardiac function. TRβ1 is predominantly expressed in kidney and liver and TRβ2 in hypothalamus, pituitary, eye and inner ear (Epstein & Brent, 1994; Flamant & Samarut, 2003; Ortiga-Carvalho et al., 2014; Yen, 2001).

Previous studies with genetically modified mice demonstrated that TRα and TRβ are partially able to compensate each other, e.g., in terms of mediating some effects of THs or isoform-specific functions when co-expressed in the same cell (Flamant & Gauthier, 2013). In the euthyroid organism, circulating TH levels balance transcriptional repression and activation to achieve optimal target gene expression.

TRs are composed of four domains that are similar within the nuclear receptor family and have distinct modular functions (Figure 4A). TRs differ most significantly in the N-terminal A/B domain signifying the N-terminal region of the receptor. The potency of TR activity is influenced by this domain as it contains the constitutive ligand-independent transcriptional activation domain, termed autonomous activation function 1 (AF-1). The A/B region is followed by the most conserved region among nuclear receptors, the DNA-binding domain (DBD). It consists of two zinc fingers that are important for identification and binding to palindromic DNA sequences called hormone response elements. Through a short D domain often referred to as hinge domain, DBD is connected to the ligand-binding domain (LBD) region, which is ultimately responsible for binding T3. The C-terminal LBD contains residues essential for interaction with corepressors and includes ligand-dependent transcriptional activation function 2 (AF-2) (Chatonnet et al., 2013; Flamant & Gauthier, 2013; Mittag et al., 2010; Ramadoss et al., 2014).

TRs bind to specific DNA sequences called thyroid hormone response elements (TREs) which are located in the promoter region of T3-responsive genes. To regulate the expression of these genes, TRs bind to TREs as dimers, either as homodimers or as heterodimers. However, TRs frequently form heterodimers with the retinoid X receptor (RXR), and these have a higher binding affinity to TRE than TR homodimers. TRs interact with TREs in the presence and even in the absence of the ligand (i.e. T3). It has been proposed that RXR/TR heterodimers are the primary mediators of T3 action (Figure 4B) (Schweizer et al., 2017; Yen et al., 2006).

Studies revealed that a large number of genes are regulated in almost all tissues by TH. In brain, this encompasses genes for synaptic establishment and transmission, dendrite

formation, neuronal migration and maturation, axonal development, proliferation, fate and differentiation of neural cells, histone modification and DNA methylation (Bernal, 2017; Gil-Ibañez et al., 2017; Hernandez & Stohn, 2018). The two major processes for transcriptional regulation by TRs that are sensitive to TH signaling are histone modification and DNA methylation (Fonseca et al., 2021; Receptor & Development, 2018). While histone modifications regulate the accessibility of DNA to RNA polymerase II and transcription factors by modulating chromatin packaging (Javaid & Choi, 2017), DNA methylation describes the addition of a methyl group to the 5'-position of a cytosine in the sequence context of CpG dinucleotides (Demeneix, 2019; Jones, 2012; Sadakierska-Chudy & Filip, 2015).

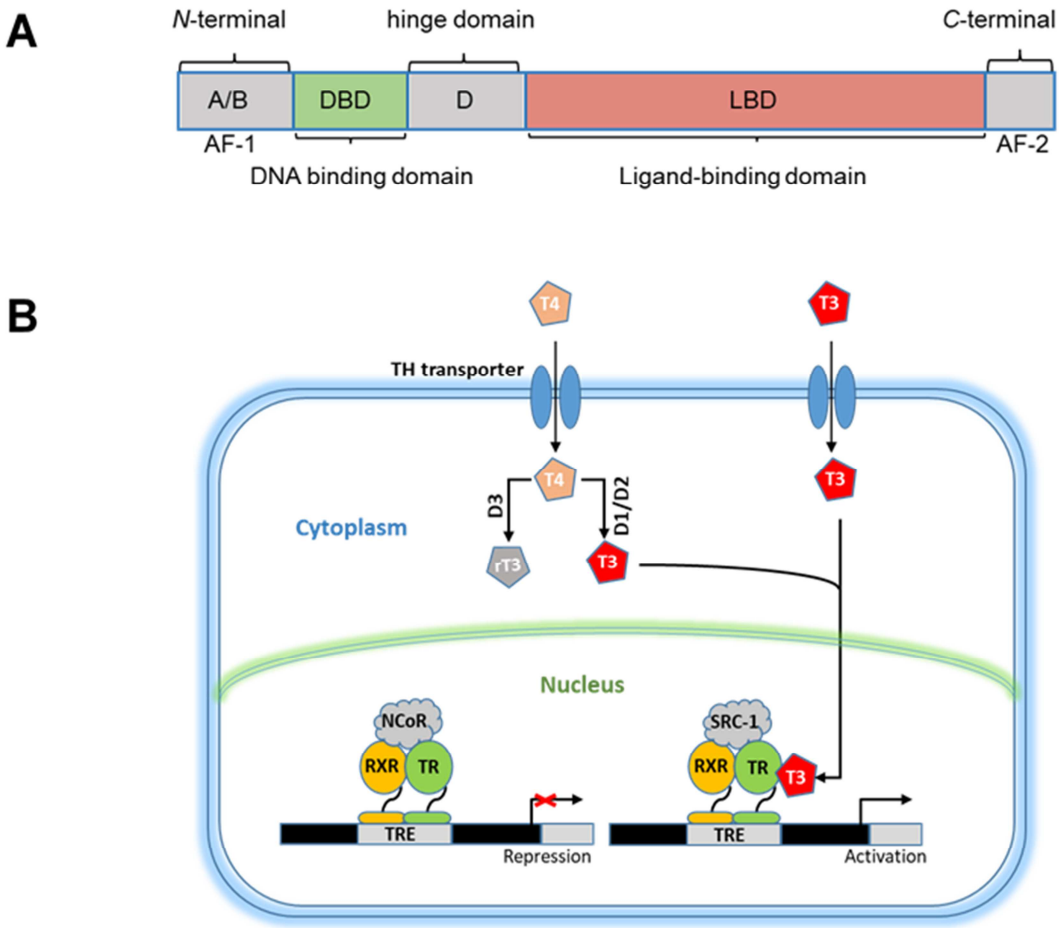

Figure 4: Mechanism of action of thyroid hormone receptors. **A)** Schematic representation of a thyroid hormone receptor showing the different functional domains. **B)** Repression and activation of a positively regulated gene. In tissues, TH transporters, such as MTC8 or MCT10, transport T4 and T3 into cells. In the cytoplasm, T4 can be inactivated by Dio3 (D3), generating reverse T3 (rT3), or T4 can be activated by Dio1 (D1) and Dio2 (D2), by conversion to T3. The unliganded thyroid hormone receptor (TR) heterodimerizes with the retinoid X receptor (RXR) and binds to the thyroid hormone response element (TRE) and to a corepressor such as NCoR or SMRT and represses the gene expression. Binding of T3 to the ligand-binding domain leads to disruption of corepressor binding and promotion of coactivator (SRC-1) binding, which then leads to recruitment of polymerase III and initiation of gene transcription.

In the regulation of TR-mediated gene expression, coregulators play a physiologically important role by recruiting either coactivating or corepressing proteins. In the absence of ligand, TRs, when bound to TREs, can act as constitutive repressors due to their association with corepressors like NCoR (nuclear receptor corepressor) or SMRT (silencing mediator of retinoic and thyroid receptor). Both proteins belong to multicomponent repressor complex that possesses histone deacetylase (HDAC) activity. This complex can thus keep surrounding histones deacetylated, facilitate chromatin condensation, and thereby repressing transcription of the target gene. When T3 binds to the LBD of TR, the TR/corepressor complex dissociates and is replaced by a coactivator complex, resulting in histone acetylation and remodeling of chromatin structure, making DNA more accessible and thereby enhancing TR-driven gene transcription. Therefore, ligand-bound TRs function as transcriptional activators, requiring coactivator proteins, such as SRC-1 (steroid receptor coactivator 1) and TIF2 (transcriptional intermediary factor 2) (Brent, 2012; Cheng et al., 2010; Minakhina et al., 2021).

1.7 Thyroid Hormone Disorders

In euthyroid serum, TH levels are stable and well balanced through the HPT axis. However, deregulation of TH levels may occur due to certain disorders such as autoimmune diseases or also during pregnancy (Krassas et al., 2015; Sinclair, 2015).

The most common cause of TH disorders is insufficient iodide intake. Consequently, the TH system cannot perform its function properly, which leads to serious health impairments of the organism. An abnormally low level of circulating TH is termed hypothyroidism, whereas an elevated level of free TH is referred to as hyperthyroidism (Boelaert & Franklyn, 2005; Evans, 2003; Gessl et al., 2012).

The symptoms of hypothyroidism vary widely, from asymptomatic to even life-threatening, depending on the duration of the condition and the severity of the hormone deficiency. The most common symptoms in adults are bradycardia, fatigue, weight gain, lethargy, dry skin, cold intolerance, constipation, and voice change. These clinical symptoms may vary by age and gender (Chaker et al., 2017). Two different types of hypothyroidism are distinguished. In overt or clinical primary hypothyroidism, the thyroid gland is directly affected and this condition is diagnosed by TSH levels above and free T4 levels below the reference range. Mild or subclinical hypothyroidism is considered as incipient thyroid failure and is diagnosed by slightly elevated TSH levels along with free T4 concentrations in the normal range (Calsolaro et al., 2019; Khandelwal & Tandon, 2012; Wartofsky et al., 2006).

Hyperthyroidism is a pathological disorder in which TH synthesis and secretion is increased. Symptoms of TH excess commonly include fatigue, anxiety, palpitations, sweating, tachycardia and heat intolerance. Graves' disease is the major cause of hyperthyroidism, followed by toxic nodular goiter.

Hyperthyroidism can also be divided into two types: overt and subclinical hyperthyroidism. Overt hyperthyroidism is characterized by low TSH levels along with elevated concentrations of T4, T3, or both. In contrast, subclinical hyperthyroidism is diagnosed by low TSH levels and normal concentrations of free T4 and free T3 (Donangelo & Suh, 2017; Manolis et al., 2020). A special form of hyperthyroidism is thyrotoxicosis, which refers to the clinical syndrome of excess circulating THs, regardless of the source. It can include for instance an excessive oral uptake of TH, either accidentally or with the purpose of losing weight. The physical signs of thyrotoxicosis resemble a severe hyperthyroidism and include tachycardia, trembling of the extremities, fever, and weight loss (Cooper, 2003; Doubleday & Sippel, 2020; Goichot et al., 2016; Leo et al., 2016).

If hypo- and hyperthyroidism are detected early, they can be treated in time with hormone preparations or thyrostatics, and fortunately, further severe disorders can usually be avoided (Papaleontiou & Haymart, 2012).

1.8 Thyroid Hormone Dysfunction during Pregnancy

Hormonal balance and metabolism change during pregnancy, resulting also in profound alterations in thyroid function. This usually includes a marked increase in serum TBG (T4-binding globulin) levels and consequently an increase in total TH levels (T4 and T3), elevated serum levels of thyroglobulin, and an increase in renal clearance of iodide. However, It should be noted that human chorionic gonadotropin (hCG) produced during pregnancy behaves like a weak thyroid stimulator. In brief, pregnancy leads to an overall increase in thyroid activity, but euthyroidism is maintained in healthy pregnant women. Nevertheless, hyperthyroidism or hypothyroidism might occur during pregnancy and affects 8-10% of pregnant women (Krassas et al., 2015; Moleti et al., 2014; Teng et al., 2013; Yalamanchi & Cooper, 2015).

In humans, the fetal thyroid gland begins to produce hormones around D130 (de Escobar et al., 2004), in mice approximately on E17.5 (Figure 1) (Nilsson & Fagman, 2017). For this reason, embryonic demand for THs before this point must be met primarily by the maternal

thyroid gland (De Escobar et al., 2007). Consequently, defects in maternal thyroid function can have serious effects on the fetus, especially on the developing brain (Harder et al., 2018), as well as outcomes on pregnancy, such as premature birth, miscarriage, growth retardation, and impaired neurodevelopment of the child (Kalra et al., 2017; Okosieme et al., 2018).

Due to pregnancy-related changes in thyroid physiology and function, it is very important to establish reference ranges for normal function during pregnancy to avoid complications associated with thyroid dysfunction. TSH reference ranges are recommended between 0.1 - 2.5 mU/L for the first and second trimesters and between 0.2 - 3.0 mU/L for the third trimester. These ranges are described in detail in the guidelines of the Endocrine Society, the American Thyroid Association and the European Thyroid Association (De Groot et al., 2012; Lazarus et al., 2014; Stagnaro-Green et al., 2011). Severe alteration of TH function during pregnancy leads to overt or subclinical hypothyroidism, which can have serious consequences for the mother and the fetus. Women with overt hypothyroidism during pregnancy, characterized by elevated serum TSH or a TSH >10 mIU/L and decreased free T4 levels in serum, are known to be at increased risk for preterm birth and infants with intrauterine growth retardation. Subclinical hypothyroidism is usually diagnosed by elevated TSH levels and normal free T4 levels (Sullivan, 2019; Taylor & Lazarus, 2019). Women with this type of thyroid insufficiency have an increased risk of hypertensive disorders.

It should be noted that fluctuations within the normal range during pregnancy may also resemble the clinical phenotype of overt or subclinical forms of hypothyroidism (Korevaar et al., 2016), making it difficult to differentiate between these two forms during pregnancy.

Despite the detrimental effects of hypo- and hyperthyroidism during pregnancy, it is still controversial whether pregnant women should be routinely monitored for thyroid status and whether treatment should be initiated in subclinical hypothyroidism (Brabant et al., 2015).

1.9 Thyroid Hormone Action in Specific Tissues

TH is an essential key regulator for metabolic processes, including growth and energy consumption, brain development, cardiovascular function, sexual behavior, and embryonic development. Furthermore, it is known that TH has multiple effects on many organs in both sexes. This section briefly describes important functions of TH that are relevant for this thesis.

1.9.1 Thyroid Hormone and the Cardiovascular System

The cardiovascular system (CV) represents a complex network of organs and tissues that ensures the supply of blood to the various parts of the body. It consists of the heart, lung, blood and blood vessels (Yelon et al., 2002).

The CV is involved in two main functions: Firstly, it interacts directly with the pulmonary system and transports oxygen and nutrients to all cells in the body, and secondly, it transports hormones produced by the endocrine system to the target tissues and organs.

Cardiovascular function is highly regulated by THs. These hormones are known to enhance cardiac contractility and heart rate (HR), stimulate the force of systolic contraction and rate of diastolic relaxation of the heart, and decrease the systemic vascular resistance. Therefore, even a mild thyroid disorder can significantly affect the cardiovascular system and its function (Cini et al., 2009; Mittag et al., 2013).

These diverse TH effects on the heart are largely mediated by the action of the TR subtypes α and β. Both types are expressed in the heart, whereas TRα is the more predominant receptor. TRα regulates contractile and electrophysiological functions in the heart, and TRβ has a minor contributing role (Ishii et al., 2021; Lazar, 1993).

TRs influence the expression of various cardiac genes (Danzi & Klein, 2002, 2012; Morkin, 2000; Small & Krieg, 2004), including myosin heavy chain (*Mhc*) α and β (Danzi & Klein, 2005) and sarcoplasmic reticulum Ca^{2+} ATPase (*Serca2*) (Campanha et al., 2016).

In addition, genomic and non-genomic TH activities regulate the expression of cardiac pacemaker genes such as hyperpolarization-activated cyclic nucleotide-gated channel 2 and 4 genes (*Hcn2* and *Hcn4*), which positively affect heart rate (DiFrancesco & DiFrancesco, 2015; Pachucki et al., 1999; Rivolta et al., 2020).

It is already known that T3 can contribute to the development of hypertension (i.e. increased blood pressure) and to an increase in cardiac output (Danzi & Klein, 2014; Dillmann, 2002), however the precise mechanisms are still somewhat unclear. Several humoral factors and mechanisms are involved in the regulation of blood pressure and can be altered by thyroid dysfunction, e.g. the renin-angiotensin-aldosterone system. TH normally increases renin synthesis and secretion. Therefore, plasma renin levels are increased in hyperthyroidism, and conversely, renin levels are lower than normal in hypothyroidism (Kobori et al., 2001). The hepatic production of angiotensinogen, the substrate for the action of plasma renin, is also increased by THs. It is therefore plausible that the changes in renin-angiotensin-aldosterone system are present in hyperthyroidism and hypothyroidism and contribute to the

increase in plasma volume in hyperthyroidism and the decrease in volume in hypothyroidism (Vargas et al., 2012).

1.9.2 Thyroid Hormone and the Metabolism

TH also regulates metabolic processes that are extremely important for normal growth and development in prenatal life, in childhood and in adult humans (Cheng et al., 2010; Mullur et al., 2014).

TH regulates energy expenditure (EE), for instance by maintaining basal metabolic rate (BMR), facilitating adaptive thermogenesis, modulating food intake, and regulating body weight. BMR is the most important source of energy expenditure, and a decrease can lead to obesity and weight gain. So, BMR was found to correlate with lean body mass and TH levels (Fox et al., 2008; Iwen et al., 2013). An abnormality in TH function such as hyper- or hypometabolism results in significant changes in BMR (Teixeira et al., 2020).

Hyperthyroidism facilitates a hypermetabolic state, which is reflected by increased resting EE, elevated lipolysis, weight loss, gluconeogenesis, and decreased cholesterol levels. Additionally, oxygen consumption in peripheral tissues augments, which in turn elevates metabolic demand and tissue thermogenesis. The strong effect of T3 is evidenced by the fact that 40% of the body's oxygen consumption at rest is regulated by THs (Badman et al., 2007; Barbe et al., 2001). In contrast, hypothyroidism is considered a hypometabolic state reflected by decreased resting EE, reduced lipolysis, weight gain, decreased gluconeogenesis, and elevated cholesterol levels (Brent, 2012).

Regulation of metabolic function by TH occurs through several specific actions in the body, including cellular actions of TH on metabolite transport and utilization (Yen, 2001), facultative thermogenesis (Silva, 2011a), the role of corepressors in metabolic regulation (Mottis et al., 2013), cross-talk with nuclear receptors (Liu & Brent, 2010), adrenergic interactions of TH (Silva & Bianco, 2008), regulation of lipids (Webb, 2010), and metabolic effects on the central regulation of TH. This regulation takes place predominantly through activities in brain, white and brown fat, skeletal muscle, and liver (Table 2) (Iwen et al., 2018; Oelkrug et al., 2020).

Table 2: Effect of thyroid hormone action on metabolic regulation.

Process	Elements regulating metabolism	Basic mechanism	Examples of physiological actions	Reference
Thyroid hormone action	TR isoforms	TR isoform specificity	Increased basal metabolic rate (BMR)	(Brent, 2000)
	Corepressor action (NCoR and SMRT)	Histone modification	Stimulate lipolysis/lipogenesis	(Astapova et al., 2008)
	Nutrient feedback	Sumoylation	Increase in adaptive thermogenesis	(Silva, 2005)
	Nongenomic action	Corepressor interactions	Stimulate β-oxidation of fatty acids	(Silva, 2005)
	Tissue-selective thyroid hormone transport	Modulation of signal transduction pathways	Stimulate β-oxidation of fatty acids	(Chen et al., 2013)
Thermogenesis and body weight	Basal metabolic rate	Integration of adrenergic signaling	Reduces body fat	(Silva, 2011b)
	Adaptive thermogenesis	Central and local adrenergic actions	Increases β-oxidation of fatty acids	(Silva, 2011b)
	Body weight and body composition	Stimulation of CPT1α expression	Stimulates adaptive thermogenesis	(Silva, 2011b)
Cholesterol and triglycerides	Cholesterol synthesis	Stimulates LDL-R	Reduces serum cholesterol	(Ladenson et al., 2010)
	Reverse cholesterol transport	Stimulates ABCA1	Reduces serum triglycerides	(Liu & Brent, 2010)
	Lipolysis/lipogenesis	Stimulates ABCA1	Reduces hepatic steatosis	(Pucci et al., 2000)
Carbohydrate metabolism	Pancreatic islet development	TR expression in developing islets	Stimulates gluconeogenesis	(Crunkhorn & Patti, 2008)
	Pancreatic islet proliferation	D2 required for developing islets and islet function	Reduces insulin sensitivity	(Crunkhorn & Patti, 2008)
	Insulin production	Insulin signaling	Increase in insulin metabolism	(Crunkhorn & Patti, 2008)
	Gluconeogenesis	Stimulation of mitochondrial respiration	Increase in insulin metabolism	(Crunkhorn & Patti, 2008)

Abbreviations: **ABCA1**: ATP-binding cassette transporter A1; **BMR**: basal metabolic rate; **CPT1α**: carnitine palmitoyl transferase 1a; **D2**: 5′-deiodinase type 2; **LDL-R**: low-density lipoprotein receptor; **NCoR**: nuclear corepressor; **SMRT**: silencing mediator for retinoic and thyroid hormone receptor; **TR**: thyroid receptor.

1.10 Aim of the Study

In recent decades, THs were found to play an important role in fetal development and adulthood by regulating tissue differentiation, tissue development, and metabolic function throughout the body. Although many women develop thyroid disorders during pregnancy (Korevaar et al., 2013), only a few of them are routinely screened for TH levels in Europe (Vaidya et al., 2012). Despite the detrimental effect of impaired TH action during development, it is currently controversial whether all pregnant women should be routinely screened for thyroid function and whether it is important to substitute in subclinical cases (Taylor et al., 2018).

Unfortunately, the majority of clinical studies investigating the role of maternal TH on offspring development have largely focused on motoric and intellectual endpoints. As recent clinical and preclinical data have shown that maternal TH is also crucial for central control of metabolism and cardiovascular function in the offspring, it seems necessary to evaluate the connection of maternal TH with these endpoints in greater detail. Therefore, this thesis aims to define the precise consequences of altered TH signaling during pregnancy on metabolism and cardiovascular functions in the offspring using a sophisticated animal model combining a genetic loss of function model with pharmacological rescue experiments during different developmental periods.

In particular, this thesis aimed to answer the following research questions:

1. What is the effect of TH treatment at different periods of pregnancy on metabolism and growth of the offspring?

2. What are the effects of thyroid treatment at different periods of pregnancy on cardiovascular development and function in the adult offspring?

3. Is there a sexual dimorphism in the studied parameters, given that male mice are usually more susceptible to changes in uterine environment?

2. MATERIALS AND METHODS

2.1 Materials

The following tables list the devices (Table 3), consumables and glassware (Table 4) used in this thesis.

Table 3: Devices used in this thesis.

Device	Supplier
Binocular microscope, SZB 250	VWR International, Germany
Blood Pressure Device, Model SC-100	Hatteras Instrument Incorporated, USA
Centrifuge 4°C (5430R)	Eppendorf, Germany
ChemiDoc Touch Imaging System	Bio-Rad Laboratories, USA
Comb, 12-well, 1.0 mm	Thermo Fisher Scientific, USA
Cryostat, CM3050s	Leica, USA
Dual short period timer TR 118 OS	Carl Roth GmbH, Germany
Eppendorf Research (R) Plus (0.5-10, 10-100, 100-1000)	Eppendorf, Germany
Filter plate A, 0.6 mL/well	Eppendorf, Germany
Gel Chamber (Horizon)	Thermo Fisher Scientific, USA
Glucometer (Accu Chek Aviva®)	Roche Diagnostics, Germany
Green Line individually ventilated cage Sealsafe cage system GM500	Tecniplast, Italy
Infrared Camera T335	FLIR Systems, Inc. Sweden
Magnetic stirrer Combimag RCT	IKA, Germany
MC6 Centrifuge	Sarstedt AG, Germany
Microplate Spectrophotometer (Plate: Take3)	Epoch, BioTek Instruments, USA
Microplate Reader 3550 with incubator	Bio-Rad Laboratories, USA
Mini Gel Tank	Invitrogen, USA
Mini-Centrifuge (C1301P-230)	Labnet International, USA
Minispec BCA analyzer NMR (LF110)	Bruker; Germany
Multistep pipette MultipetteR E3	Eppendorf, Germany
PhenoMaster	TSE Systems GmbH, Germany
Precision scale, 440-47N	Kern, Germany
Precision scale, Atilon	Acculab, Germany
Precision scale, PCB 1000-1	Kern, Germany
Precision scale, PT 1200	Sartorius, Germany
PyroMark Q48 Autoprep	QIAGEN, Germany
qPCR machine (QuantStudio 5, A28134)	Thermo Fisher Scientific, USA

Device	Supplier
Quantstudio Applied Biosystems	Thermo Fisher Scientific, USA
Quantus™ Fluorometer	Promega, USA
Rack Iso FreezeR for PCR set-up	Sarstedt AG, Germany
Rack, PCR tubes, 96-well	TH. Geyer, Germany
Rectal Thermometer Probe (BAT-12)	Physitemp Inc., USA
SPECTROstar Nano	BMG Labtech, Germany
Surgical instruments	Fine Science Tools, Canada
Syringes (Injekt-F)	Braun, Germany
Thermometer	Th. Geyer, Germany
Tissue Homogenizer (Bead Mill 24)	Fisherbrand, USA
TXRF analyzer, S4 T-STAR	Bruker Nano GmbH, Germany
Vortex PV-1	Grant Instruments, UK
Western Blot Equipment	Bio-Rad Laboratories, USA

Table 4: Consumables and glassware used in this thesis.

Consumable / glassware	Catalog #	Supplier
96 PCR Plate half skirt flat	72.1979.102	Sarstedt AG, Germany
Adhesive Clear PCR Seal Sheets	600208	Biozym Scientific GmbH, Germany
Alcohol Pads	9160612	Braun, Germany
Ceramic beads (1.4 mm, 325 g)	432-0356	VWR International, USA
Eppendorf Tubes 5.0 mL	30119401	Eppendorf, Germany
Falcon Tube 15 mL	62.554.002	Sarstedt AG, Germany
Falcon Tube 50 mL	62.559.001	Sarstedt AG, Germany
Filter tip (10 µL / 100 µL / 1000 µL)	701114210 / 70760212 / 70762211	Sarstedt AG, Germany
Immobilon®-P Transfer Membrane Pore Size 0.45 µm	IPVH00010	Merck Milipore, USA
Micro Tube 1.5 mL SafeSeal	72.706.400	Sarstedt AG, Germany
Micro Tube 2 mL SafeSeal	72.695.500	Sarstedt AG, Germany
MicroAmpR clear adhesive film	Z369667-100EA	Sigma-Aldrich, USA
PCR stripe lid chain	410092	Sarstedt AG, Germany
PyroMark Q48 Absorber Strips	974912	QIAGEN, Germany
PyroMark Q48 Discs	974901	QIAGEN, Germany
Reaction tubes low binding, 1.5 mL	72.706.700	Sarstedt AG, Germany
Screw cap micro tubes	637440	Sarstedt AG, Germany
Surgical blade stainless No. 11 pfm	18071067	Pfm medical, Japan
Western Blotting Filter Paper	8860	Thermo Fisher Scientific, USA

Chemicals used in this thesis are listed in Table 5.

Table 5: Chemicals used in this thesis.

Chemical	Catalog #	Supplier
100 bp Standard DNA Ladder	MWD100	NIPPON Genetics EUROPE GmbH
2-Mercaptoethanol	M3148	Sigma-Aldrich, USA
3,3',5-Triiodo-L-Thyronine sodium salt (T3)	T6397	Sigma-Aldrich, USA
Acetic acid	W200603	Merck Millipore, USA
Agarose Powder	2267.4	Carl Roth GmbH, Germany
Ammonium persulfate (APS)	9592.1	Carl Roth GmbH, Germany
Ammonium cerium (IV) sulfate hydrate	483680	Sigma-Aldrich, USA
Bicinchoninic Acid solution	B-9643	Sigma-Aldrich, USA
Bovine Serum Albumin (BSA)	A7906	Sigma-Aldrich, USA
Calcium Chloride Dihydrate ($CaCl_2$ $2H_2O$)	HN04.2	Th. Geyer GmbH, Germany
Chloroform (Trichloromethane)	C2432	Honeywell, Sigma-Aldrich, Germany
Clarity Western ECL Substrate	1705060	Bio-Rad Laboratories, USA
Collagenase, type I (Clostridium histolyticum)	LS004194	Worthington Biochemical Corporation, USA
Complete Ultra Tablets Mini	5892791001	Roche Diagnostics, Germany
DEPC-treated Water	AM9906	Thermo Fisher Scientific, USA
D-Glucose	G7021	Sigma-Aldrich, USA
Diethyl Ether Rotipuran >99%	3942.1	Carl Roth GmbH, Germany
Dipotassium hydrogen phosphate (K_2HPO_4)	231-834-5	Carl Roth GmbH, Germany
Dimethylsulfoxid (DMSO)	D8418	Sigma-Aldrich, USA
DNA Away	43944	Thermo Fisher Scientific, USA
dNTP Mix (10 mM)	R0191	Thermo Fisher Scientific, USA
DreamTaq Buffer	B65	Thermo Fisher Scientific, USA
DreamTaq DNA Polymerase 500 U	EP0702	Thermo Fisher Scientific, USA
DL-Dithiothreitol (DTT)	D0632	Sigma-Aldrich, USA
Dowex W50-X2	217441	Merck Millipore, USA
Ethanol (denatured)	24194	Sigma-Aldrich, USA
Ethanol 99% (extra pure)	5054.4	Th. Geyer GmbH, Germany
Ethylenediaminetetraacetic Acid (EDTA)	E26282	Merck Millipore, USA
Ethylenglycol 99,5% p.A.	6881.1	Th. Geyer GmbH, Germany
Gallium standard	16639	Merck Millipore, USA
Glutathion	G4251	Sigma-Aldrich, USA
Glutathion reductase	10105678001	Roche Diagnostics, Germany
Glycine	G8898	Sigma-Aldrich, USA
GoTaqRqPCR Master Mix	A6002	Promega, USA
Hydrochloric Acid	K025.1	Carl Roth GmbH, Germany
Hydrogen peroxidase	18304	Sigma-Aldrich, USA
Isoflurane	TU061220	Zoetis, USA

Chemical	Catalog #	Supplier
Isopropanol 99%	17024	Th. Geyer GmbH, Germany
Magnesium Chloride	KK36.2	Carl Roth GmbH, Germany
Methanol >99%	8388.5	Carl Roth GmbH, Germany
Milk Powder	T145.3	Carl Roth GmbH, Germany
Nicotinamide adenine dinucleotide phosphate (NADPH)	481973	Merck Millipore, USA
Normal goat serum (NGS)	0005-000-001	Dianova/ USA
PageRulerTM Plus Prestained Protein Ladder	26619	Thermo Fisher Scientific, USA
Paraformaldehyde powder, 95%	158127	Sigma-Aldrich, USA
Phenylmethylsulfonyl Fluoride (PMSF)	93482	Sigma-Aldrich, USA
Potassiumphosphat (KPO_4)	12665087	Fischer Scientific
Propylthiouracil (PTU)	P3700000	Merck Millipore, USA
RNase ZAP™	R2020	Th. Geyer GmbH, Germany
Saline (0.9%)	S9888	Berlin-Chemie AG, Germany
Serenom serum standard	210105	Sero AS, Norway
Sodium acid (NaN_3)	S2002	Sigma-Aldrich, USA
Sodium Chloride (NaCl)	9265.2	Carl Roth GmbH, Germany
Sodium Deoxycholate ($C_{24}H_{39}NaO_4$)	A1531.0025	AppliChem, Germany
Sodium Dodecylsulfate Solution 10%	A0676,1000	AppliChem, Germany
Sodium Fluoride Solution (NaF)	450022	Sigma-Aldrich, USA
Sodium Hydroxide (NaOH)	6771.3	Carl Roth GmbH, Germany
Sodium Orthovanadate, activated (Na_3VO_4)	450243	Sigma-Aldrich, USA
Sodium (meta) arsenite ($NaAsO_2$)	S7400	Sigma-Aldrich, USA
Standard DNA Ladder (100 bp)	MWD100	NIPPON Genetics EUROPE GmbH, Germany
Sucrose ≥ 99.5% (GC)	59378	Sigma LifeScience, USA
Sulfuric acid (H_2SO_4)	339741	Sigma-Aldrich, USA
SYBRTM Safe DNA Gel Stain	S33102	Thermo Fisher Scientific, USA
TBE Buffer 10x pH 8.3	106177	Th. Geyer GmbH, Germany
Tetramethylethylenediamine (TEMED)	2367.1	Carl Roth GmbH, Germany
Trichloroacetic Acid	T9159	Sigma-Aldrich, USA
Tris	AE15.2	Carl Roth GmbH, Germany
Tris-EDTA (TE) Buffer	T9285	Sigma-Aldrich, USA
Tween®-20	P1379	Sigma-Aldrich, USA
Vaseline	V125	Balea, Germany

2.1.1 Buffer and Solution Recipes

The following table (Table 6) lists all buffers and their composition that were used in this thesis.

Table 6: Buffer and solution recipes used in this thesis.

Buffer / Solution	Recipe	
4% Formaldehyde Solution (PFA, for 300 mL)	37.5 mL	PFA (32%)
	262.5 mL	1x PBS
Genotyping Buffer (for 100 mL)	1 mL	EDTA (0.5 M)
	4 mL	NaCl (5 M)
	1 mL	20% v/v SDS
	10 mL	Tris (1M, pH 8.5)
Lysis Buffer (10 mL)	10 mL	RIPA-Puffer
	1 pc.	Protease Inhibitor tablets
	50 µL	200 mM Na_3VO_4
	200 µL	500 mM NaF
	1 mL	100 mM PMSF
Phosphate Buffered Saline (10× PBS, 0.1 M, pH = 7.4, for 1 L)	2 g	KCl
	2.4 g	KH_2PO_4
	26.8 g	Na_2HPO_4
	80 g	NaCl
Resolving Gel 12% in H_2O (for 10 mL)	4.04 mL	Acrylamid
	40 µL	APS
	0.21 mL	SDS
	20 µL	TEMED
	2.53 mL	Tris Base (1.5 M)
RIPA Buffer (100 mL)	3.33 mL	1.5 M Tris-HCl (pH 7.4)
	3 mL	5 M NaCl
	1 mL	100 % Nonidet P-40
	5 mL	10 % Na-deoxycholate
	200 µL	500 mM EDTA
	87.47 mL	PBS
Running Buffer (1 L)	30.3 g	Tris (0.25 M)
	144.13 g	Glycin (1.92 M)
	10 g	SDS (1% w/v)
Stacking Gel (for 1 Gel with TGX Stain-FreeTM FastCastTM Acrylamide Kit)	1.5 mL	Stacker 1 (ready to use solution, Kit)
	1.5 mL	Stacker 2 (ready to use solution, Kit)
	15 µL	APS (10%) 0.5%
	4.5 µL	TEMED (0.15%)

Buffer / Solution	Recipe	
Sample Buffer (4× 20 mL)	10 mL	Glycerol (50% v/v)
	2 g	SDS (10% w/v)
	6.25 mL	1 M Tris / HCl pH 6.8
	1.75 g	Bromphenolblau
	Before use: add 1-part β-Mercaptoethanol to 4 parts buffer	
Stacking Gel in H_2O (for 10 mL)	1.66 mL	Acrylamid
	40 µL	APS
	0.08 mL	SDS
	20 µL	TEMED
	2.48 mL	Tris Base (0.5 M)
TBS pH 7.4 10× (1 L)	12.1 g	0.1 M Tris
	87.7 g	1.5 M NaCl
Transfer Buffer or Blotting buffer 10× (1 L)	30.3 g	Tris (0.025 M)
	144.13 g	Glycin (0.192 M)
	-	Methanol (20%)
	10× Buffer without MeOH for 1× Buffer: 700 mL VE H_2O + 100 mL 10× blotting buffer + 200 mL MeOH	
Tris Buffered Saline with Tween 20 (1× TBS-T, pH = 7.4, 1 L)	8.77 g	NaCl
	1.21 g	Tris Base
	1 mL	Tween 20

2.1.2 Primer

Table 7 shows all primers and their sequences used for qPCR in this thesis. All primers were obtained from Integrated DNA Technologies Inc. or Thermo Fisher Scientific.

Table 7: Primer sequences for qPCR in this thesis.

Gene	Gene name	Primer Sequence 5'→ 3'	
Acc1	Acetyl-Coenzyme A carboxylase 1	Fw:	GTC CCC AGG GAT GAA CCA ATA
		Rev:	GCC ATG CTC AAC CAA AGT AGC
Ace1	Angiotensin converting enzyme	Fw:	TCC AAG CAG GAA GCT AAT CC
		Rev:	CAG CCT ACC TGC TTC CTT CC
Adrb3	Beta 3-adrenergic receptor	Fw:	AGA AAC GGC TCT CTG GCT TTG
		Rev:	TGG TTA TGG TCT GTA GTC TCG G
Agt	Angiotensinogen	Fw:	TTC CAA GGA ACG ATG AGA GG
		Rev:	ACT CCA GTG CTG GAA GTT GC

Gene	Gene name	Primer Sequence 5'→ 3'	
Cyclo	Peptidylprolyl isomerase D	Fw:	TCA CAA CAG TTC CGA CTC CTC
		Rev:	ACC TCT ACA TTT TCA AGC GTC C
Dio1	iodothyronine deiodinase type I	Fw:	GCT GAA GCG GCT TGT GAT ATT
		Rev:	GTT GTC AGG GGC GAA TCG G
Dio2	iodothyronine deiodinase type II	Fw:	ATG GGA CTC CTC AGC GTA GAC
		Rev:	ACT CTC CGC GAG TGG ACTT
Fasn	Fatty Acid Synthase	Fw:	GGA GGT GGT GAT AGC CGG TAT
		Rev:	TGG GTA ATC CAT AGA GCC CAG
Gh	Growth hormone	Fw:	GCT ACA GAC TCT CGG ACC TC
		Rev:	CGG AGC ACA GCA TTA GAA AAC AG
Gpd2	Glycerol -3-phosphate dehydrogenase 2, Mitochondrial	Fw:	GAA GGG GAC TAT TCT TGT GGG T
		Rev:	GGA TGT CAA ATT CGG GTG TGT
Hcn2	Hyperpolarization Activated Cyclic Nucleotide Gated Potassium and Sodium Channel 2	Fw:	TCC GCA CCG GCA AAG TTA
		Rev:	CCG GGA TGG ATG ACA CGA AG
Hcn4	Hyperpolarization Activated Cyclic Nucleotide Gated Potassium and Sodium Channel 4	Fw:	ACC CGC AGA GGA TCA AGA TGA
		Rev:	AAT GCG AGT CTC CAC TAT AAG GA
Hprt	Hypoxanthine Phosphoribosyl transferase	Fw:	GCA GTA CAG CCC CAA AAT GG
		Rev:	AAC AAA GTC TGG CCT GTA TCC AA
Hsl	Hormone sensitive lipase	Fw:	CAC CCA TAG TCA AGA ACC CCT C
		Rev:	TCT ACC ACT TTC AGC GTC ACC G
Igf1	Insulin-like growth factor 1	Fw:	CTG GAC CAG AGA CCC TTT GC
		Rev:	GGA CGG GGA CTT CTG AGT CTT
Myh1	Myosin heavy chain 1	Fw:	CTC TTC CCG CTT TGG TAA GTT
		Rev:	CAG GAG CAT TTC GAT TAG ATC CG
Myh4	Myosin heavy chain 4	Fw:	CTT TGC TTA CGT CAG TCA AGG T
		Rev:	AGC GCC TGT GAG CTT GTA AA
Pepck	Phosphoenolpyruvate Carboxylase	Fw:	ATC TTT GGT GGC CGT AGA CCT
		Rev:	GCC AGT GGG CCA GGT ATT T
Pparδ	Peroxisome proliferator activated receptor delta	Fw:	TCC ATC GTC AAC AAA GAC GGG
		Rev:	ACT TGG GCT CAA TGA TGT CAC
Pyrkl	Pyruvate kinase (liver)	Fw:	TCA AGG CAG GGA TGA ACA TTG
		Rev:	CAC GGG TCT GTA GCT GAG TG
Pyrkm	Pyruvate Kinase (muscle)	Fw:	CGC CTG GAC ATT GAC TCT G
		Rev:	GAA ATT CAG CCG AGC CAC ATT
Serca2	Calcium-Transporting ATPase Sarcoplasmic Reticulum type 2	Fw:	TCC GCT ACC TCA TCT CAT CC
		Rev:	CAG GTC TGG AGG ATT GAA CC
Sln	Sarcolipin	Fw:	GAG GTG GAG AGA CTG AGG TCC
		Rev:	GAA GCT CGG GGC ACA CAG CAG
Spot14	TH responsive protein	Fw:	AAG GTG GCT GGC AAC GAA A
		Rev:	GGG TCA GGT GGG TAA GGA TG

Gene	Gene name	Primer Sequence 5'→ 3'	
Tshb	Thyroid stimulating hormone beta	Fw:	CCG CAC CAT GTT ACT CCT TA
		Rev:	GTT CTG ACA GCC TCG TGT AT
Ucp1	Uncoupling Protein 1	Fw:	ACT CAG GAT TGG CCT CTA CG
		Rev:	CCA CAC CTC CAG TCA TTA AGC
α-Mhc (Myh6)	Myosin heavy chain 6 (alpha)	Fw:	GCC CAG TAC CTC CGA AAG TC
		Rev:	GCC TTA ACA TAC TCC TCC TTG TC
β-Mhc (Myh7)	Myosin heavy chain 7 (beta)	Fw:	GGA ATC CTT TGG AAA TGC GAA GA
		Rev:	GCC CCA ACA ATA TAG CCA GTT AC

2.1.3 Antibodies

For western blot analysis, the following antibodies were used in this thesis.

Table 8: Primary (a) and secondary (b) antibodies used for western blot analysis.

	Antibody	Species	Dilution	Catalog #	Supplier
(a)	anti-HCN2	Rabbit	1:1,000	APC-30	Alomone labs, Israel
	anti-HCN4	Rabbit	1:10,000	APC-052	Alomone labs, Israel
(b)	anti-rabbit IgG	Goat	1:5,000	P0448	Dako, Denmark

2.1.4 Commercial Kits

The kits used for experiments in this thesis are listed in Table 9.

Table 9: Commercial kits used in this thesis.

Kit	Catalog #	Supplier
EpiTectR Fast DNA Bisulfite Kit	59802	QIAGEN, Germany
PyroMark PCR Kit	978703	QIAGEN, Germany
PyroMark Q48 Advanced CpG Reagents	974022	QIAGEN, Germany
RevertAid First Strand cDNA Synthesis Kit	K1622	Thermo Fisher Scientific, USA
RNase-Free DNase Set	79256	QIAGEN, Germany
RNeasy Fibrous Kit	74704	QIAGEN, Germany
RNeasy Lipid Tissue Kit	74804	QIAGEN, Germany
RNeasy Lipid Tissue Mini Kit	74804	QIAGEN, Germany
RNeasy Mini Kit	74106	QIAGEN, Germany
Total T3 ELISA 96 wells	DNOV053	NovaTec GmbH, Germany
Total T4 ELISA 96 wells	EIA-1781	DRG Instruments, Germany

2.1.5 Software

Software used for experiments are listed in Table 10.

Table 10: Software used in this thesis.

Software	Supplier
EndNote X9	Clarivate Analytics, USA
FLIR Tools 5.3.15268.1001	FLIR Systems, Inc. Sweden
Gen5™ 2.00.17	BioTek, USA
GraphPad Prism® 7	GraphPad Software Inc, USA
ImageLabTM Software	Bio-Rad Laboratories, USA
Microsoft Office 2016	Microsoft, USA
PyroMarkR Assay Design 2.0.1.15	QIAGEN, Germany
PyroMarkR Q48 Autoprep Software 2.4.2 build 3	QIAGEN, Germany
QuantStudioTM Design & Analysis Software	Thermo Fisher Scientific, USA
SPECTROstar Nano 2.10	BMG Labtech, USA
Unipro UGENE v1.25.3	Unipro, USA

2.2 Methods

2.2.1 Animal Husbandry and Study Design

TRα1 mice, carrying the dominant-negative R384C mutation in TRα1, have been described by Tinnikov et al. (2002). The heterozygous mutant TRα1 (TRα1+/m) male mice were obtained at the age of 10 weeks from the GTH of the University of Luebeck, Germany. And wildtype C57BL6/6NCr female mice were purchased at the age of 10 weeks from Charles River Laboratory, Germany.

The TRα1+/m mice used for the experiments have been backcrossed to C57BL6/6NCr for 12 generations and were bred in the GTH Luebeck animal core facility. Littermate male mutant and wildtype mice were born by wildtype females. At least 6 animals per group were used for the experiments at the age of 4 months.

To decipher effects related to maternal thyroid hormone receptor α signaling, offspring obtained from male TRα1 heterozygous (TRα1+/m) and wildtype females were compared. The animals were housed at 21°C on a 12 h light/12 h dark cycle with free access to food and water.

The dams received 0.5 µg/mL T3 (3,3',5-Triiodo-L-thyronine; T6397, Sigma Aldrich, USA) via drinking water containing 0.01% BSA (A7906, Sigma Aldrich, USA). The treatment started either from the first day after positive plug check and was continued until embryonic day E12.5 (i.e. first half of pregnancy) or at E12.5 until day E17.5, the day before birth (i.e. second half of pregnancy) (Figure 5) (Flamant, Gauthier, and Richard 2017).

All animal procedures were conducted in accordance with the Directive 2010/63/EU of the European Parliament and of the Council and approved by MELUND Schleswig-Holstein, Germany (Ministerium für Energiewende, Landwirtschaft, Umwelt, Natur and Digitalisierung). All required animal permissions were obtained from the local Ethics Committee.

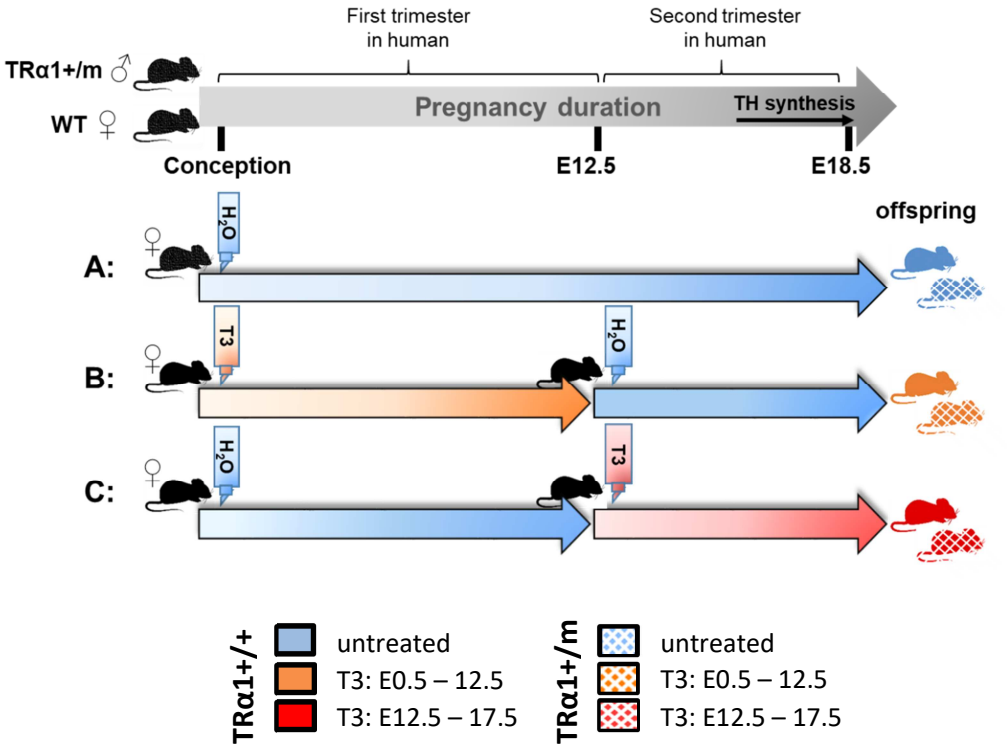

Figure 5: Breeding scheme of T3 treatment during pregnancy. A: *Dams were treated with H_2O either from conception until birth (blue arrow) or* ***B:*** *in the first (orange arrow) or* ***C:*** *second half of pregnancy (red arrow) with T3 in drinking water.*

2.2.2 *In vivo* Methods

2.2.2.1 Metabolic Characterization

To investigate the metabolic phenotype of the offspring, their water bottles and food were weighed daily. Based on the weight changes, the food and water intake of the offspring was

ultimately determined. In addition, the body weight of the offspring was measured once a week after weaning. Subsequently, several experiments were performed to investigate the metabolic changes that occur during thyroid hormone treatment. For instance the following metabolic parameters were assessed in the offspring: thermoregulation, glucose tolerance, energy expenditure and body composition (lean and fat mass).

2.2.2.2 Infrared Thermography

Infrared (IR) thermography, a non-invasive method, was used to measure the body surface temperature of various body parts of freely moving mice.

Infrared images of interscapular brown adipose tissue (iBAT), inner ear, and tail base were taken when the offspring were 4 months old. For image acquisition the mice were placed on their cage grid for a maximum of 3 minutes. Three images of each body part were taken to determine body temperature, heat production, and heat loss.

On four consecutive days, the measurement was performed always at the same time. While the first day served to accustom the animal to this procedure, day 2 to 4 were used for the evaluation.

Before images of the iBAT were taken, it was necessary to apply a small amount of Vaseline between the shoulder blades of the mice to brush up the fur of the neck (Oelkrug and Mittag 2021).

For the analysis of the IR images, the highest temperature of the regions mentioned above was taken. The images were analyzed with the software FLIR Tools (FLIR Systems, Inc. Sweden).

2.2.2.3 Rectal Body Temperature

Rectal body temperature was determined using a thermal probe (BAT-12, Physitemp, USA) and taken as an estimate of the core body temperature of the experimental mice.

The measurement was performed on four consecutive days. The measurement on the first day was used to accustom the animal to this procedure. The values from day 2 to 4 were used for evaluation.

First, some Vaseline was applied to the probe. Then it was inserted rectally into the animal and the measurement could be started. As soon as the device displayed a value, the measurement was finished.

2.2.2.4 Blood Pressure Measurement

For blood pressure measurements of the offspring, specifically systolic and diastolic blood pressure, mean arterial pressure (MAP) as well as pulse rate, a non-invasive tail-cuff system with a temperature-controlled platform (100°F) was used. MAP is the average arterial pressure during one cardiac cycle.

The device can measure the blood pressure of a single conscious mouse at a time. The principle of this technique is based on the illumination of the tail blood volume by a red light-emitting diode (LED); the light passes through the tail and is monitored by the photodiode. With each heartbeat, the blood volume varies and consequently the light intensity changes as well. Finally, the intensity is converted into digital numbers displayed on the device.

As the measurement procedure is very sensitive to movements, the mouse was placed in a chamber and their tails were pulled through a cuff and fixed.

To accustom the animals to the device and minimize their stress response, several days before the start of the experiment, their blood pressure was already measured once a day. Furthermore, the mice were allowed to get used to the device for 3 minutes each time before the measurement began.

During the experiment blood pressure of the mice was measured on three consecutive days and 15 times in one session for 30 seconds. At the end of each session, both platform and chamber were disinfected with ethanol to avoid contamination between the experimental mice.

For analysis, diastolic blood pressure values below 40 mmHg were excluded. Then the mean for each mouse was calculated from the three days, and finally these mean values were used to determine the mean for each genotype. The detailed settings for blood pressure measurements are presented in the table below (Table 11).

Table 11: Detailed setting for blood pressure measurement.

Task	Duration
Measurement cycles	15
Minimum Pulse Amplitude	5%
No. of consecutive peaks	70
Ignore Peaks Smaller than	0.5%
Maximum Pressure	242 mmHg
Pulse Time Out	30 sec
Measurement time	30 sec
Time between measurements	2 sec
Systolic Threshold	20%
Diastolic Threshold	50%
Platform Temperature	100°F / 37.8°C

2.2.2.5 Measurement of Glucose Metabolism in Mice (ipGTT)

Glucose tolerance and clearance was assessed in the offspring by conducting an intraperitoneal glucose tolerance test (ipGTT).

The experimental offspring were fasted for six hours prior to performance of the test. Basal blood glucose was measured by scratching the tip of the tail with a scalpel after sterilizing the tail with 70% ethanol. The first drop of blood was removed, and the second drop was used to determine blood glucose with a glucometer (Accu Chek Aviva®, Roche Diagnostics, Germany). The baseline blood glucose was noted. Then the mice were injected i.p. with 2 g/kg glucose. After injection, the tail was scratched again for blood glucose measuring after 15 min, 30 min, 60 min, 90 min and 120 min.

2.2.2.6 Body Composition Analysis by Nuclear Magnetic Resonance (NMR)

Body composition was quantified by nuclear magnetic resonance (NMR) technology.

For NMR analysis, the minispec Body Composition Analyzer (Bruker, Germany) was used according to the manufacturer's instructions. Mice were fixed in a restrainer and measured for 2 minutes. By this non-invasive method, free fluid, fat mass, and lean mass could be analyzed in mice and finally differences in body composition due to genotype or different treatments of offspring could be assessed.

2.2.2.7 Indirect Calorimetry

Indirect calorimetry is a method that uses respiratory gas exchange (i.e. oxygen consumption (VO_2) and carbon dioxide production (VCO_2)) to analyze energy metabolism. The measurements in mice were performed using an open flow respirometric system (PhenoMaster, TSE Systems GmbH, Germany) and a temperature-controlled climate chamber (23 ± 0.5°C).

The respiration quotient (RQ) value gives an indication of which macromolecules are metabolized. If the metabolism consists only of lipids, the RQ value is about 0.7, for proteins about 0.8 and for carbohydrates about 1.0 (Tschöp et al. 2012). The RQ value was calculated as follows:

$$RQ = \frac{VCO_2}{VO_2}$$

Daily energy expenditure (DEE) was measured for 48 hours after the experimental offspring were individually housed and acclimated for at least 2 days. DEE was calculated using RQ and caloric equivalents as given by Heldmaier (1975):

$$DEE = (4.44 + 1.43 \times RQ) \times VO_2 \times 0.001$$

To measure basal metabolic rate (BMR) the offspring were measured in the inactive phase of mice (light on). The experimental mice should not have access to food or water for up to six hours to avoid heat production due to the acute increase in metabolism after eating. Thermoneutrality, the state in which active thermoregulation and physical activity are lowest, is about 30°C in mice (Meyer, Ootsuka, and Romanovsky 2017). This temperature is therefore best suited for determining the BMR.

2.2.3 Molecular Methods

2.2.3.1 Plasma Preparation

Whole blood samples from mice were collected by cardiac puncture and transferred into a 1 mL tube. The blood was immediately stored on ice for maximum 20 min. Subsequently, the samples were centrifuged at 2,000×g for 2x15 min to remove the cells from the plasma and to deplete platelets. Finally, the resulting supernatant (i.e. plasma) was transferred into a new tube and stored at -20°C.

2.2.3.2 Genes

The following table (Table 12) provides an overview of the tissue-specific genes studied in this thesis.

Table 12: Tested genes in different tissues in this thesis.

Tissues	Tested genes
Houskeeping	*Cyclo, Hprt*
Heart	*α-Mhc, β-Mhc, Serca2, Hcn2, Hcn4*
Liver	*Spot14, Pepck, Pyrkl, Fasn, Igf1, Agt, Dio1, Acc1*
Lung	*Ace*
iWAT	*Adrb3, Hsl*
iBAT	*Dio2, Ucp1, Adrb3, Hsl*
gWAT	*Acc1, Hsl*
Muscle gastrocnemius	*Pyrkm, Pepck, Myh1, Myh4, Gpd2, Sln, Pparδ*
Muscle soleus	*Pyrkm, Pepck, Myh1, Myh4, Gpd2, Sln, Pparδ*
Pituitary	*Tshb, Gh, Dio2*

2.2.3.3 DIO1 and GPx1 Activity Assay

DIO1 activity was analyzed using a nonradioactive iodide-release assay (Renko et al. 2012). Briefly, liver homogenates (20 µL per sample) and four random samples as inhibited controls were mixed with 10 µL of DMSO or 1mM PTU (6-n-propyl-2-thio-uracil), respectively. The deiodinase reaction was started by adding 80 µL freshly prepared substrate mixture (10 µM rT3, 0.2 M KPO_4 (pH 6.8), 2 mM EDTA, 80 mM DTT) and incubated at 37°C for 2 h. The reactions were stopped on ice and centrifuged (5 min at 4°C and 15,000×g). The supernatants (75 µL each) were applied to Dowex W50-X2 resin in 96-well column package (0.6 mL/well, Filter Plate A, Eppendorf Perfectprep Plasmid 96 Vac Direct Bind kit) to separate the released iodide. Then, the columns were washed (100 µL, 10% acetic acid) and free iodide was eluted by centrifugation (6 min at 20°C and 200×g). The eluate was diluted 1:2 or 1:4 with 10% acetic acid, and 50 µL were transferred to a microtiter plate for determination of iodide content by the Sandell/Kolthoff reaction. After adding 50 µL cerium solution (22 mM $(NH_4)_4Ce(SO_4)_4$ in 0.44 M H_2SO_4) and 50 µL arsenite solution (25 mM $NaAsO_2$, 0.8 M NaCl in 0.5 M H_2SO_4), changes in absorption at 415 nm were assessed over 20 min incubation time at 25°C (Microplate Reader 3550 with incubator; Bio-Rad), and converted into iodide concentrations using an iodide standard curve after subtraction of background from the PTU-inhibited controls.

DIO1 activity is expressed as pmol iodide per min per mg protein. The inter-assay of the assay was determined to be below 20%.

GPx1 activity was evaluated using a coupled enzymatic assay monitoring reduced nicotinamide adenine dinucleotide phosphate (NADPH) consumption at 340 nm (Flohé and Günzler 1984). Briefly, liver homogenates were diluted to protein concentrations of 2.5 mg/mL to reach the dynamic range of the assay. Subsequently, liver homogenates of 1 µL were applied to 96-well plates and assayed in triplicates. For quality control, a constant serum sample was included in triplicate in each assay run. After the addition of 200 µL of a test mixture containing 1 mM NaN_3, 3.4 mM reduced glutathione, 0.3 U/mL glutathione reductase and 0.27 mg/mL NADPH, the reaction was started with 10 µL of 0.00375% hydrogen peroxide. The decrease in NADPH absorbance per minute measured at 340 nm as readout is proportional to the Gpx1 activity in the sample and is expressed as pmol NADPH per min per mg total protein (pmol/min/mg). The inter- and intra-assay was determined to be below 15%.

Both the DIO1 and GPx1 activity assays were performed by a collaborator (Prof. Dr. Lutz Schomburg, Charité Berlin, Germany) for this thesis.

2.2.3.4 Genotyping of TRα1+/m Mutant Mice

The genotype of TRα1+/m mutant mice was analyzed by isolating DNA from ear punches. For isolation, the tissue was incubated overnight in 500 µL genotyping buffer with 5 µL Proteinase K (100 µg/mL) at 55°C and 450 rpm. Subsequently, the samples were centrifuged for 5 min at 18,000×g (RT). Then the supernatant was transferred into a new tube. Afterwards the DNA was precipitated by adding 500 µL isopropanol and separated by centrifugation for 30 min at 18,000×g (RT). The supernatant was discarded and the pellet was washed with 100 µL 80 % ethanol and centrifuged again for 30 min at 18,000×g (RT). Subsequently, the supernatant was discarded and the pellet was air-dried at RT. Finally, the DNA was resolved in 100 µL 10% TE buffer for 30 – 60 min at 55°C, 450 rpm and then stored at 4°C. The isolated DNA was used together with the relevant primer pair (Table 13) for genotyping.

The primer sequences used for genotyping of TRα1+/m mutant mice are listed in Table 13. The program for running the PCR is included in Table 15.

Table 13: Primer sequences used for genotyping.

Strain	Primer Sequence 5' → 3'
Thrα1+/m	Fw: GGA CAA GAT CGA GAA GAG TCA GGA
	Rev: CAC TGC ATT CTA GTT GTG GTT TGT CC

The following table (Table 14) shows the pipetting scheme and the corresponding components of the PCR mix.

Table 14: PCR mix for genotyping with a total volume of 10 µL per reaction.

Substance	Volume per reaction
Taq buffer (10×)	1 µL
dNTP	1 µL
Forward primer 5 µM	1 µL
wt / ko reverse primer 5 µM	1 µL
Taq polymerase	0.5 µL
Sample (ear)	1 µL
dH_2O	4.5 µL

Table 15: PCR program used for genotyping of TRα1+/m mutant mice.

Step	Temperature	Time	Repeat
Activation	95°C	2 min	1
Denaturation	95°C	15 sec	40
Annealing	55°C	15 sec	
Elongation	72°C	15 sec	
Final elongation	72°C	1 min	1
Hold	4°C	∞	

For separation of DNA fragments, PCR reactions were diluted with 6× loading dye. Gel electrophoresis was performed on a 1.5% agarose gel in 1× TBE and 0.01% SYBR safe at 150 V for 30-45 min. For determination of DNA size, a 100 bp DNA ladder was used.

2.2.3.5 RNA Isolation, cDNA Synthesis and Quantitative RT PCR (qPCR)

For gene expression analysis, RNA was isolated from different snap-frozen tissues. For iBAT, iWAT, and gWAT, RNeasy Lipid Tissue Mini Kit (QIAGEN, Germany); for liver, lung,

and pituitary, RNeasy Mini Kit (QIAGEN, Germany) and for heart, muscle gastrocnemius and muscle soleus, RNeasy Fibrous Kit (QIAGEN, Germany) was used according to the manufacturer's instructions. Subsequently, RNA concentration was measured in a UV photometer. Complementary DNA (cDNA) was then synthesized from 0.5 - 1 µg of total RNA using the Molecular Biology RevertAid strand cDNA kit (Thermo Fisher Scientific, USA) with oligo $(dT)_{18}$ primer (Invitrogen, USA). Afterwards, the cDNA was diluted in nuclease-free water to reach a final concentration of 1.25 - 5 ng/µL. The corresponding cDNA was used as a template for the qPCR reaction. The detailed pipetting scheme is shown in Table 16.

Table 16: Preparation of the qPCR mix with a total volume of 20 µL per reaction. *To the first mix, the substances of the second mix were added. All substances together are the complete qPCR mix.*

	Substance	Amount per reaction
1st Mix	Total RNA	0.5 - 1 µg
	Nuclease-free water	ad 11 µL
	Oligo$(dT)_{18}$ Primer	1 µL
	Total volume	12 µL
2nd Mix	5× Reaction buffer	4 µL
	10 mM dNTP Mix	2 µL
	RiboLock RNase Inhibitor (20 U/µL)	1 µL
	RevertAid M-MuLV RT (200 U/µL)	1 µL
	Total volume	**20 µL**

The complete mix was then gently mixed and briefly centrifuged. For oligo $(dT)_{18}$-primed cDNA synthesis, the samples first had to be incubated at 42°C for 60 min and subsequently the reaction was terminated by heating at 70°C for 5 min.

To enable comparison of the gene expression, equivalent concentrations of the same tissues were used. Quantstudio Applied Biosystems (Thermo Fisher Scientific, USA) and GoTaq® qPCR Master Mix (Promega, USA) were used for quantitative real-time PCR analysis, which was performed according to the conditions in Table 17.

Table 17: Cycling conditions for qPCR.

Temperature	Time	Repeats
95°C	10 min	1
95°C	15 sec	40
60°C	1 min	
95°C	15 sec	1
60°C	1 min	
95°C	1 min	
melting curve program		

In the last step of the qPCR program, a melting curve was generated from 60°C up to 95°C for 1 min to confirm the specificity of the primers. Furthermore, standard curves were calculated with the following equation for each individual gene to correct for PCR efficiency:

E = 10 (-1/slope of the standard curve).

All primer sequences utilized are listed in Table 7.

The most stable reference genes were determined using NormFinder (https://moma.dk/normfinder-software, Denmark) and used as housekeeping gene, that were required to normalize gene expression levels. For heart, iBAT and liver cyclophilin (*Cyclo*) was used as housekeeping gene and for gWAT, iWAT, lung, muscle gastrocnemius, muscle soleus and pituitary hypoxanthine guanine phosphoribosyl transferase (*Hprt*) was used.

The determination of the cycle threshold (Ct) is essential for qPCR measurement. This value is the cycle number at which the fluorescence signal of a PCR product crosses a certain threshold. To obtain quantitative information, the threshold is set in the exponential phase of the amplification curve. To transform the Ct values into quantities (i.e. gene expression levels), first the difference in Ct values between the gene of interest and the housekeeping gene, termed delta Ct (ΔCt) has to be calculated and in a second step gene expression was adjusted to the primer efficiency (E) by using the equation $E^{-\Delta Ct}$.

To compare the different genotypes and treatment conditions used in this thesis, the gene expression level values were normalized. This was accomplished by dividing the mean value of the corresponding control group from the individual gene expression level value.

2.2.3.6 Total T4 and T3 ELISA for Mouse Serum Analysis

Serum levels of total T3 (tT3; i.e. protein-bound and free T3) and total T4 (tT4; i.e. protein-bound and free T4) were determined by using commercial ELISA kits according to the instructions for use provided by the manufacturer.

In the tT3 competitive ELISA, the unknown amount of T3 in a sample competes with a defined amount of HRP-labeled T3 for the antibody-binding sites in the microtiter strip wells. After incubation, unbound antigen was removed by washing and the formed immune complexes were visualized with the substrate 3,3',5,5'-Tetramethylbenzidine (TMB). The color reaction was stopped with sulfuric acid solution and absorption at 450 nm was measured with the SPECTROstar Nano Microplate Reader. The color intensity inversely correlates with the tT3 concentration in the sample.

Serum tT4 concentration was also determined by competitive ELISA, following a very similar principle as in tT3 ELISA described above. In brief, a serum sample was mixed with labeled T4, containing 8-anilino-1-napthalene sulfonic acid (ANS) to inhibit binding of T4 to proteins in serum, and T4 antibody. A certain amount of the labeled T4 competes with the unlabeled T4 in the sample for the binding sites on the specific T4 antibody. Unbound antigen was then removed by washing. After addition of TMB solution, a color reaction started. This was terminated by adding 1 N HCl. Finally, the color intensity, which is inversely proportional to the concentration of tT4 in the serum sample, was measured with a microplate reader (SPECTROstar Nano Microplate Reader) at 450 nm.

2.2.3.7 Western Blot Analysis

For protein isolation, the snap-frozen tissues were homogenized in RIPA buffer and freshly added protease inhibitors. Protein concentrations were measured by a bicinchoninic acid assay (BCA, Sigma, Germany). Therefore, 30-50 µg protein were separated on a 12% SDS polyacrylamide gel (Bio-Rad Laboratories, USA) and finally transferred to a polyvinylidene fluoride membrane (PVDF, Merck Millipore, USA). Thereafter the membranes were blocked for 1 hour in 5 % BSA or 5 % non-fat dry milk (in 1× TBS-T) and incubated with primary antibodies for HCN2 or HCN4 (Table 8(a)) overnight at 4°C.

After washing 4×10 min in TBS-T the blots were incubated for 1 hour at RT with the corresponding peroxidase conjugated secondary antibody (Table 8(b)). Then the blots were washed again for 4×10 min in TBS-T. The antigens were visualized using a clarity western ECL substrate. Afterwards, the blots were stripped with Restore PLUS Western Blot Stripping Buffer (Thermo Fisher Scientific, USA) for 15 min. The band intensity was quantified with Image Lab™ software (Bio-Rad Laboratories, USA). Protein expression was normalized to total protein load.

2.2.3.8 DNA Methylation by Bisulfite Pyrosequencing

Bisulfite pyrosequencing is a method commonly used for quantitative analysis of DNA methylation.

First, genomic DNA was extracted from snap-frozen heart tissue using the QIAampR Fast DNA Tissue Kit (QIAGEN, Germany) and subsequently quantified using the Quantus™ Fluorometer (Promega, USA). For this purpose, the DNA is mixed with a fluorescent dye that

binds to double-stranded DNA (dsDNA) and shows fluorescence when excited with light of a specific wavelength.

The DNA concentration in the sample correlates with the fluorescence. First, 200 µL QuantiFluor® ONE dsDNA Dye was dispensed into 0.5 mL PCR tubes and then 1 µL of QuantiFluor® ONE Lambda DNA standard (equivalent to 400 ng) or 1 µL 1xTE buffer for the blank or 1 µL sample was added. Afterwards the mix was vortexed thoroughly and incubated for 5 min at RT, protected from light. Finally the dsDNA concentration was determined via the ONE DNA protocol on the fluorometer.

Following DNA quantification, genomic DNA (1,650 – 2,000 ng in a volume of 20 µL) was treated with sodium bisulfite using the EpiTect Fast DNA Bisulfite Kit (QIAGEN, Germany) according to the manufacturer's instructions. Bisulfite mediates deamination of the DNA base cytosine to the RNA base uracil. Whereas 5'-methylcytosine bases are not converted by sodium bisulfite. For the conversion, the protocol for highly concentrated samples was used. First, DNA was diluted to 2 µg in 20 µL with DEPC-treated water. After adding the bisulfite solution and DNA protection buffer, the reaction mixture was mixed until the buffer turned from green to blue, indicating the correct pH for the reaction. The bisulfite reaction was performed in a thermal cycler using the program listed in Table 18.

Table 18: Bisulfite thermal cycling program.

Step	Time	Temperature
Denaturation	5 min	95°C
Incubation	30 min	60°C
Denaturation	5 min	95°C
Incubation	20 min	60°C
Hold	∞	4°C

After incubation, the samples could be stored overnight at 4°C. Subsequently, bisulfite converted DNA was purified according to the manufacturer's instructions.

To dry the columns after the final washing step, additional centrifugation was performed using new collection tubes. Subsequently, to ensure evaporation of residual liquid, the columns were dried by incubation at 60°C for 5 min in a heating block. Finally, the bisulfite-converted DNA was eluted from the column by adding 40 µL of elution buffer and the purified DNA was stored at -20°C.

PCR was then performed using the PyroMark PCR Kit (QIAGEN, Germany), which enables amplification of DNA for pyrosequencing analysis. PCR and sequencing primers for *Hcn2*

and *Hcn4* genes were generated with the PyroMark Assay Design Software 2.0 (QIAGEN, Germany).

For bisulfite pyrosequencing analysis, one of the PCR primers has to be biotinylated at the 5' end, in this case the reverse primer. The bisulfite PCR reaction mix was pipetted as listed in the Table 19.

Table 19: Reaction mix for bisulfite PCR with a total volume of 25 µL per reaction.

Component	Final concentration	Volume per reaction
PyroMark PCR Master Mix (2×) (contains HotStarTaq DNA Polymerase and PyroMark PCR Buffer (with 3 mM $MgCl_2$ and dNTPs))	1×	12.5 µL
CoralLoad® Concentrate (10×)	1×	2.5 µL
Fw primer (10 µM)	0.2 µM	0.5 µL
Rev primer (10 µM)	0.2 µM	0.5 µL
RNase-Free water	---	8.0 µL
Bisulfite-DNA	10-20 ng	1.0 µL

Then, the bisulfite-PCR was performed for the region of interest in *Hcn2* and *Hcn4* genes with the cycling protocol in Table 20. The primer annealing temperatures as well as the amplicon sizes are shown in Table 21.

Table 20: Cycling program for bisulfite PCR.

Step	Temperature	Time	Repeats
Activation	95°C	15 min	1
Denaturation	94°C	30 sec	35-45
Annealing	Primer-dependent	30 sec	
Elongation	72°C	30 sec	
Final elongation	72°C	10 min	1
Hold	4°C	∞	

Pyrosequencing was performed on a PyroMark Q48 Autoprep (QIAGEN, Germany). To program the sequencing assay, the associated software (PyroMark Q48 Autoprep software) with "CpG Assay" mode was used.

Table 21: Annealing temperature, amplicon size and template strand of primer used in this thesis.

Name	Template strand of the primer (5' → 3')		Annealing Temperature	Amplicon size
Hcn2_79192273-7919231 lower strand_ Intron 4, chr10	Standard:	GTT TAT GTT TGG GTG AG	44.9°C	170 bp
	Fw:	TGG GTG GTA GTA TTA GTT TAT GTT TG	52.9°C	260 bp
	Rev:	/5Biosg/CCC TTA CTC TCT ACA ATA AAT CTC AAT	52.4°C	270 bp
Hcn4_58672018-58672051 upper strand_ Exon 1, chr9	Standard:	GGT TAA TAA ATT TTT TTT AAG GAT G	45.9°C	250 bp
	Fw:	GGT GTT ATG TTG TAA TTT GGG GTT AAT A	53.9°C	280 bp
	Rev:	/5Biosg/ACC CTA CTA ACT TAA CCC TCT	52.0°C	210 bp

Prior to pyrosequencing, all sequencing reagents were brought to RT. Primers used for sequencing were diluted to 4 µM with PyroMark Annealing Buffer and the PyroMark Q48 Autoprep was prepared as per the instructions of the instrument. The PyroMark Q48 Disc was loaded with 3 µL of bead mix (PyroMark Q48 Magnetic Beads), i.e. streptavidin-coated beads that bind later to the biotin-labeled PCR strand, and with 10 µL of biotinylated PCR product for the pyrosequencing reaction. Finally, the disc was correctly inserted into the PyroMark Q48 Autoprep and pyrosequencing was started.

If manual primer loading was selected, 2 µL of sequencing primer were added after PCR product purification. The final concentration of the sequencing primer was 800 nM in 10 µL reaction mix.

After each pyrosequencing run, the cartridges of the instrument were cleaned with high purity water and lint-free cloths according to the cleaning program.

Finally, to calculate the percentage of DNA methylation, the amount of thymine and cytosine at the target CpG position was measured and then the C:T ratio was calculated (C represents the proportion of methylated and T the proportion of unmethylated cytosines). The results were analyzed using the PyroMark Q48 Autoprep Software and Microsoft Excel.

Quality was evaluated by a standard curve with 0%, 25%, 50%, 75%, and 100% methylated DNA and by testing for possible primer self-annealing.

This experiment was performed in collaboration with Cathleen Geißler, member of Prof. Dr. Henriette Kirchner's research group at CBBM, Luebeck.

2.2.3.9 Trace Element Measurements

Total concentrations of the trace elements copper and selenium in serum and liver homogenate samples were determined by total reflection X-ray fluorescence (TXRF) spectroscopy using a benchtop TXRF analyzer (S4 T-STAR, Bruker Nano GmbH, Berlin, Germany) as described by Hughes et al. (2015).

Briefly, samples were diluted with a gallium standard (1,000 µg/L), applied to a polished quartz glass slide, and dried overnight. Seronorm serum standard (Sero AS, Billingstad, Norway) served as control in each analytical run.

This experiment was performed by a collaborator (Prof. Dr. Lutz Schomburg, Charité Berlin, Germany) for this thesis.

2.2.4 Statistical Analysis

GraphPad Prism 7 software (GraphPad Software Inc., San Diego, CA, USA) was used for statistical analysis. Data were analyzed using 2-way ANOVA with post-hoc Holm-Sidak test for differences between gender and genotypes of the offspring to examine the effects of maternal T3 treatment during different periods of pregnancy. Males and females were tested separately. All values are represented as mean ± SEM. Statistical significance was defined as $p < 0.05$ (*), $p < 0.01$ (**), $p < 0.0001$ (***) and $p < 0.0001$ (****).

3. RESULTS

To dissect the influence of maternal thyroid hormone (TH) at different periods during pregnancy on adult male and female offspring, mice heterozygous for the dominant negative R384C mutation in TRα1 (TRα1+/m mice) were used in combination with maternal pharmacological TH treatments to characterize the temporal role of prenatal TRα1 signaling. Taking advantage of the fact that the TRα1R384C can be reactivated by elevating T3 (3,3',5-triiodothyronine) levels *in vivo* (Tinnikov et al. 2002; Wallis et al. 2008), an experimental paradigm was established in which TRα1 signaling was selectively restored in the TRα1+/m embryo during the first or second half of pregnancy. They were compared with wildtype littermates (TRα1+/+ mice) exposed to high levels of T3 during the same periods and with untreated controls. As the respective TRα1+/+ littermates were exposed to elevated TH during the same periods, the full spectrum of impaired or enhanced TH signaling in the developing embryos was assessed.

3.1 Effect of Maternal Hypothyroidism on Offspring Development and Phenotype

3.1.1 Maternal T3 Treatment during the First or Second Half of Pregnancy Has No Effect on Water and Food Intake in Dams

First, it was investigated whether T3 treatment influences water and food intake of dams during pregnancy. For this purpose, water (+T3) and food intake were measured every day from conception until birth. No significant effect of T3 treatment on water and food intake of dams could be detected either in the first or in the second half of pregnancy (Figure 6A+B).

3.1.2 Maternal T3 Treatment Has No Effect on Body Weight and Body Length in the Offspring

To determine whether maternal T3 treatment during the first or second half of pregnancy had an effect on the offspring, postnatal weight development of the offspring was measured once a week after weaning. No significant changes were detected in either male or female offspring after maternal T3 treatment (Figure 7); however, females were lighter than males

and body weight was lower in TRα1+/m offspring as expected (Tinnikov et al. 2002).

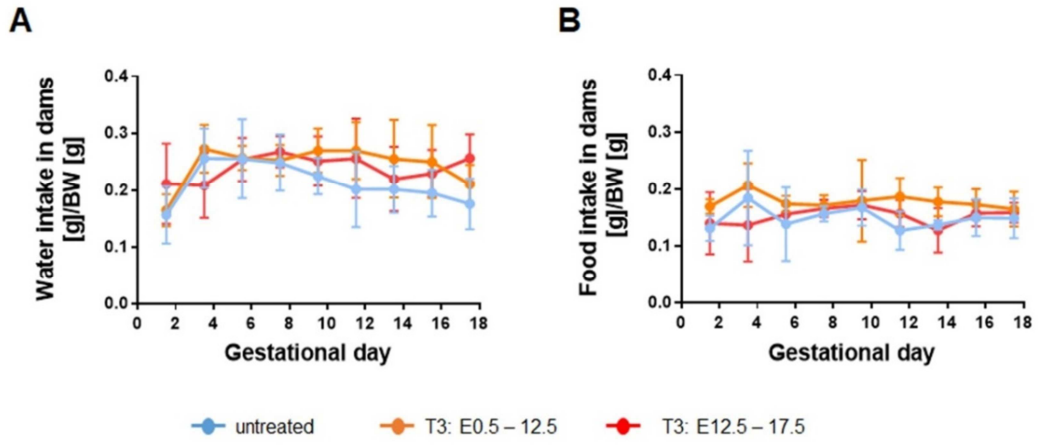

Figure 6: Water and food intake in dams. The dams were treated with H_2O from conception until birth (blue) or with T3 in the drinking water during the first (orange) or second half of pregnancy (red). **A)** Water and **B)** food intake in the respective dams was measured every two days and normalized to body weight. All values are shown as mean ± SEM and were analyzed with two-way ANOVA with Holm-Sidak's multiple comparisons test; n=6 for each group. The figures were adapted from "Pedaran et al. 2021 Thyroid".

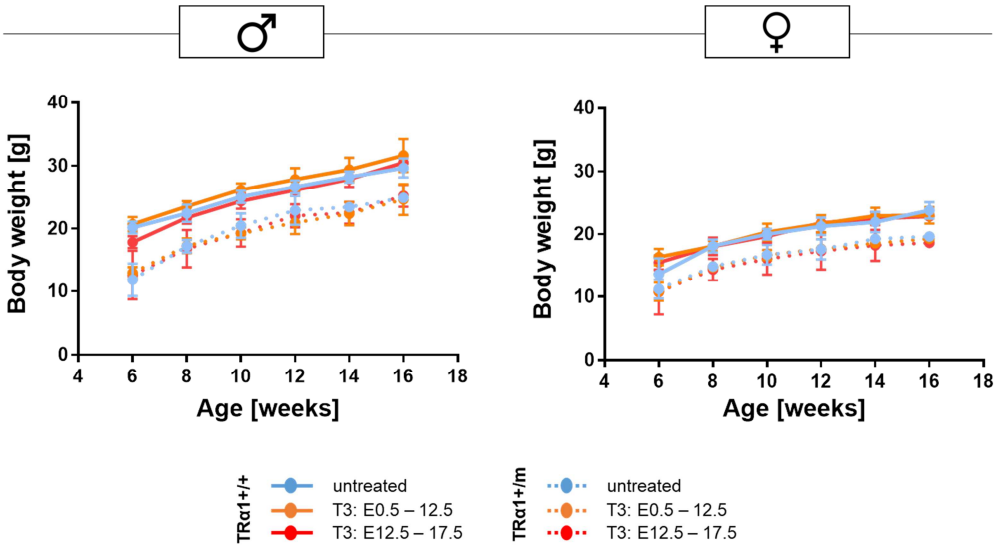

Figure 7: Postnatal body weight development of male and female offspring. Offspring are shown either in blue (dams were treated with H_2O from conception until birth), orange (dams were treated in the first half of pregnancy with T3 in drinking water), or red (dams were treated in the second half of pregnancy in drinking water). Body weights of male and female offspring of both genotypes were determined once per week. All values are shown as mean ± SEM and were analyzed with two-way ANOVA with Holm-Sidak's multiple comparisons test; n=6 for each group. The figures were adapted from "Pedaran et al. 2021 Thyroid".

Total body length at 16 weeks of age reflected this pattern, with no effect of maternal T3 treatment in male and female offspring of both genotypes (Figure 8A). Examination of

hepatic *Igf1* (Insulin-Like growth factor 1) and *Gh* (Growth hormone) gene expression in the pituitary gland of the offspring revealed no significant alteration that could affect body length in these offspring (Figure 8B-C).

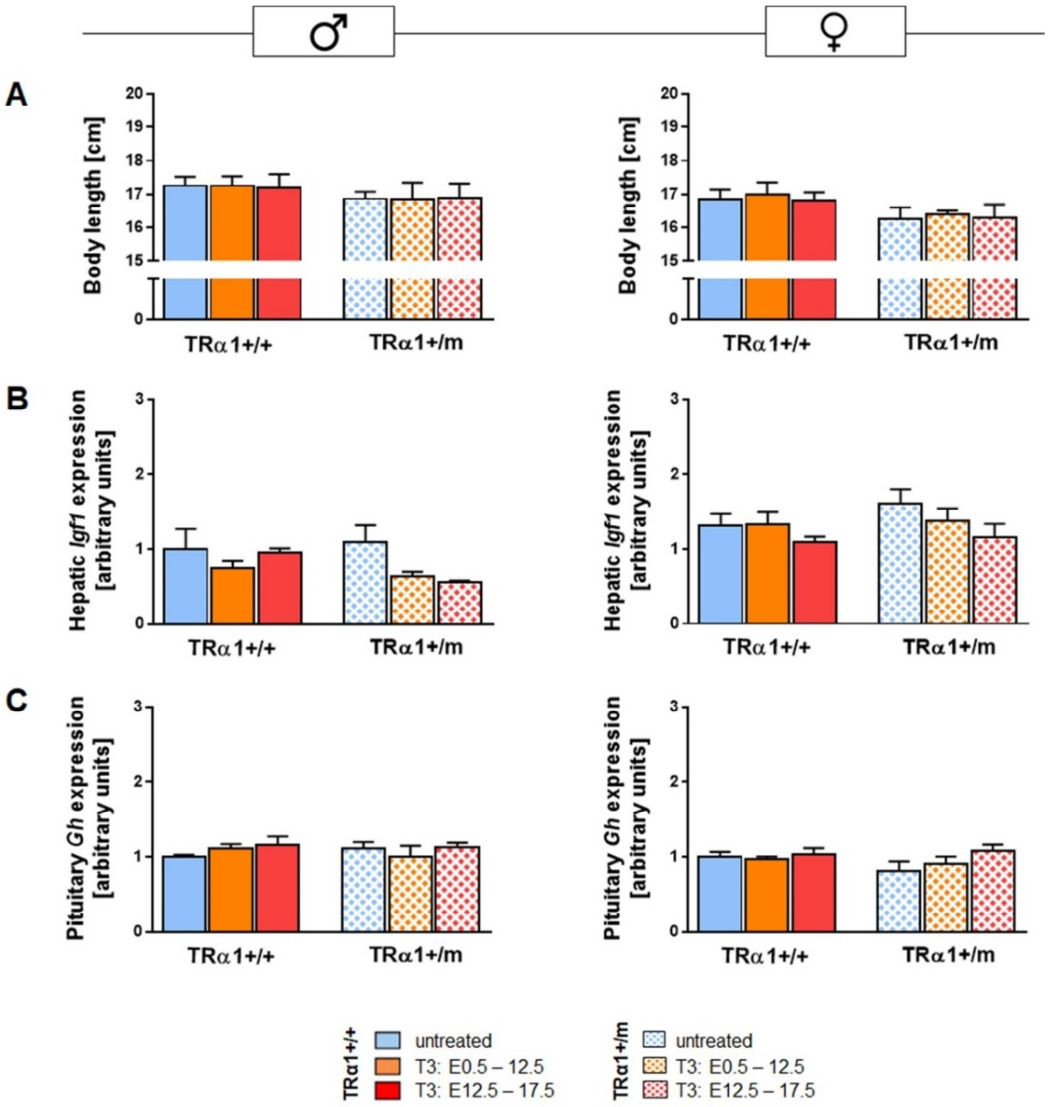

Figure 8: Total body length at 16 weeks of age and expression of Igf1 and Gh genes in male and female offspring. **A)** Analysis of body length of male and female offspring of both genotypes whose dams were treated with T3 in drinking water in either the first half (orange) or in the second half (red) of pregnancy compared to untreated offspring (blue). In addition, the relative gene expression of **B)** *Igf1* (Insulin-Like growth factor 1) in the liver and **C)** *Gh* (Growth hormone) in the pituitary gland of the offspring was measured by qPCR. All values are shown as mean ± SEM and were analyzed with two-way ANOVA with Holm-Sidak's multiple comparisons test; n=6 for each group.

Taken together, these data demonstrate that maternal T3 treatment during the first or second half of pregnancy has no effect on body weight and body length of the offspring in both genders, suggesting that T3 administration during pregnancy at the dose used in this thesis has no severe catabolic effects on fetal development.

3.2 Effect of Maternal Hypothyroidism on Cardiovascular Development in the Offspring

3.2.1 T3 Treatment during Pregnancy Causes Gender and Genotype Specific Cardiovascular Alterations in the Offspring

It is well established long time ago that maternal TH affects the cardiovascular set point (Harder et al. 2018; Lompre, Nadal-Ginard, and Mahdavi 1984; Mai et al. 2004; Mittag et al. 2013). Therefore, a detailed cardiovascular analysis was performed in adult offspring to find out whether maternal T3 treatment at different periods in pregnancy has a different effect on the cardiovascular system in postnatal life.

To identify alterations in heart rate and blood pressure, adult offspring were tested while conscious using a non-invasive tail-cuff system with a temperature-controlled platform (100°F). During the experiment, the blood pressure and heart rate of the offspring were measured on three consecutive days and 15 times in one session for 30 seconds.

Blood pressure (systolic and diastolic) was slightly elevated but not significantly affected in male offspring, while there was a significant increase in mean arterial pressure (MAP) in wildtype males treated in the second half of pregnancy. Whereas, a decrease in systolic and diastolic pressure was observed in female wildtype offspring, which was significant in female TRα1+/m offspring treated in the second half of pregnancy (Figure 9A-B). MAP is significantly decreased after T3 treatment in the second half of pregnancy in both genotypes of female offspring (Figure 9C).

It was also observed that T3 treatment in the second half of pregnancy resulted in a significant increase of heart rate in male offspring of wildtype and TRα1+/m mice, while no effect was observed in female wildtype and it was even reversed in female TRα1+/m mice (Figure 9D). As expected, heart rate was generally lower in TRα1+/m offspring than in wildtypes, consistent with TRα1 acutely regulating heart rate (Mittag et al. 2012; Mittag, Behrends, et al. 2010; Mittag, Davis, et al. 2010).

After sacrificing the offspring, the hearts were weighed and significant hypertrophy was found in male and female wildtype offspring (Figure 9E), when dams were treated with T3 in the second half of pregnancy. Heart weights were lower in TRα1+/m as expected but were further decreased by maternal T3 treatment selectively in males.

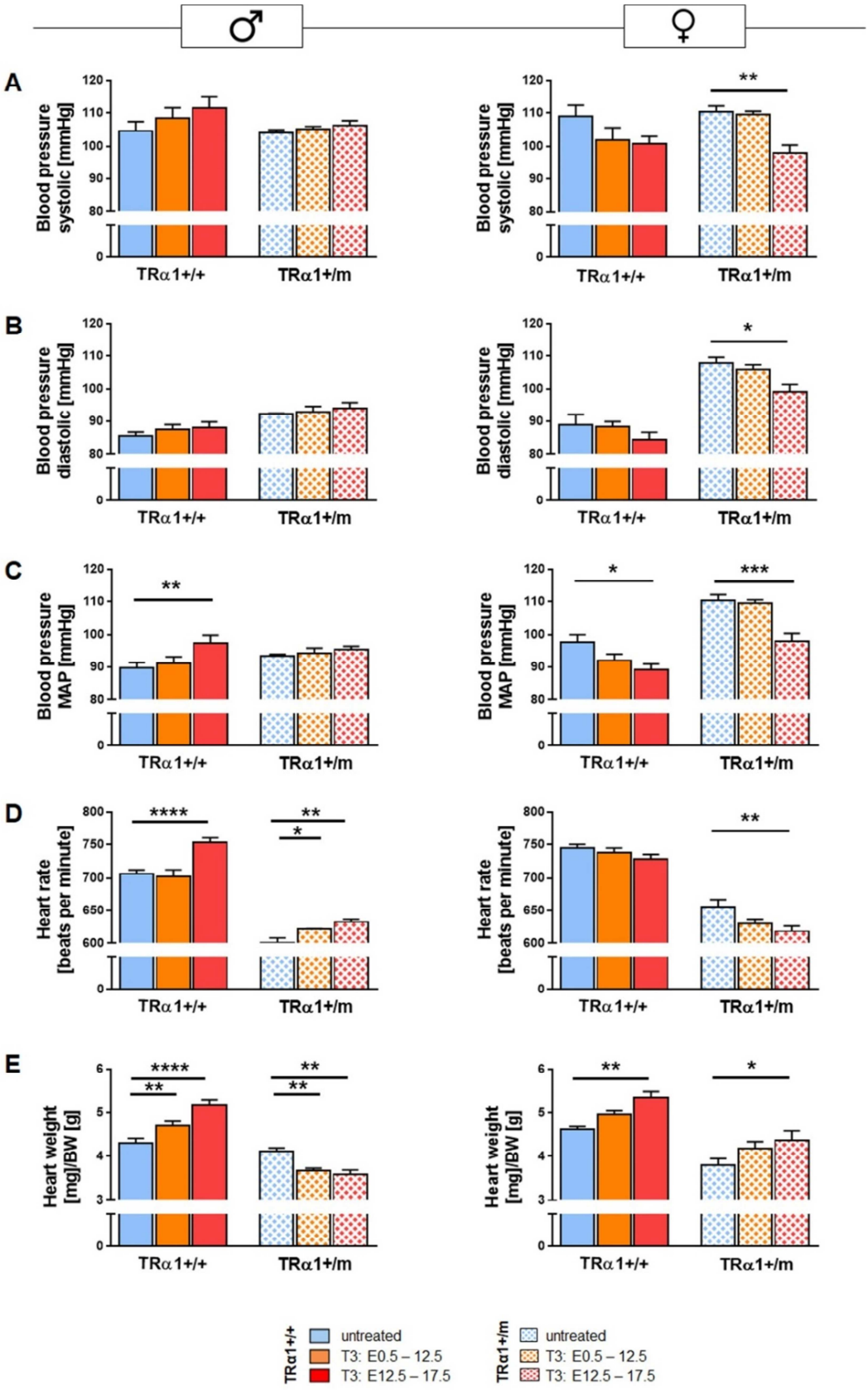

Figure 9: The effect of maternal T3 treatment on blood pressure, heart rate, and heart weight in adult offspring. The effect was measured in adult offspring whose dams were treated with T3 in either the first half (orange) or in the second half of pregnancy (red) and compared with the control group (blue). Heart rate and blood pressure were measured in restrained but conscious mice using a non-invasive tail cuff system. The following parameters were analyzed in adult offspring of both

genders: Blood pressure **A)** systolic, **B)** diastolic, **C)** mean arterial pressure (MAP), **D)** heart rate (beats per minute), and **E)** heart weight (mg) relative to body weight (g). All values are shown as mean ± SEM of all animals and analyzed with two-way ANOVA with Holm-Sidak's multiple comparisons test. $p<0.05$ (*), $p<0.01$ (**), $p<0.001$ (***) and $p<0.0001$ (****); n=6 for each group. The figures were adapted from "Pedaran et al. 2021 Thyroid".

Mittag et al. (2013) found that pulmonary angiotensin-converting enzyme (*Ace*) was reduced and hepatic angiotensinogen (*Agt*) was increased in male TRα1+/m mice compared to wildtype, but blood pressure remained unaltered in both groups. They showed that after T3 treatment, systolic, diastolic, and mean arterial pressure (MAP) were increased by approximately 25% and, consequently, mRNA levels of *Ace* and *Agt* were also increased.

To investigate whether the slight increase in systolic and diastolic values and MAP after T3 treatment in the second half of pregnancy was caused by an increase in pulmonary *Ace* or hepatic *Agt*, mRNA gene expression of these two genes was measured. There was a significant increase in *Ace* mRNA expression in TRα1+/+ mice after T3 treatment in the second half of pregnancy and a significant increase in *Agt* expression in TRα1+/m male offspring, while there were no significant differences in female offspring (Figure 10A-B).

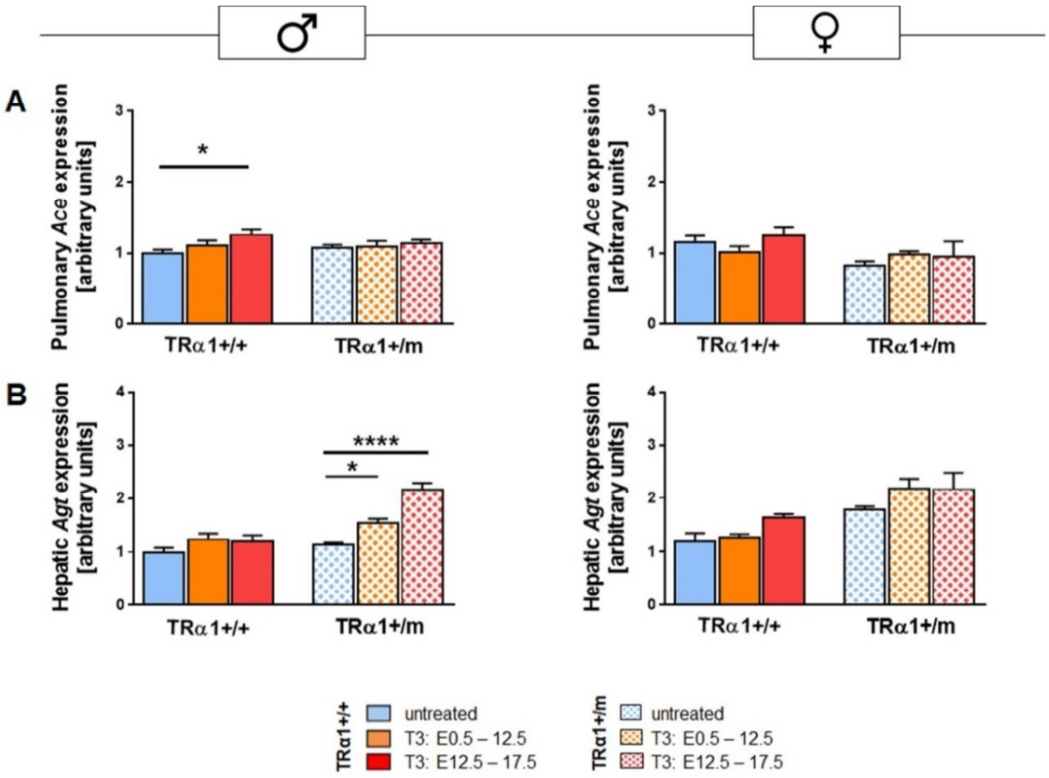

Figure 10: Analysis of mRNA genes responsible for blood pressure. **A)** Pulmonary angiotensin-converting enzyme (*Ace*) and **B)** hepatic angiotensinogen (*Agt*) levels in male and female wildtype offspring and offspring heterozygous for a mutant TRα1 (TRα1+/m). The dams of these offspring were treated either in the first half (orange) or in the second half of pregnancy (red) and compared with the control group (blue). All values are shown as mean ± SEM of all animals and analyzed with two-way

ANOVA with Holm-Sidak's multiple comparisons test. $p<0.05$ (*) and $p<0.0001$ (****); n=6 for each group.

3.2.2 Maternal T3 Treatment during the Second Half of Pregnancy Leads to a Significant Alteration in Gene Expression Level in the Heart of Adult Offspring

To better elucidate cardiac gene expression after T3 treatment in the first or second half of pregnancy and to compare with the control group, several essential cardiac genes were measured by qPCR, i.e. sarcoplasmic/endoplasmic reticulum calcium ATPase 2 (*Serca2*), cardiac muscle alpha myosin heavy chain (*α-Mhc*), and cardiac muscle beta myosin heavy chain (*β-Mhc*) (Danzi and Klein 2012, 2020; Mittag, Davis, et al. 2010) and hyperpolarization-activated cyclic nucleotide gated channel 2 and 4 (*Hcn2* and *Hcn4*) (Chen et al. 2018; Difrancesco 2010).

It was found that T3 treatment in pregnancy resulted in significant upregulation of *α-Mhc*, *β-Mhc*, *Serca2*, *Hcn2* and *Hcn4,* particularly in male offspring of both genotypes (Figure 11A-E), with the exception of *Hcn2*, which was affected by T3 only in the second half of pregnancy. Remarkably, female offspring were less affected; mainly TRα1+/m mice whose dams were treated with T3 in the second half of pregnancy were affected.

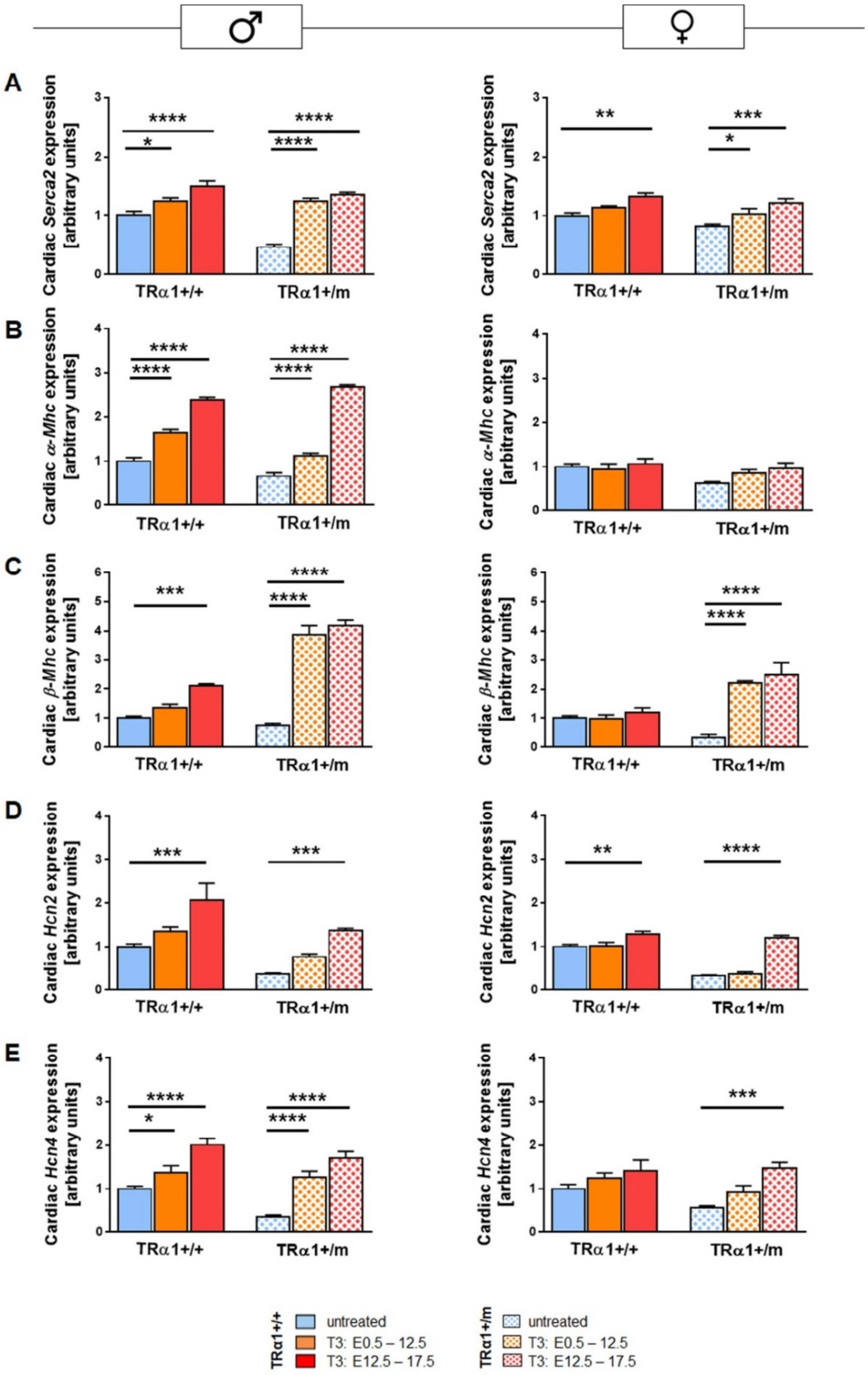

Figure 11: Analysis of cardiac gene expression using qPCR in maternal T3-treated wildtype and TRα1 mutant offspring of both genders. Dams were treated with T3 either in the first half (orange) or in the second half of pregnancy (red) for comparison with the control group (blue). The figure displays the expression results for the following cardiac genes in the adult male and female offspring: **A)** *Serca2* (sarcoplasmic/endoplasmic reticulum calcium ATPase 2, **B)** *α-Mhc* (myosin heavy chain 6 cardiac muscle alpha), **C)** *β-Mhc* (myosin heavy chain 7 cardiac muscle beta), **D)** pacemaker *Hcn2*

(hyperpolarization-activated cyclic nucleotide-gated potassium channel 2) and **E)** pacemaker *Hcn4* (hyperpolarization-activated cyclic nucleotide-gated potassium channel 4). All values are shown as mean ± SEM of all animals and analyzed with two-way ANOVA with Holm-Sidak's multiple comparisons test. p<0.05 (*), p<0.01 (**), p<0.001 (***) and p<0.0001 (****); n=6 for each group. The figures were adapted from "Pedaran et al. 2021 Thyroid".

Since the pacemaker genes (*Hcn2* and *Hcn4*) are very important for cardiac function (Rivolta et al. 2020), the protein levels of these genes were measured to determine whether T3 treatment in the second half of pregnancy also increases the protein levels.

It was found that the protein levels of both genes were significantly increased in the male offspring after T3 treatment in the second half of pregnancy (Figure 12A-B).

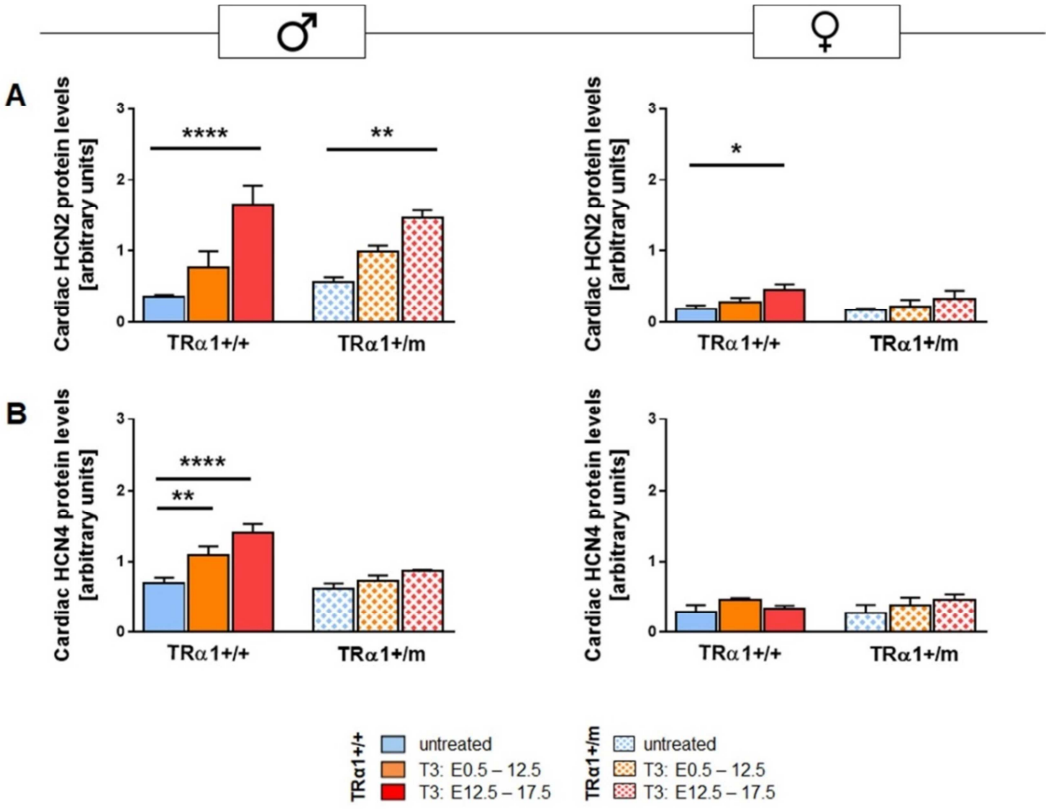

Figure 12: HCN2 and HCN4 protein levels in heart. **A)** HCN2 protein level in heart of male and female offspring of control dams (blue) or dams either treated with T3 in the first (orange) or second half of pregnancy (red). **B)** HCN4 protein levels in heart of these experimental mice. All values are shown as mean ± SEM and were analyzed with two-way ANOVA with Holm-Sidak's multiple comparisons test. p<0.05 (*), p<0.01 (**) and p<0.0001 (****); n=6 for each group. The figures were adapted from "Pedaran et al. 2021 Thyroid".

To obtain information on whether gene expression of *Hcn2* or *Hcn4* could be linked to the altered heart rate, a Pearson correlation analysis was performed for *Hcn2* and *Hcn4* gene expression with heart rate. Of note, there is a significant positive correlation between these 2

genes (*Hcn2* and *Hcn4*) and heart rate in male offspring, regardless of genotype (Figure 13A-B).

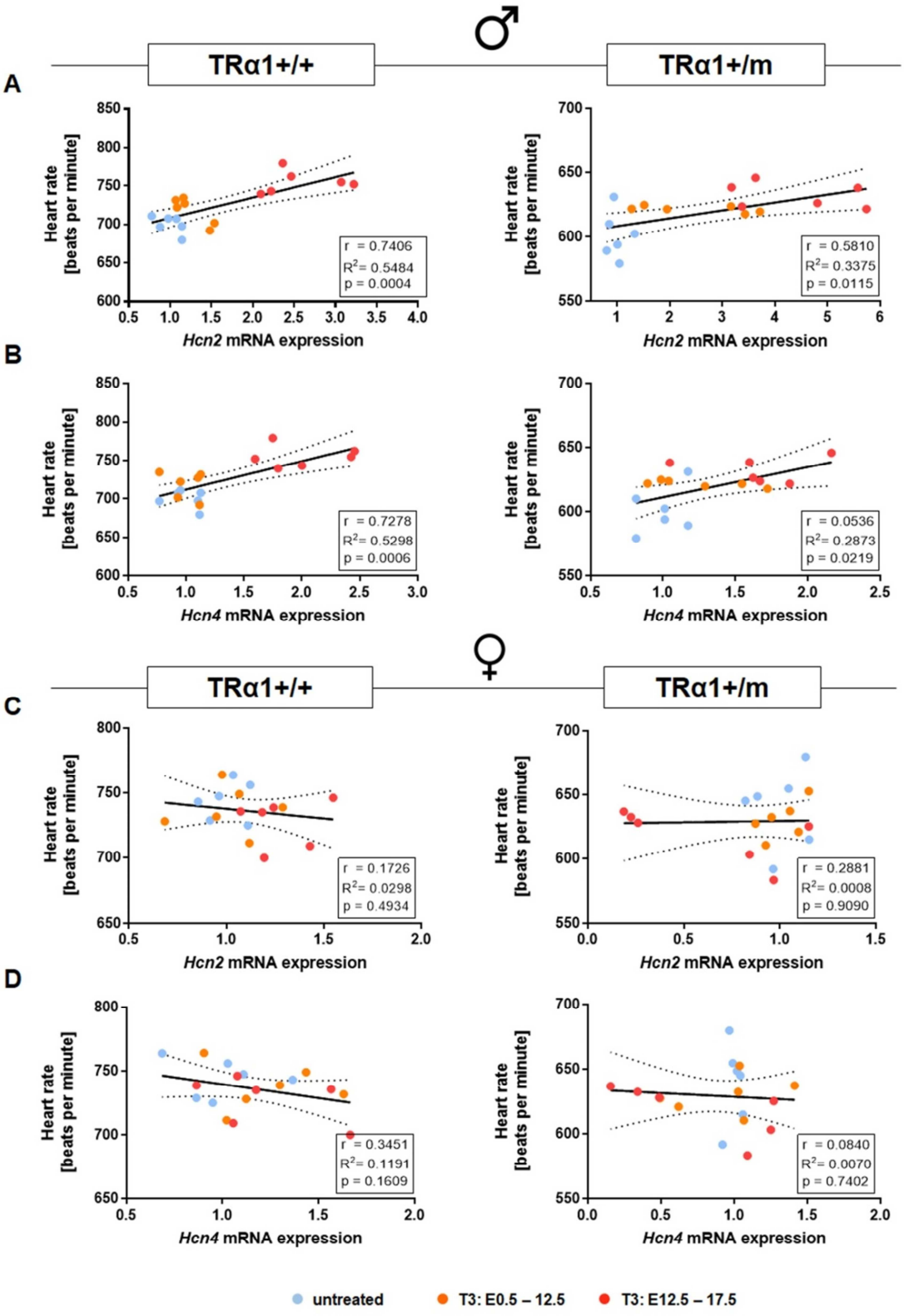

Figure 13: Correlation analysis of pacemaker gene expression with heart rate in male and female offspring. Control offspring were shown in blue dots and the offspring whose dams were treated with T3 in the first half of pregnancy in orange and in the second half in red dots. The figure shows the correlation analysis of *Hcn2* gene expression with heart rate in the offspring of both genotypes in **A)** male and **C)** female offspring and the same correlation analysis for *Hcn4* gene

expression with heart rate in **B)** male and **D)** female offspring. The respective raw P value is given in the figure (r: Pearson correlation coefficient; R^2: coefficient of determination; p: p-value; dashed lines indicate 95% confidence interval); n=6 for each group. The figures were adapted from "Pedaran et al. 2021 Thyroid".

3.2.3 Maternal T3 Treatment in the Second Half of Pregnancy Leads to a Decrease of DNA Methylation in *Hcn2* Gene and Increased DNA Methylation in *Hcn4* Gene

Given that pacemaker *Hcn2* and *Hcn4* expression was highly correlated with heart rate (Figure 13A-D), it was speculated that altered fetal programming by DNA methylation could underlie the persistently elevated gene expression.

Using the publicly available genome-wide methylation datasets GSE21415 (Liang et al. 2011) and ENCSR397YEG (He et al. 2020), the CpG sites in these genes that are actively methylated or demethylated during heart development were identified, expecting that they might be most sensitive to reprogramming by maternal TH. Subsequently, DNA methylation was measured. It was observed a similar effect of maternal TH on DNA methylation of *Hcn2* and *Hcn4*, especially since intronic regions are known to be of regulatory importance for the regulation of *Hcn* genes (Kuratomi et al. 2007). For *Hcn2* the most dynamic regulation was observed in intron 4, for *Hcn4* this was at the border in exon 1.

Since the most dynamic regulation for *Hcn2* was observed in intron 4, DNA methylation was measured in this part of the gene, i.e. on chromosome 10. A consistent decrease was found at 3 of 5 CpG sites (chr10:79,192,307; chr10:79,192,303 and chr10:79,192,274) in male offspring of both genotypes as a consequence of maternal T3 treatment in the second half of pregnancy (Figure 14A-C and Figure Supplement 1A-B). Within exon 1 of *Hcn4* on chromosome 9, 3 of the 4 CpG sites (chr9:58,672,034; chr9:58,672,042 and chr9:58,672,044) showed a significant increase in DNA methylation after T3 treatment in the second half of pregnancy (Figure 14D-F and Figure Supplement 1C). Moreover, the expression of *Hcn2* at the affected CpG sites correlated negatively and that of *Hcn4* positively with DNA methylation (Figure Supplement 2A), suggesting an altered chromatin state in these key regulatory regions.

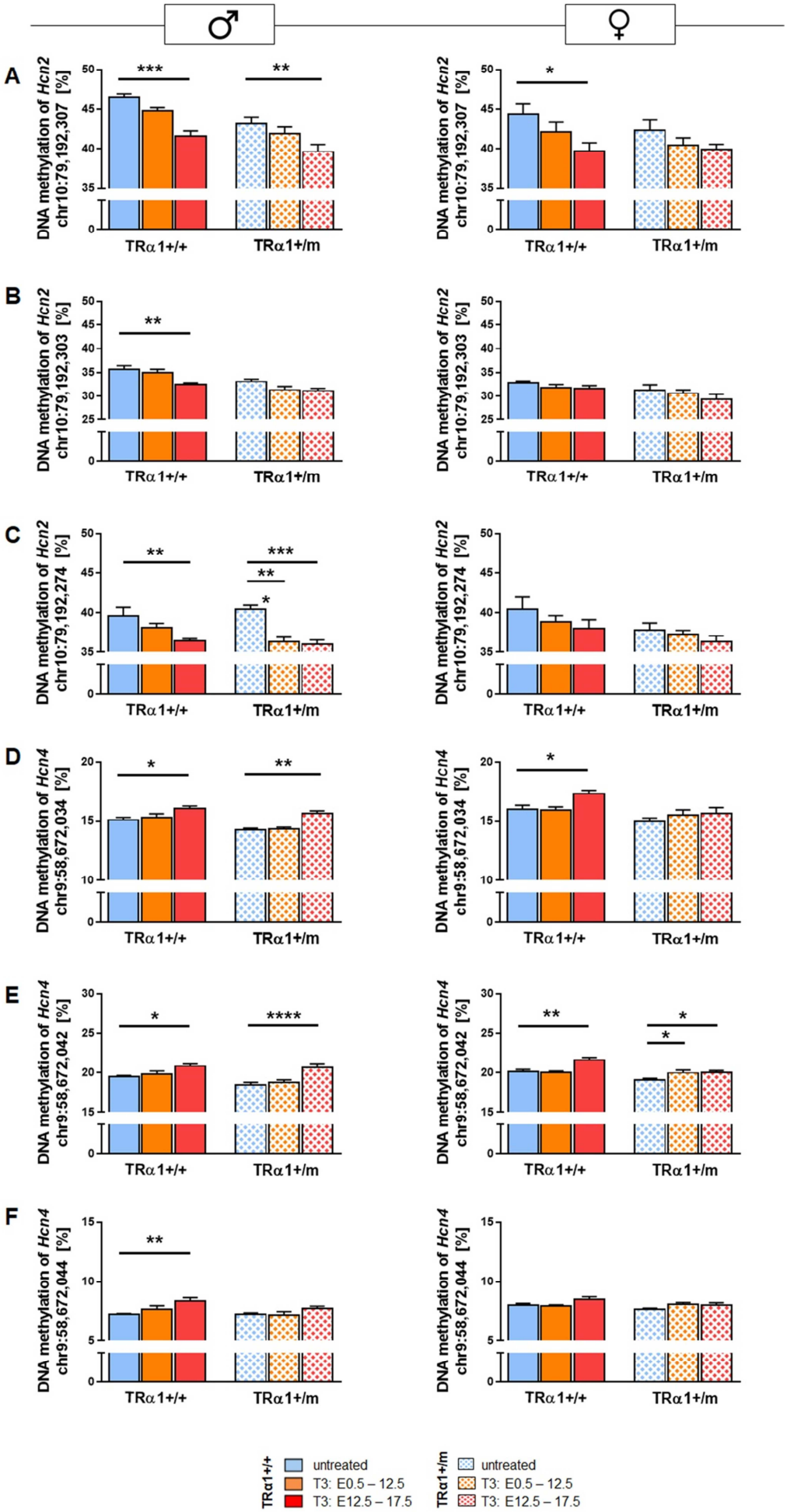
♂
♀
A
DNA methylation of Hcn2 chr10:79,192,307 [%]
B
DNA methylation of Hcn2 chr10:79,192,303 [%]
C
DNA methylation of Hcn2 chr10:79,192,274 [%]
D
DNA methylation of Hcn4 chr9:58,672,034 [%]
E
DNA methylation of Hcn4 chr9:58,672,042 [%]
F
DNA methylation of Hcn4 chr9:58,672,044 [%]
TRα1+/+
TRα1+/m
TRα1+/+ untreated
T3: E0.5 – 12.5
T3: E12.5 – 17.5
TRα1+/m untreated
T3: E0.5 – 12.5
T3: E12.5 – 17.5

Figure 14: Cytosine-methylation quantification by bisulfite-pyrosequencing. Genomic DNA was extracted from snap-frozen heart of adult male and female offspring, whose dams were treated either in the first half (orange) or in the second half of pregnancy (red) compared with the control group (blue). DNA methylation of *Hcn2* was measured at 5 CpG sites (3 CpG sites are shown) within the fourth intron: **A)** chr10:79,192,307, **B)** chr10: 79,192,303 and **C)** chr10,79,192,274. DNA methylation of *Hcn4* was analyzed at 4 CpG sites (3 CpG sites are shown) within exon 1: **D)** chr9:58,672,034, **E)** chr9: 58,672,042 and **F)** chr9: 58,672,044. All values are shown as mean ± SEM and were analyzed with two-way ANOVA with Holm-Sidak's multiple comparisons test. $p<0.05$ (*), $p<0.01$ (**) and $p<0.001$ (***); n=6 for each group. The figures were adapted from "Pedaran et al. 2021 Thyroid".

3.3 Effect of Maternal Hypothyroidism on Metabolism of the Offspring

It is well established that TH plays an important role in the maintenance of metabolic homeostasis (Benedetti et al. 2019; Huget-Penner and Feig 2020; Lucaccioni et al. 2021). An increase or decrease in maternal TH leads to various metabolic diseases in the offspring (Andersen et al. 2021; Tapia-Martínez et al. 2019).

Moreover, in 2002 it was found that the TRα1+/m mice display a 10-fold reduction in TRα ligand affinity, resulting in aporeceptor activity at physiological T3 concentrations, whereas elevated T3 concentration facilitates holoreceptor (Tinnikov et al. 2002). Suppressing TH signaling in TRα1+/m mice improves basal metabolic rate by increasing sympathetic outflow and these mice are resistant to obesity and thus have a lean phenotype (Sjögren et al. 2007). However, little is known about how maternal T3 treatment at different periods during pregnancy affects metabolic function in the offspring. This part of the thesis aimed to investigate the effects of maternal hypothyroidism on metabolic function and offspring development.

3.3.1 Maternal T3 Treatment during Pregnancy Decreases T3 Level in TRα1+/m Male Offspring

The Hypothalamus-Pituitary-Thyroid (HPT) axis is one of several hormone regulatory systems that lead from the hypothalamus to the pituitary gland and conclusively to peripheral target organs (Feldt-Rasmussen, Effraimidis, and Klose 2021). For a long time, it was well established that maternal thyroid disease can affect the setting of the HPT axis (Korevaar et al. 2016). To identify whether maternal T3 treatment in the first or second half of pregnancy differentially alters TH metabolism in the offspring, serum total T3 and T4 levels were determined in these mice.

It was found that maternal T3 treatment resulted in decreased T3 levels only in the adult TRα1+/m offspring (Figure 15A). However, neither serum total T4 (Figure 15B) nor pituitary mRNA expression of *Tshb* or *Dio2* were altered (Figure 15C+D), indicating that the HPT axis is largely unaffected by the treatment paradigm used in this thesis.

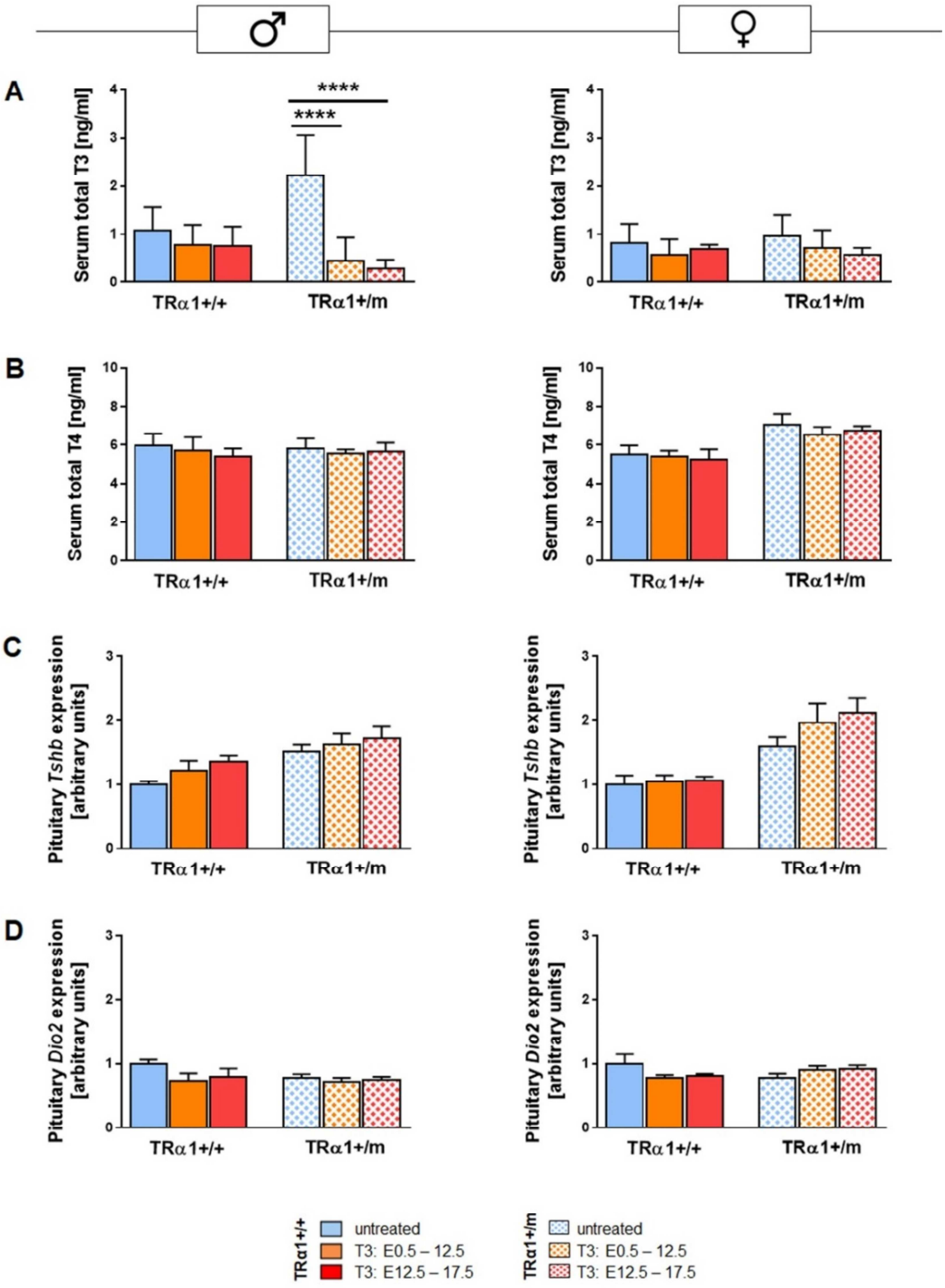

Figure 15: Measurement of T3 and T4 production and expression of Tshb and Dio2 after T3 treatment during pregnancy. **A)** Total T3 in serum of adult male and female offspring from control dams (blue) or from dams treated with T3 in either the first (orange) or the second half of pregnancy (red) and **B)** Total T4 in serum in these mice. Moreover, pituitary mRNA expression of **C)** thyroid

stimulating hormone subunit beta (*Tshb*) and **D)** deiodinase type II (*Dio2*) were analyzed in these adult offspring. All values are shown as mean ± SEM and were analyzed with two-way ANOVA with Holm-Sidak's multiple comparisons test. p<0.0001 (****); n=6 for each group. The figures were adapted from "Pedaran et al. 2021 Thyroid".

This result was supported by measurements of hepatic TH target genes: *Dio1* mRNA and DIO1 activity were higher in TRα1+/m offspring, as expected (Venero et al. 2005); however, alterations due to maternal treatment were not significant in either period (Figure 16A+B). Interestingly, maternal T3 reduced *Spot14* mRNA in female but not male offspring (Figure 16C), constituting a sexual dimorphism that is frequently observed in fetal programming.

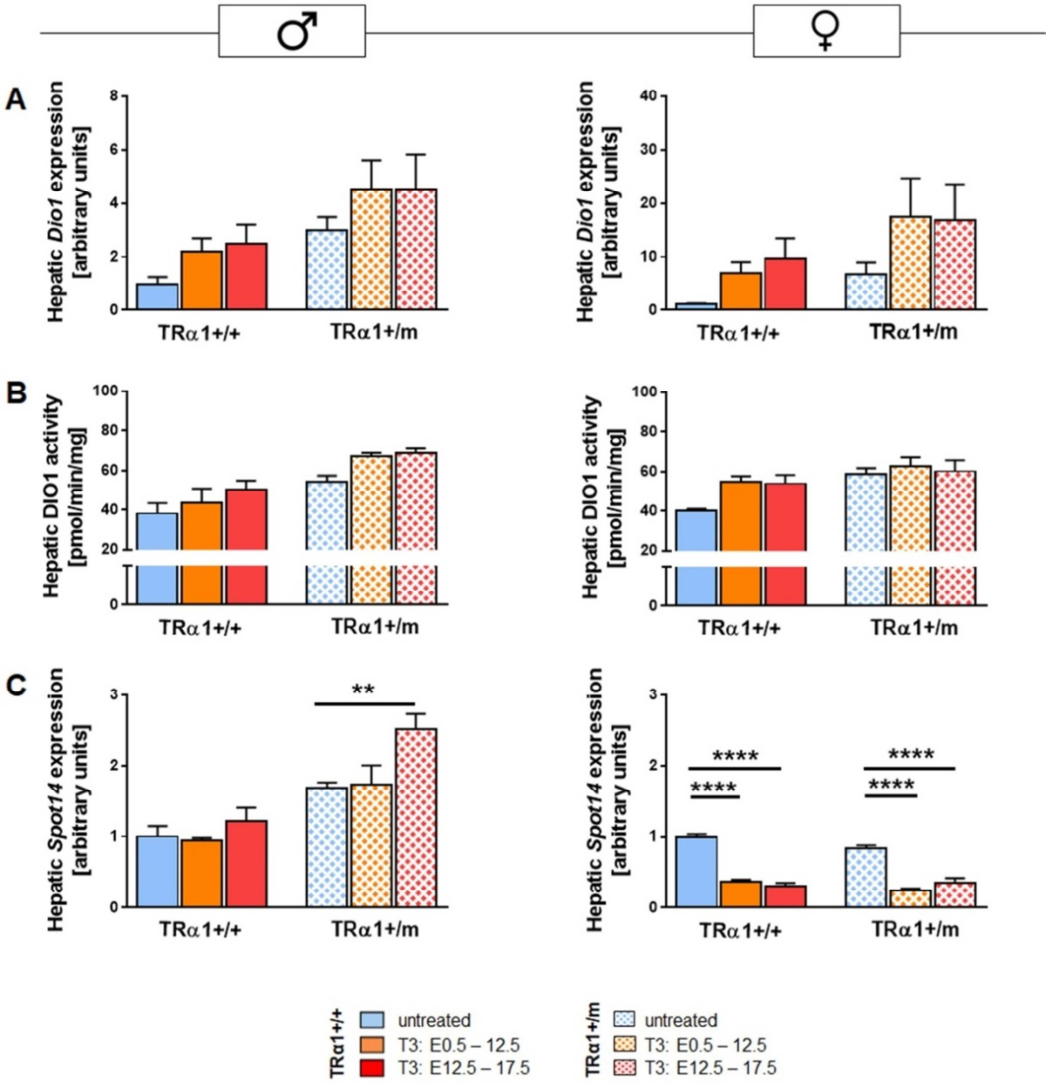

Figure 16: Analysis of hepatic TH target genes. **A)** mRNA expression of hepatic deiodinase type I (*Dio1*), **B)** hepatic DIO1 activity and **C)** hepatic expression of *Spot14* in male and female adult offspring from control dams (blue bars) or from dams treated with T3 in either the first (orange bars) or the second half of pregnancy (red bars). All values are shown as mean ± SEM and were analyzed with two-way ANOVA with Holm-Sidak's multiple comparisons test. p<0.01 (**) and p<0.0001 (****); n=6 for each group. The figures were adapted from "Pedaran et al. 2021 Thyroid".

3.3.2 Maternal T3 Treatment during Pregnancy Decreases Serum Selenium in the Offspring

Several trace elements are very crucial for normal thyroid hormone synthesis and metabolism, such as selenium (Se) and copper (Cu) (Köhrle 2015). It has been previously shown that low Se and Cu status is associated with adverse pregnancy outcomes such as miscarriages, cardiovascular disease, premature birth, low birth weight, glucose intolerance, and gestational diabetes (Perkins and Vanderlelie 2016).

Therefore, Se, Cu as well as GPx1 (glutathione peroxidase 1) levels were measured in the offspring. GPx1 is an intracellular antioxidant enzyme that enzymatically reduces hydrogen peroxide to water to protect cells from oxidative stress (Lubos, Loscalzo, and Handy 2011).

Hepatic Se, Cu and GPx1 levels were found to be unaltered in both T3 treatment conditions in both genotypes (Figure 17A-C), concurring with previous studies (Mittag, Behrends, et al. 2010). Remarkably, serum selenium levels were strongly reduced by maternal T3 treatment in males of both genotypes and in wildtype females (Figure 17D). Serum Cu levels, which are also regulated by TH (Mittag et al. 2012), were not altered in male offspring (Figure 17E).

Taken together, maternal T3 treatment in both halves of pregnancy did not significantly affect hepatic Se and Cu metabolism in the offspring, however seemed to have a permanent effect on serum Se levels, which was more pronounced in males.

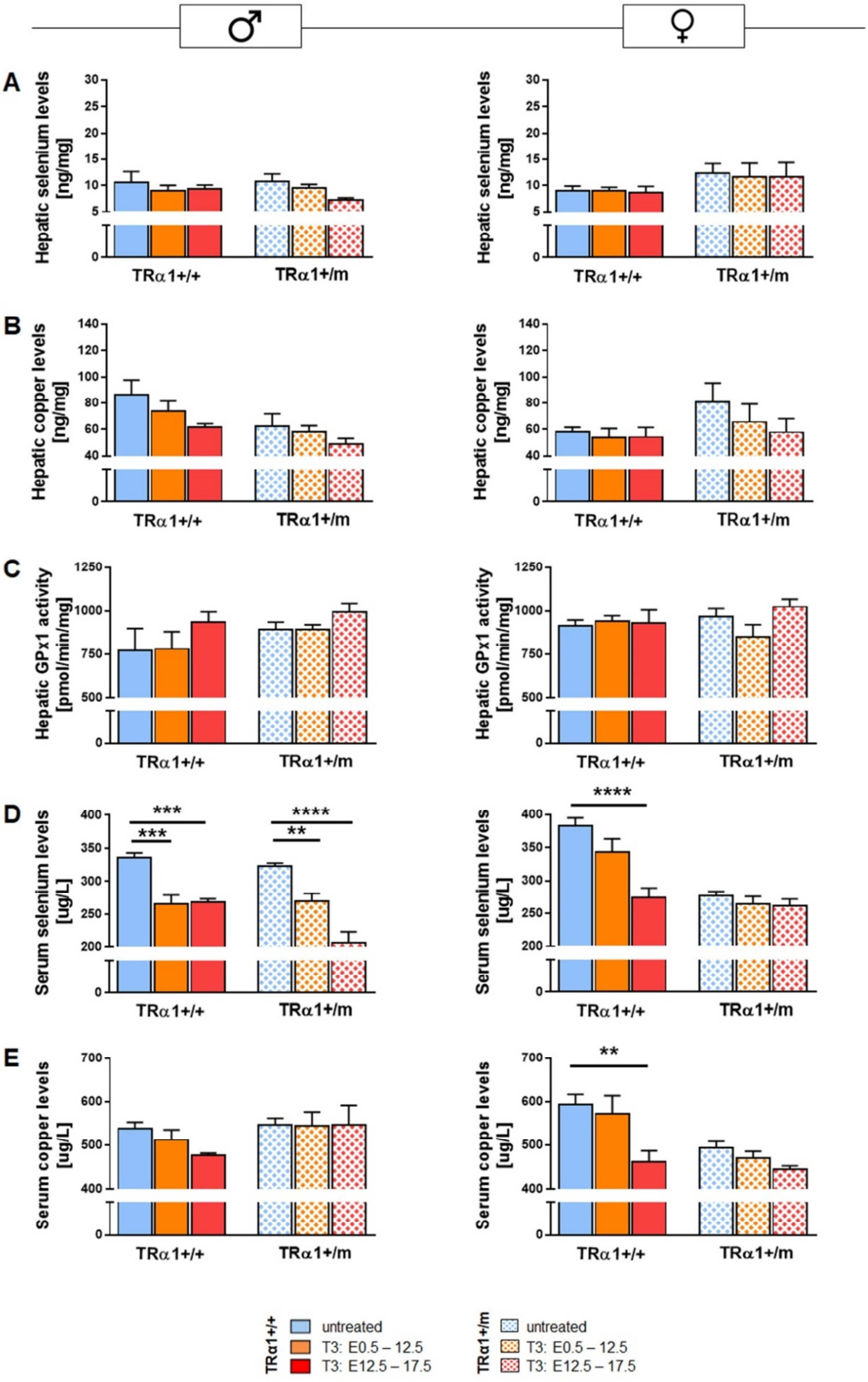

Figure 17: Measurement of hepatic and serum trace elements in offspring. **A)** Hepatic selenium, **B)** copper, **C)** GPx1 levels, **D)** serum selenium, and **E)** serum copper levels were measured in male and female wildtype (TRα1+/+) and TRα1+/m mutant mice. The results of the offspring whose dams were treated with T3 in the first half of pregnancy are shown in orange, and those with treatment in the second half in red. The control group is illustrated in blue. All values are shown as mean ± SEM of all

animals and analyzed with two-way ANOVA with Holm-Sidak's multiple comparisons test. $p<0.01$ (**), $p<0.001$ (***) and $p<0.0001$ (****); n=6 for each group. The figures were adapted from "Pedaran et al. 2021 Thyroid".

3.3.3 Maternal T3 Treatment Does Not Affect Glucose Metabolism in the Offspring

Thyroid hormones have an important role in metabolism and in particular glucose metabolism. During pregnancy, maternal hypothyroidism may alter fetal glucose homeostasis and lead to glucose intolerance in the adult offspring (Kemkem et al. 2020; Safayee et al. 2016). To investigate whether maternal T3 treatment in the first or second half of pregnancy also has effects on glucose intolerance and clearance in male and female offspring, an intraperitoneal glucose tolerance test (ipGTT) was performed. After the experimental mice fasted for six hours, basal blood glucose was measured. Then 2 g/kg glucose was injected i.p. and blood glucose was measured after 15 min, 30 min, 60 min, 90 min, and 120 min.

The offspring showed no significant differences in basal glucose or tolerance upon T3 treatment during different time periods of pregnancy, however the TRα1+/m offspring demonstrated an accelerated glucose clearance as expected (Figure 18A-B) (Sjögren et al. 2007).

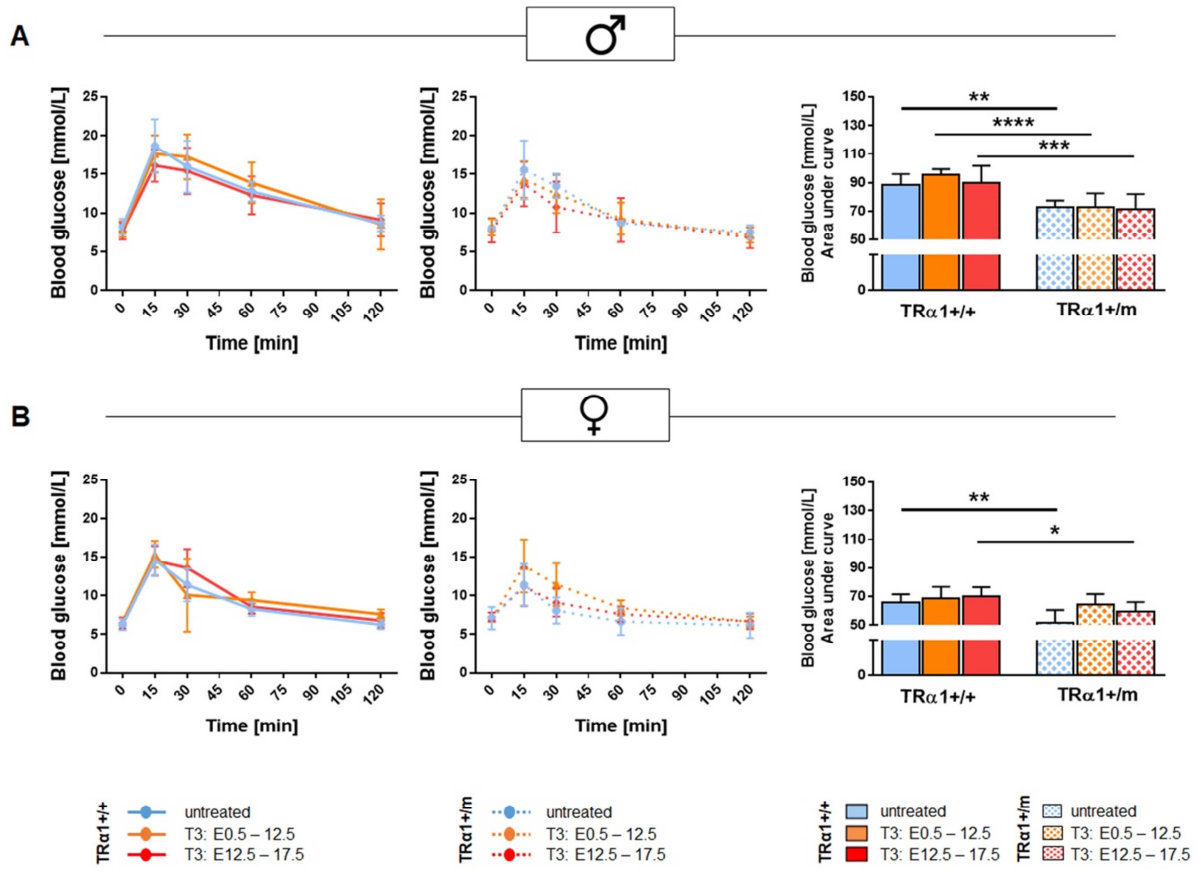

Figure 18: Blood glucose and area under the curve (AUC) during the ipGTT. IpGTT was performed on **A)** male and **B)** female TRα1+/+ and TRα1+/m offspring. The offspring are displayed in blue (dams received H_2O from conception until birth), orange (dams were treated in the first half of pregnancy with T3 in drinking water), or red (dams were treated in the second half of pregnancy in drinking water). All values are shown as mean ± SEM and were analyzed with two-way ANOVA with Holm-Sidak's multiple comparisons test; n=6 for each group.

3.3.4 Maternal T3 Treatment during Different Periods of Pregnancy Shows No Severe Metabolic Effects in the Offspring

Maternal T3 treatment was observed to have no significant effects on oxygen consumption (Figure 19A-B), respiratory quotient (RQ) (Figure 19C), average daily energy expenditure (DEE) (Figure 19D), resting metabolic rate (RMR) (at 23°C), or basal metabolic rate (BMR) (at 30°C) (Figure 19E-F) in both genders and both genotypes compared to control offspring.

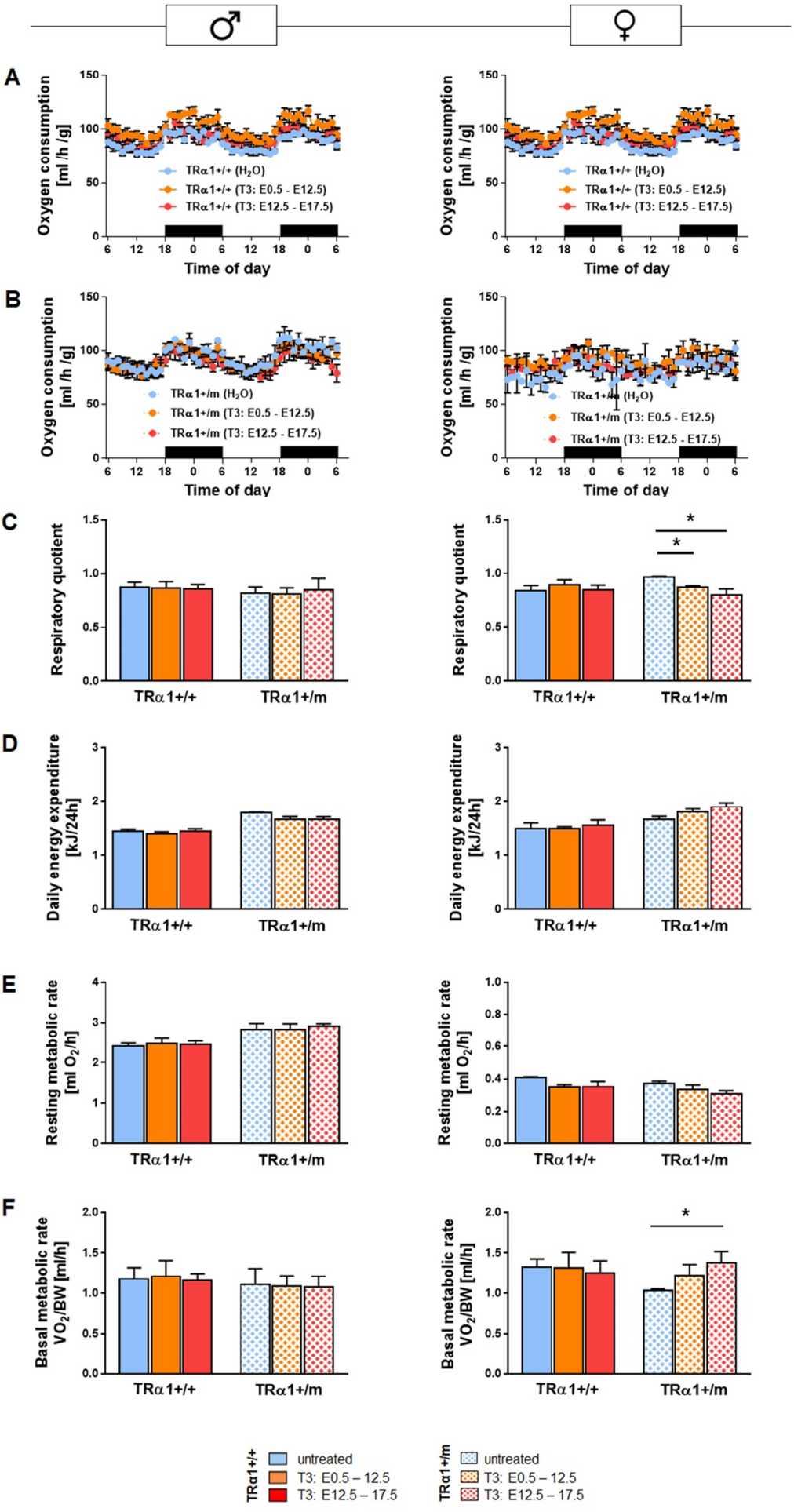
♂
♀
A
Oxygen consumption [ml /h /g]
Time of day
TRα1+/+ (H_2O)
TRα1+/+ (T3: E0.5 - E12.5)
TRα1+/+ (T3: E12.5 - E17.5)
B
TRα1+/m (H_2O)
TRα1+/m (T3: E0.5 - E12.5)
TRα1+/m (T3: E12.5 - E17.5)
C
Respiratory quotient
D
Daily energy expenditure [kJ/24h]
E
Resting metabolic rate [ml O_2/h]
F
Basal metabolic rate VO_2/BW [ml/h]
TRα1+/+
TRα1+/m
*
untreated
T3: E0.5 – 12.5
T3: E12.5 – 17.5

Figure 19: Effect of maternal TH on metabolic function in male and female offspring. Oxygen consumption during day and night (black horizontal bars indicate night-time activity) was measured in **A)** offspring of the wildtype and **B)** in TRα1+/m of both genders. Furthermore, **C)** the respiratory quotient of these offspring over the course of 2 consecutive days, **D)** daily energy expenditure per 24 hours, **E)** resting metabolic rate at room temperature (23°C) and **F)** thermoneutrality (at 30°C) were analyzed in these offspring. The dams were treated with T3 either in the first half (orange) or in the second half of pregnancy (red) compared to the control group (blue). All values are shown as mean ± SEM and were analyzed with two-way ANOVA with Holm-Sidak's multiple comparisons test. $p<0.05$ (*); n=6 for each group.

3.3.5 Maternal T3 Treatment in the Second Half of Pregnancy Improves Locomotor Activity in TR*α*1+/m Male Offspring

It is known that the TRα1+/m mice exhibit a reduction in hippocampal parvalbumin (PV) neurons associated with anxiety and memory impairment. This leads to delayed maturation of PV in the motor cortex with massive deficits in locomotor activity (Venero et al. 2005; Wallis et al. 2008). In this study, the locomotor activity of the offspring was measured and strikingly it was found, that locomotor activity significantly increased in male offspring of both genotypes after T3 treatment in the second half of pregnancy, whereas a significant decrease in locomotor activity was observed in female TRα1+/m offspring (Figure 20A).

To determine the role of maternal T3 treatment on skeletal muscle at different periods during pregnancy, the red muscle soleus and the mixed fiber type muscle gastrocnemius were also investigated. After maternal T3 treatment during pregnancy, muscle weight was found to be significantly increased by maternal T3 treatment during the second half of pregnancy in both genders and genotypes (Figure 20B-C), although locomotor activity was significantly reduced in female TRα1+/m offspring.

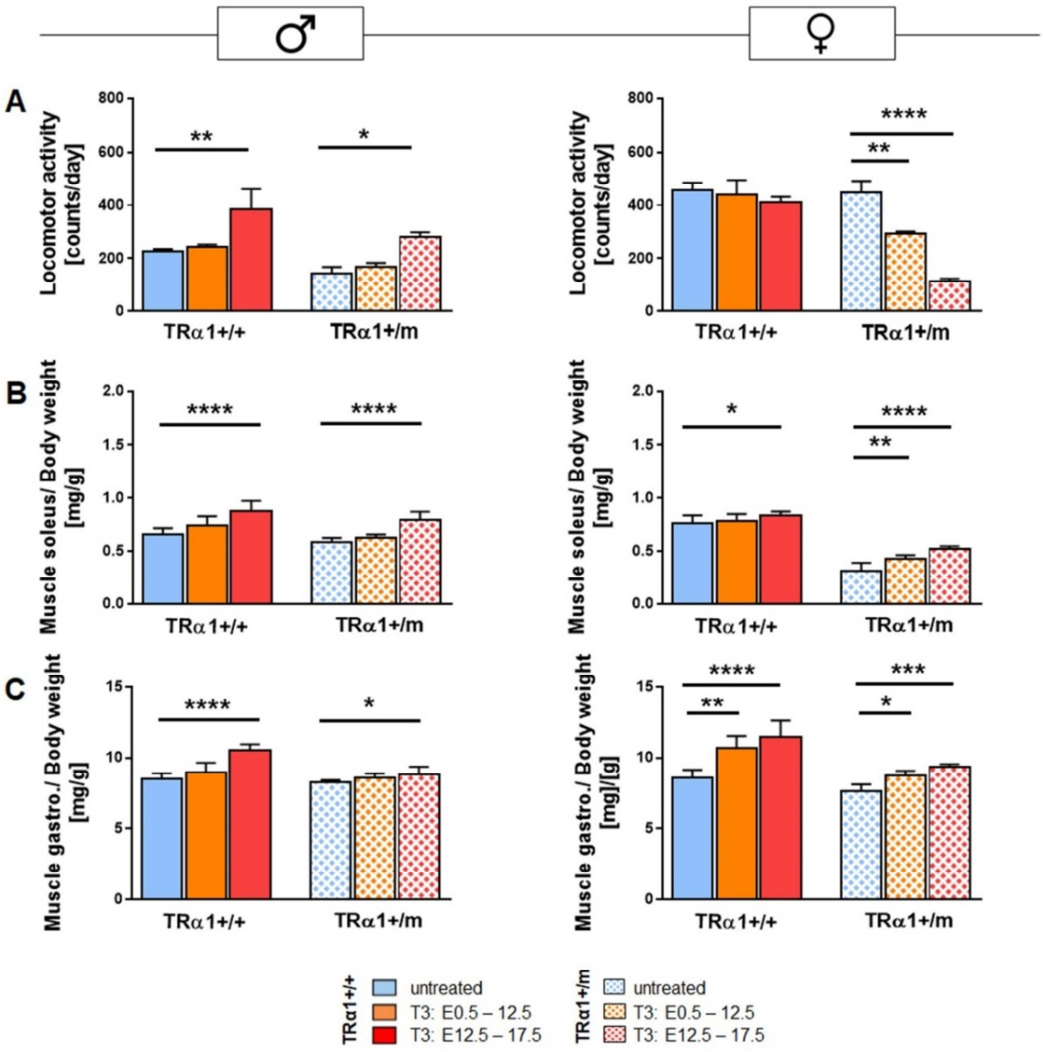

Figure 20: Locomotor activity and muscle weight/body weight ratio of soleus and gastrocnemius muscles. The dams were treated with T3 either in the first half (orange) or in the second half of pregnancy (red) and compared with the control group (blue). **A)** Locomotor activity was measured over the course of two consecutive days at 23°C in maternal T3-treated wildtype and TRα1 offspring in both genders and genotypes. Muscle weight-to-body weight ratio of **B)** soleus and **C)** gastrocnemius muscles in these experimental mice. All values are expressed as mean ± SEM and were analyzed with two-way ANOVA with Holm-Sidak's multiple comparisons test. $p<0.05$ (*), $p<0.01$ (**), $p<0.001$ (***) and $p<0.0001$ (****); n=6 for each group.

In addition genes encoding proteins such as *Pepck* (phosphoenolpyruvate carboxylase) and *Pyrkm* (Phosphoenolpyruvate carboxylase) for muscle were measured, which are involved in glucose uptake and glucose metabolism in these muscles. There is a tendency of an increase in glucose metabolism of these genes in both muscles after maternal T3 treatment in the second half of pregnancy in male offspring (Figure 21A-B). Gene expression in female offspring showed the same pattern as in male offspring (Figure Supplement 3A-B).

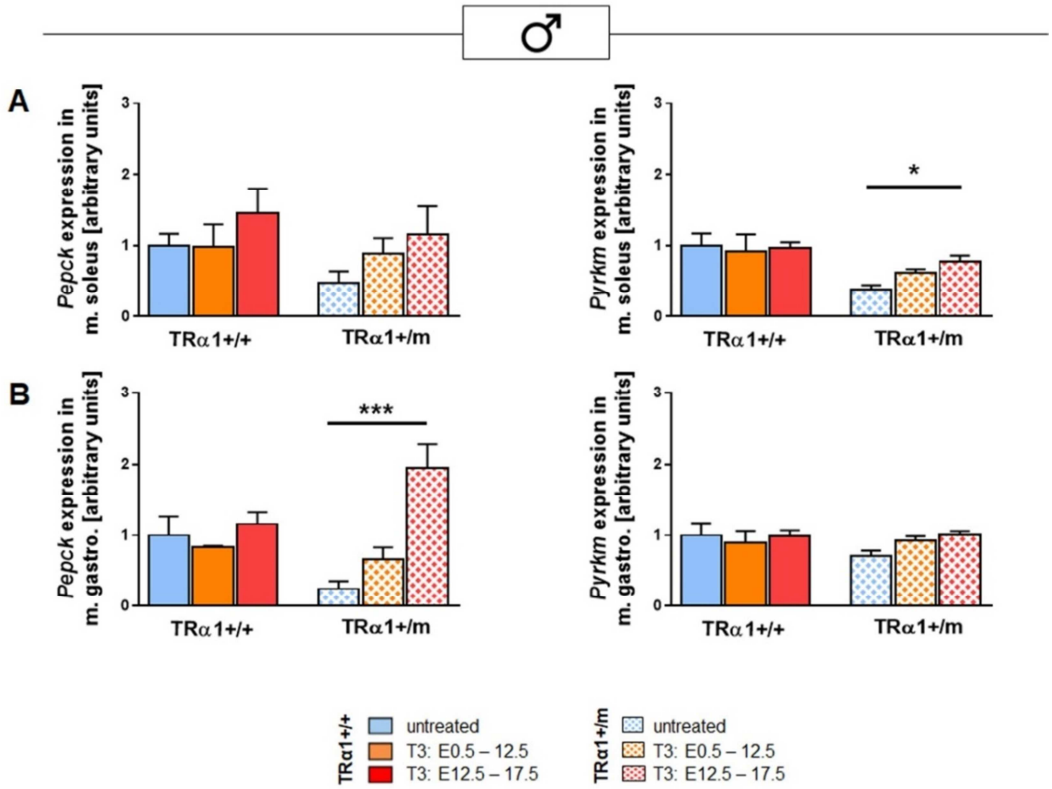

Figure 21: Gene expression of proteins involved in glucose uptake and metabolism in male offspring. Gene expression of proteins involved in glucose metabolism in male offspring whose dams were treated either in the first half (orange) or in the second half of pregnancy (red) compared to control group (blue). **A)** *Pepck* (phosphoenolpyruvate carboxylase) and *Pyrkm* (Phosphoenolpyruvate Carboxylase for muscle) in muscle soleus and **B)** muscle gastrocnemius. All values are presented as mean ± SEM and were analyzed with two-way ANOVA with Holm-Sidak's multiple comparisons test. $p<0.05$ (*) and $p<0.001$ (***); n=6 for each group.

As noted, the uptake of triglyceride-rich lipoproteins into muscle soleus and gastrocnemius was not significantly changed after maternal T3 treatment in the offspring. Therefore, the expression of *Pparδ* (Peroxisome proliferator-activated receptor delta) and *Gpd2* (Glycerol 3-phosphate dehydrogenase) genes, which are involved in β-oxidation in both muscle tissues, were measured. There was a significant increase of *Pparδ* in both muscles after the maternal T3 treatment compared to the control group while *Gpd2* was significantly decreased in wildtype offspring in muscle soleus (Figure 22A-B). Figure Supplement 4A-B demonstrates the expression of these genes in female offspring.

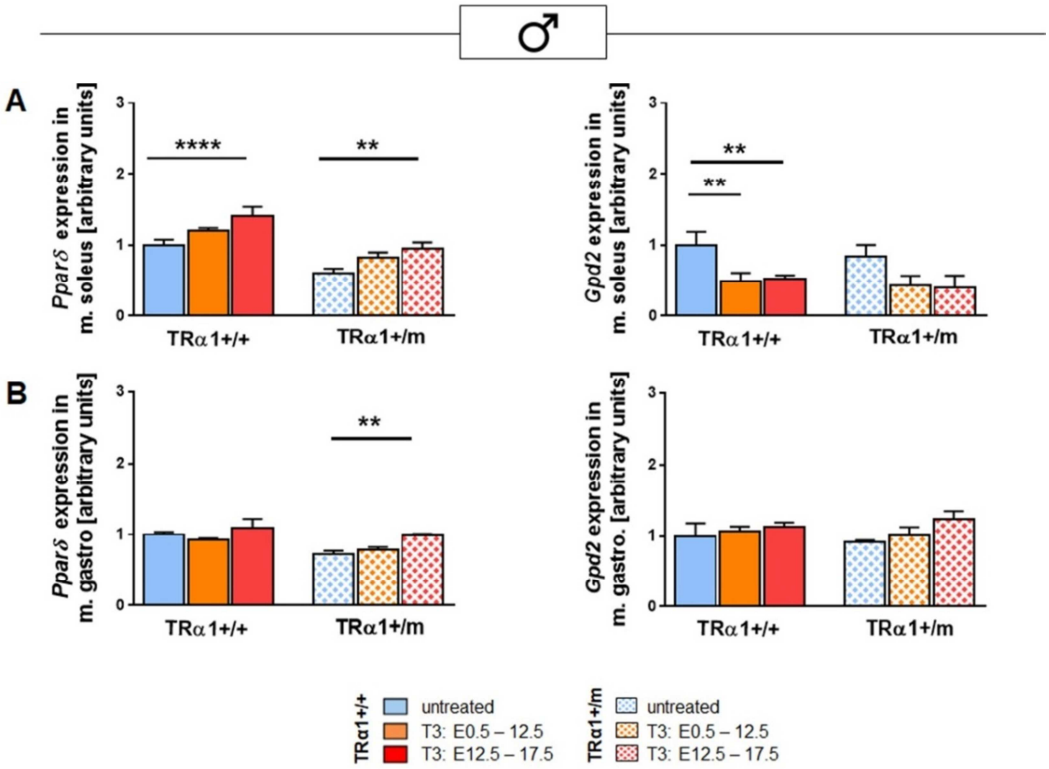

Figure 22: Gene expression of proteins involved in β-oxidation and oxidative phosphorylation in male offspring. Investigation of the gene expression in male offspring whose dams were treated in either the first half (orange) or in the second half of pregnancy (red) compared to the control group (blue). *Pparδ* (Peroxisome proliferator-activated receptor delta) and *Gpd2* (Glycerol 3-phosphate dehydrogenase) were measured in **A)** muscle soleus and **B)** muscle gastrocnemius of offspring. All values are expressed as mean ± SEM and were analyzed with two-way ANOVA with Holm-Sidak's multiple comparisons test. $p<0.01$ (**) and $p<0.0001$ (****); n=6 for each group.

Subsequently, gene expression of *Myh1* (Myosin heavy chain 1) and *Myh4* (Myosin heavy chain 4), which are responsible for activity in adult mice, was analyzed. It was detected that both genes (*Myh1* and *Myh4*) were significantly decreased in muscle soleus in female offspring after maternal T3 treatment, while no significant changes occurred in male offspring (Figure 23A-B). The same result was found for muscle gastrocnemius (Figure Supplement 5A-B).

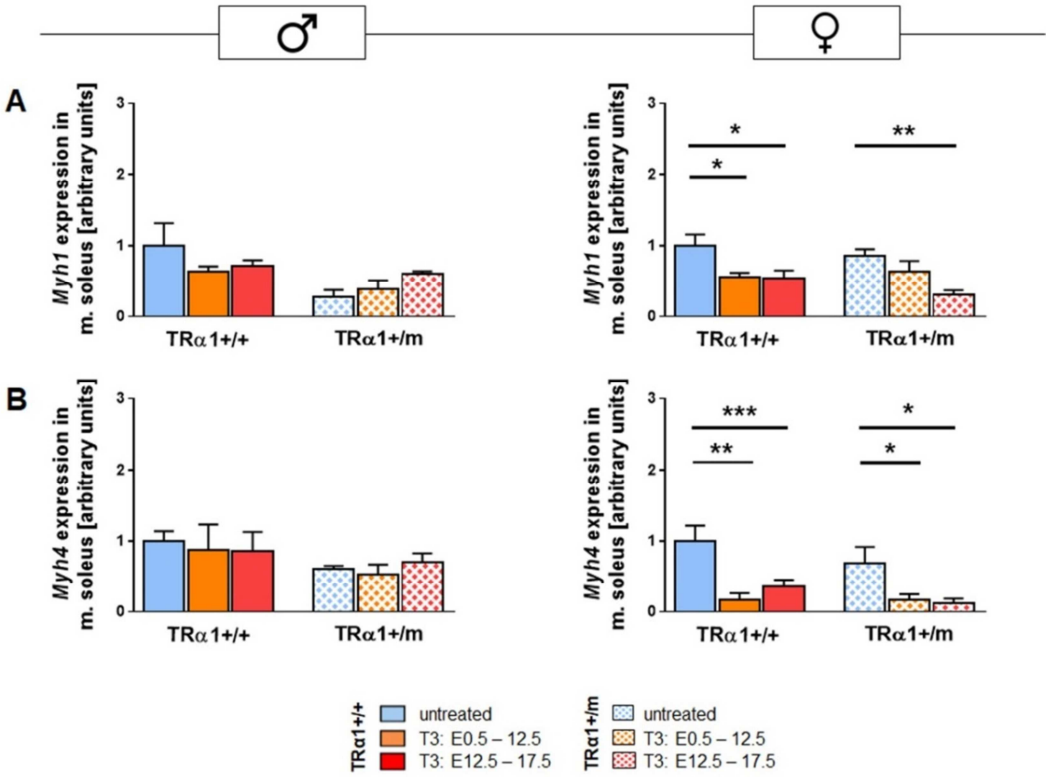

Figure 23: Gene expression of Myh1 and Myh4 in muscle soleus of offspring. Gene expression in adult male and female offspring of control dams (blue) or dams either treated with T3 in the first (orange) or second half of pregnancy (red) of **A)** *Myh1* (Myosin heavy chain 1) and **B)** *Myh4* (Myosin heavy chain 4) in muscle soleus. All values are shown as mean ± SEM and were analyzed with two-way ANOVA with Holm-Sidak's multiple comparisons test. $p<0.05$ (*), $p<0.01$ (**) and $p<0.001$ (***); n=6 for each group.

3.3.6 Maternal T3 Treatment Alters the Body Composition in the Offspring

To determine the changes in body composition of the offspring due to the different periods of maternal T3 treatment, the fat content, lean mass, and free fluid content of restrained mice were analyzed using nuclear magnetic resonance spectroscopy (NMR).

It was found that maternal T3 treatment significantly reduced lean mass and free body fluid in male offspring, while these parameters were unchanged in female offspring (Figure 24A-B). Moreover, maternal T3 treatment did not affect the fat mass of offspring of both genders and both genotypes (Figure 24C).

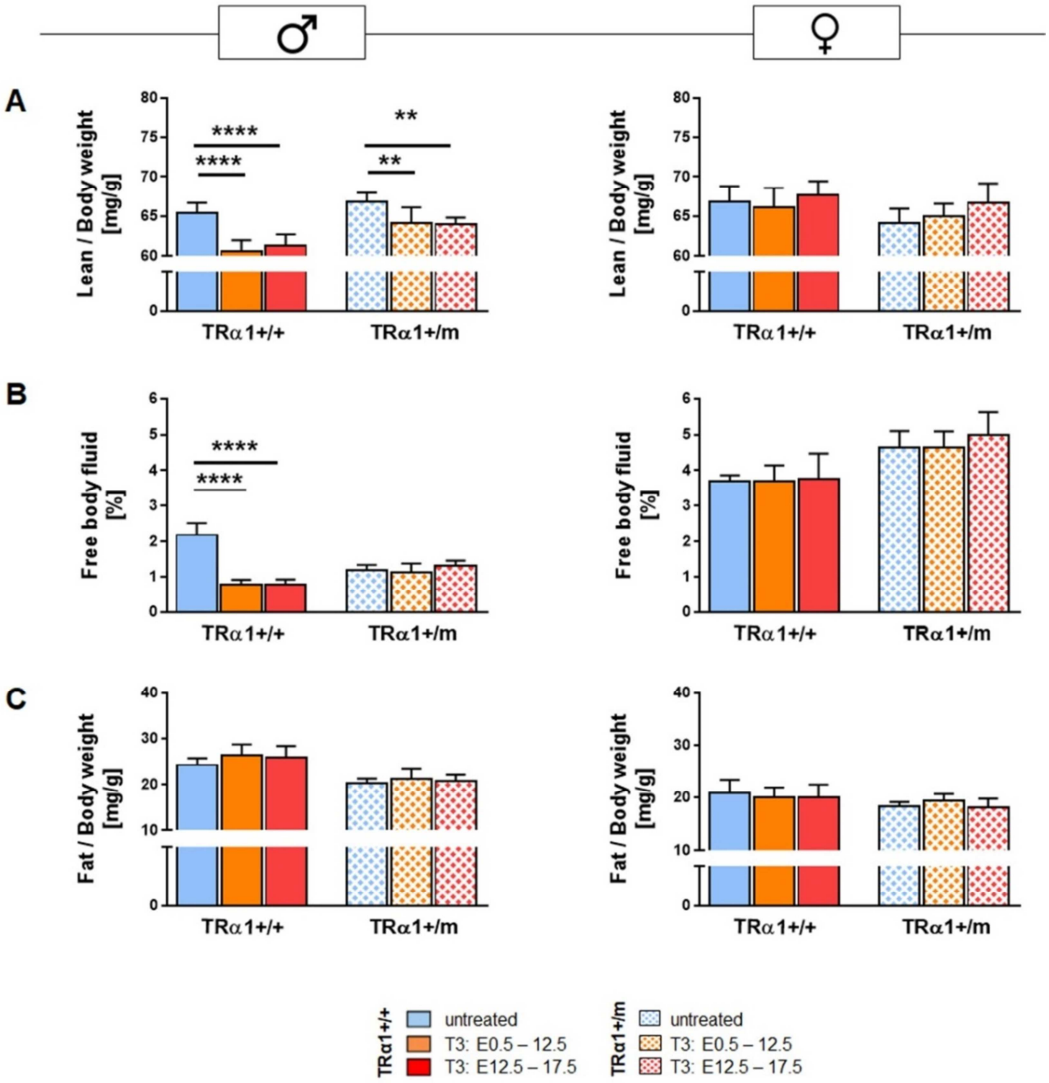

Figure 24: Determination of changes in body composition of the offspring. Effect of maternal TH on body composition in offspring of both genders whose dams were treated with T3 either in the first (orange) or in the second half of pregnancy (red) compared with untreated dams (blue). **A)** Lean mass, **B)** free body fluid and **C)** fat mass. All values are shown as mean ± SEM and were analyzed with two-way ANOVA with Holm-Sidak's multiple comparisons test. $p<0.01$ (**) and $p<0.0001$ (****); n=6 for each group.

3.3.7 Maternal T3 Treatment Decreases the Adipose Tissue Weight iWAT and gWAT in the Offspring

To further investigate how maternal T3 treatment in different periods during pregnancy affects adipose tissue development in offspring, dams were treated with T3 in the first or second half of pregnancy and TRα1+/+ and TRα1+/m offspring mice were compared with control groups. It was established that T3 treatment in the second half of pregnancy resulted in a significant decrease in inguinal white adipose tissue (iWAT) and gonadal white adipose

tissue (gWAT) weight, in both genotypes and genders. However, there was no effect of maternal T3 treatment on interscapular brown adipose tissue (iBAT) weight (Figure 25A-C).

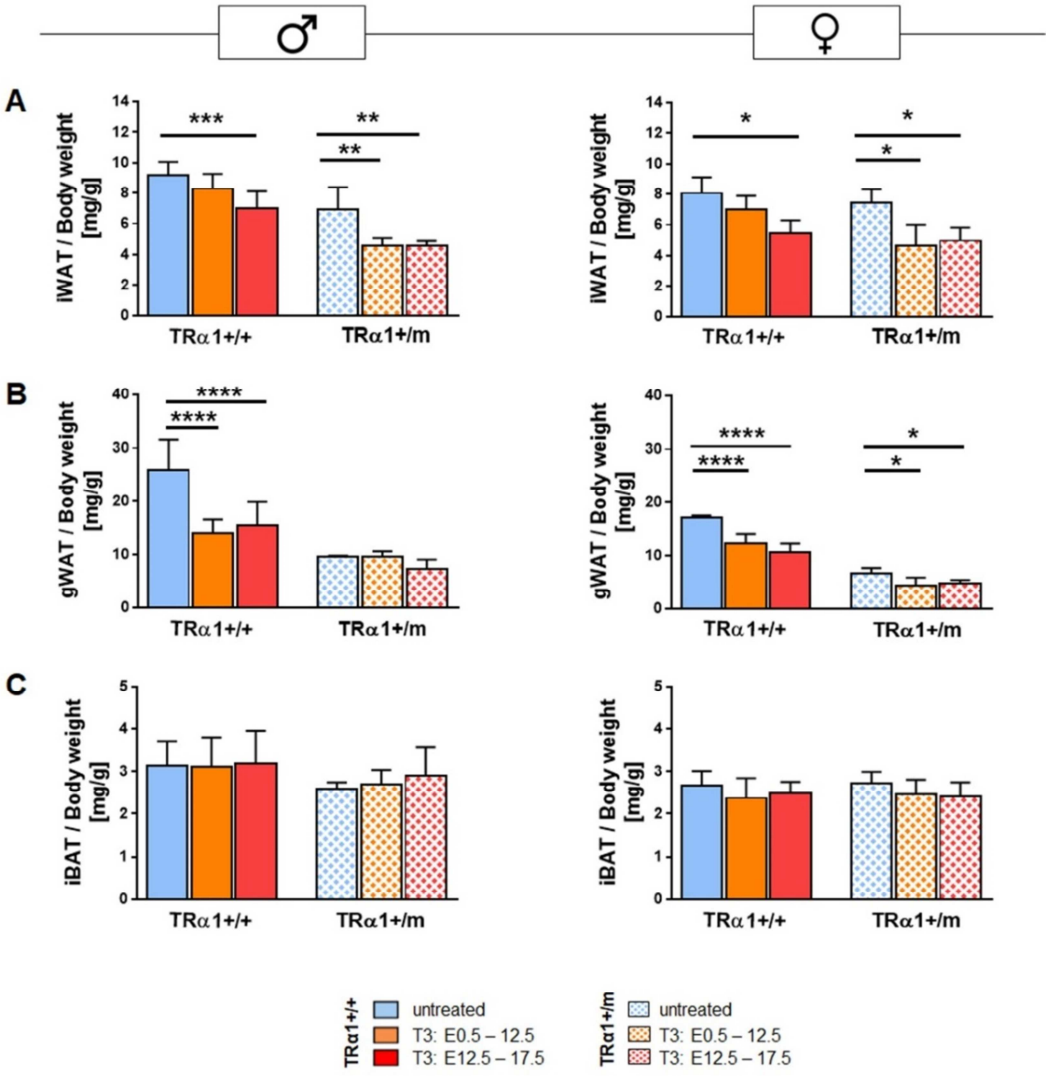

Figure 25: Adipose tissue weight in the offspring of both genders and genotypes. Offspring are displayed in blue (dams were treated with H_2O from conception until birth), orange (dams were treated in the first half of pregnancy with T3 in drinking water), or red (dams were treated in the second half of pregnancy in drinking water). Adipose tissue weight of **A)** inguinal white adipose tissue (iWAT), **B)** gonadal white adipose tissue (gWAT) and **C)** interscapular brown adipose tissue (iBAT) were anaylzed. All values are expressed as mean ± SEM and were analyzed with two-way ANOVA with Holm-Sidak's multiple comparisons test. $p<0.05$ (*), $p<0.01$ (**), $p<0.001$ (***) and $p<0.0001$ (****); n=6 for each group.

To determine molecular alterations in these tissues after maternal T3 treatment, gene expression analysis was performed for some genes involved in lipolysis and lipogenesis process. *Hsl* (hormone sensitive lipase) and *Adrb3* (beta 3-adrenergic receptor) were not altered after maternal T3 treatment in iWAT tissue (Figure 26A), whereas *Hsl* was

significantly increased in iBAT (Figure 26C). The *Hsl* and *Acc1* genes in the gWAT of the male offspring were also not changed (Figure 26B). The results for female offspring are illustrated in Figure Supplement 6A-C.

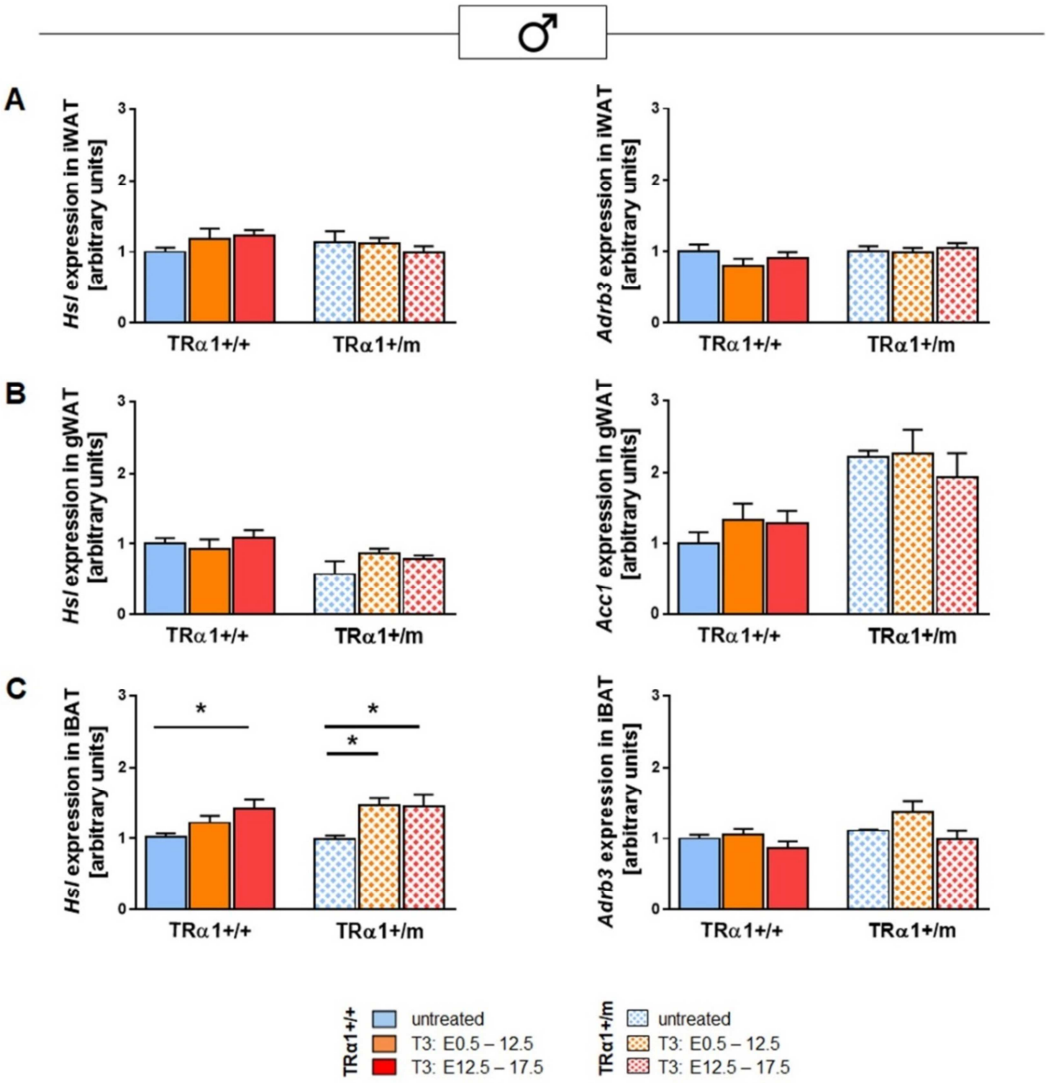

Figure 26: Determination of molecular alterations in iWAT, iBAT and gWAT in male offspring. Gene expression of proteins involved in lipid metabolism in male offspring whose dams were treated either in the first half (orange) or in the second half of pregnancy (red) compared to the control group (blue). **A)** *Hsl* (hormone sensitive lipase) and *Adrb3* (beta 3-adrenergic receptor) in iWAT, **B)** *Hsl* (hormone sensitive lipase) and *Acc1* (acetyl-Coenzyme A carboxylase 1) in gWAT and **C)** *Hsl* (hormone sensitive lipase) and *Adrb3* (beta 3-adrenergic receptor) in iBAT were analyzed. All values are presented as mean ± SEM and were analyzed with two-way ANOVA with Holm-Sidak's multiple comparisons test. $p<0.05$ (*); n=6 for each group.

3.3.8 Maternal T3 Treatment Did Not Alter Thermogenesis in the Offspring

Considering the important contribution of TH to body temperature homeostasis, thermoregulation was studied using inner ear (= auditory canal), interscapular brown adipose

tissue (iBAT), and tail base temperature as measured by infrared thermography in the offspring. Finally, rectal temperature was determined in these offspring.

There were no significant alterations in iBAT, inner ear and rectal temperature in offspring of both genders and genotypes, while interestingly, tail temperature was significantly decreased in TRα 1+/+ offspring of both genders after maternal T3 treatment (Figure 27).

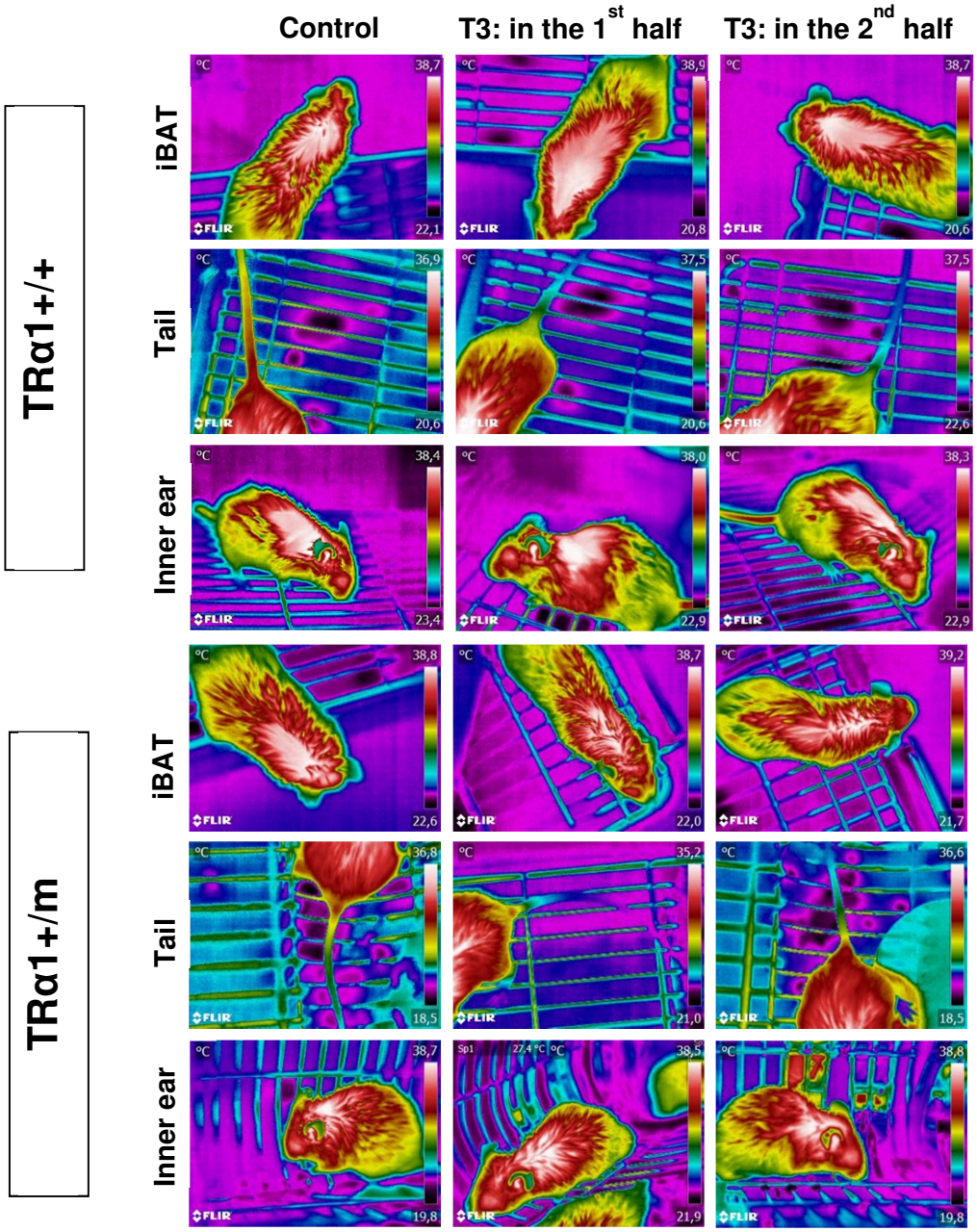

Figure 27: Investigation of the thermogenic organs by infrared thermography in male offspring. Evaluation of surface temperature changes by infrared thermography in male offspring of both genotypes born to dams treated with T3 in either the first or in the second half of pregnancy. Representative images of iBAT, tail, and inner ear. Female offspring showed the same result (data not shown).

After the infrared thermography the pictures were analyzed by FLIR systems program (Figure 28A-D).

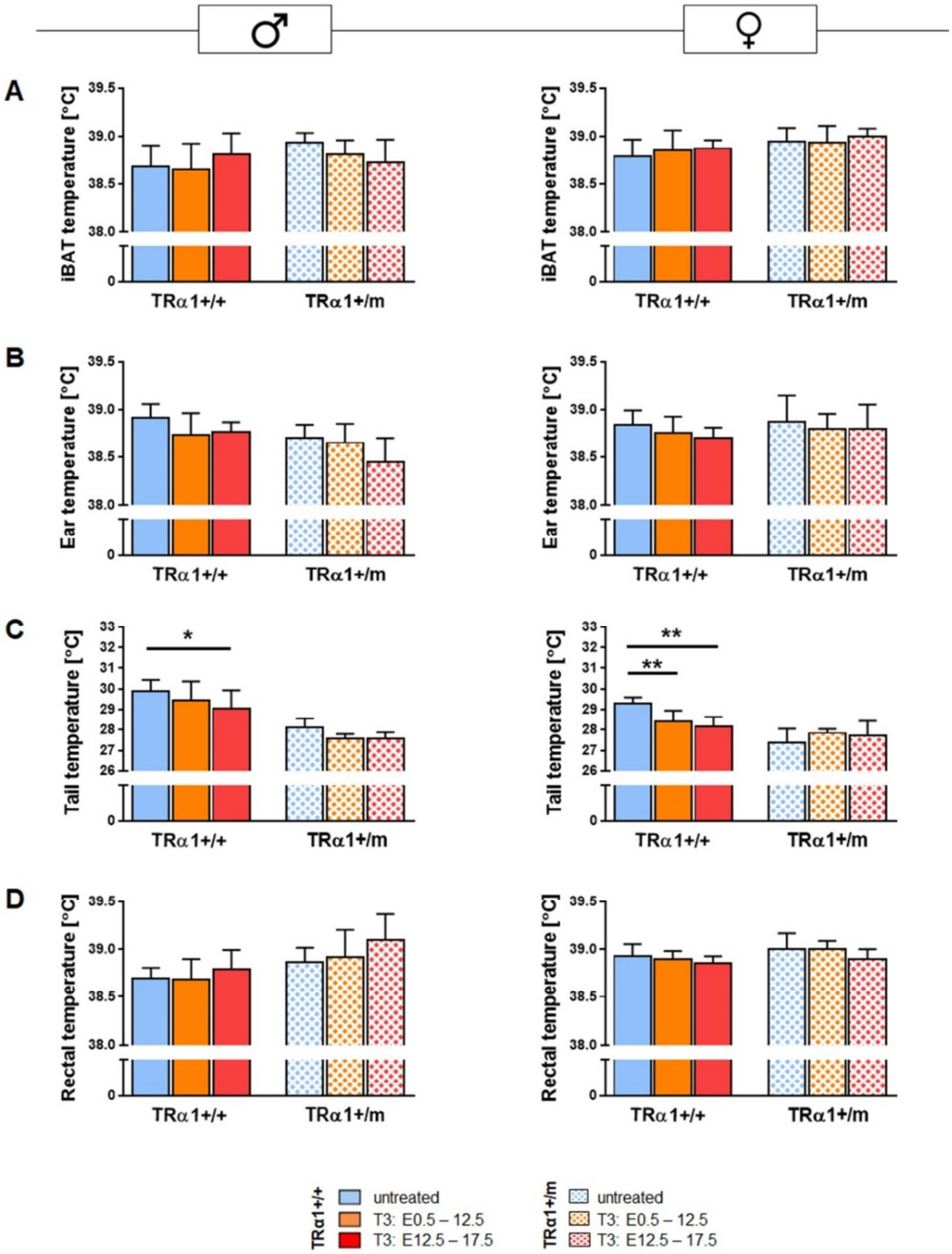

Figure 28: Body temperature of male and female offspring. Male and female WT and mutant offspring born to dams treated with T3 in either the first or second half of pregnancy were analyzed. Bar graphs show the results for **A)** iBAT, **B)** inner ear, **C)** tail, and **D)** rectal temperature. All values are expressed as mean ± SEM and were analyzed with two-way ANOVA with Holm-Sidak's multiple comparisons test. $p<0.05$ (*) and $p<0.01$ (**); n=6 for each group.

After the temperature analysis with infrared camera, some genes were tested, which are responsible for thermogenesis in the body.

Most remarkably, at the molecular level, a significant upregulation of mRNA expression of uncoupling protein 1 (*Ucp1*) is observed in male offspring of both genotypes, whereas no alteration in *Ucp1* expression is found in female offspring (Figure 29A). Deiodinase type 2 (*Dio2*) was also significantly upregulated after maternal T3 treatment, however only in male TRα1+/+ and female TRα1+/m offspring (Figure 29B).

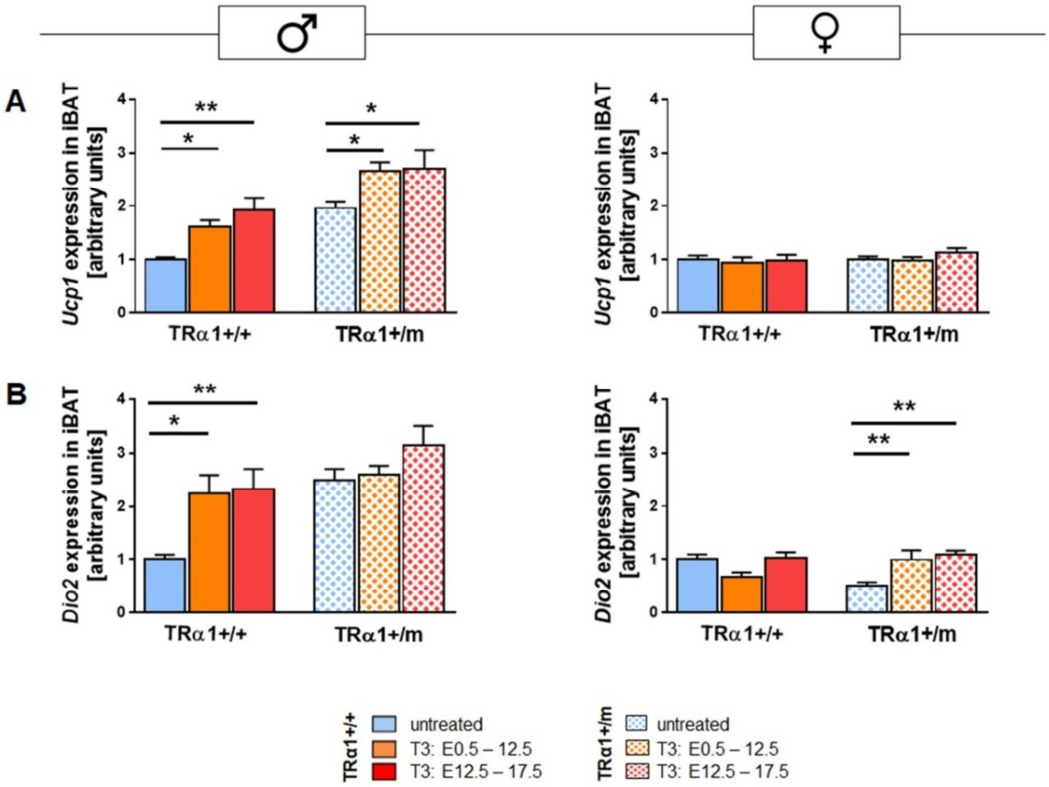

Figure 29: Gene expression in iBAT of adult male and female offspring. Dams were treated with T3 either in the first (orange) or second half of pregnancy (red) and compared to the control group (blue). **A)** *Ucp1* (uncoupling protein 1) and **B)** *Dio2* (deiodinase type II) levels in iBAT of male and female offspring. All values are presented as mean ± SEM and were analyzed with two-way ANOVA with Holm-Sidak's multiple comparisons test. $p<0.05$ (*) and $p<0.01$ (**); n=6 for each group.

Muscle was then analyzed as an alternative thermogenic organ. No major alterations in the mRNA levels of *Sln* (Sarcolipin) were detected in muscle soleus or gastrocnemius of male offspring (Figure 30). Female offspring showed the same result (Figure Supplement 7).

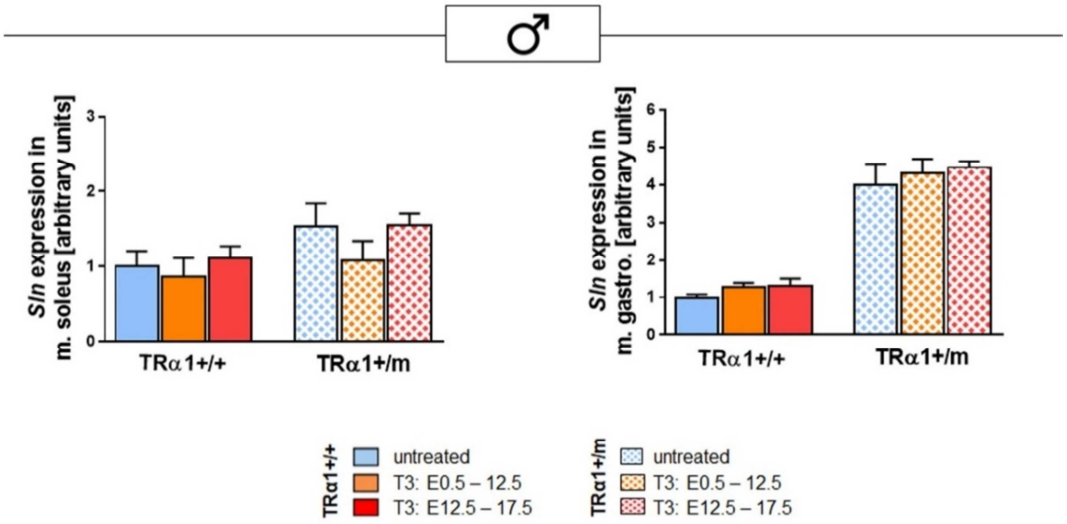

Figure 30: Sln expression in muscle soleus and gastrocnemius of adult male offspring. Dams were treated with T3 either in the first (orange) or second half of pregnancy (red) and compared to the control group (blue). All values are shown as mean ± SEM and were analyzed with two-way ANOVA with Holm-Sidak's multiple comparisons test; n=6 for each group.

3.3.9 Maternal T3 Treatment Increases the Metabolic Function of the Liver in the Offspring

To address the glucose utilization in the liver after maternal T3 treatment at different periods during pregnancy and to measure gluconeogenesis and glycolysis in the offspring, gene expression in the liver was measured.

Examination of gene expression in the liver in this study revealed significantly increased mRNA expression after T3 treatment in the second half of pregnancy in *Pepck* and *Pyrkl*. The increase in mRNA expression was also observed for genes involved in liponeogenesis and lipolysis such as acetyl-CoA carboxylase 1 (*Acc1*) and fatty acid synthase (*Fasn*) (Figure 31A-D).

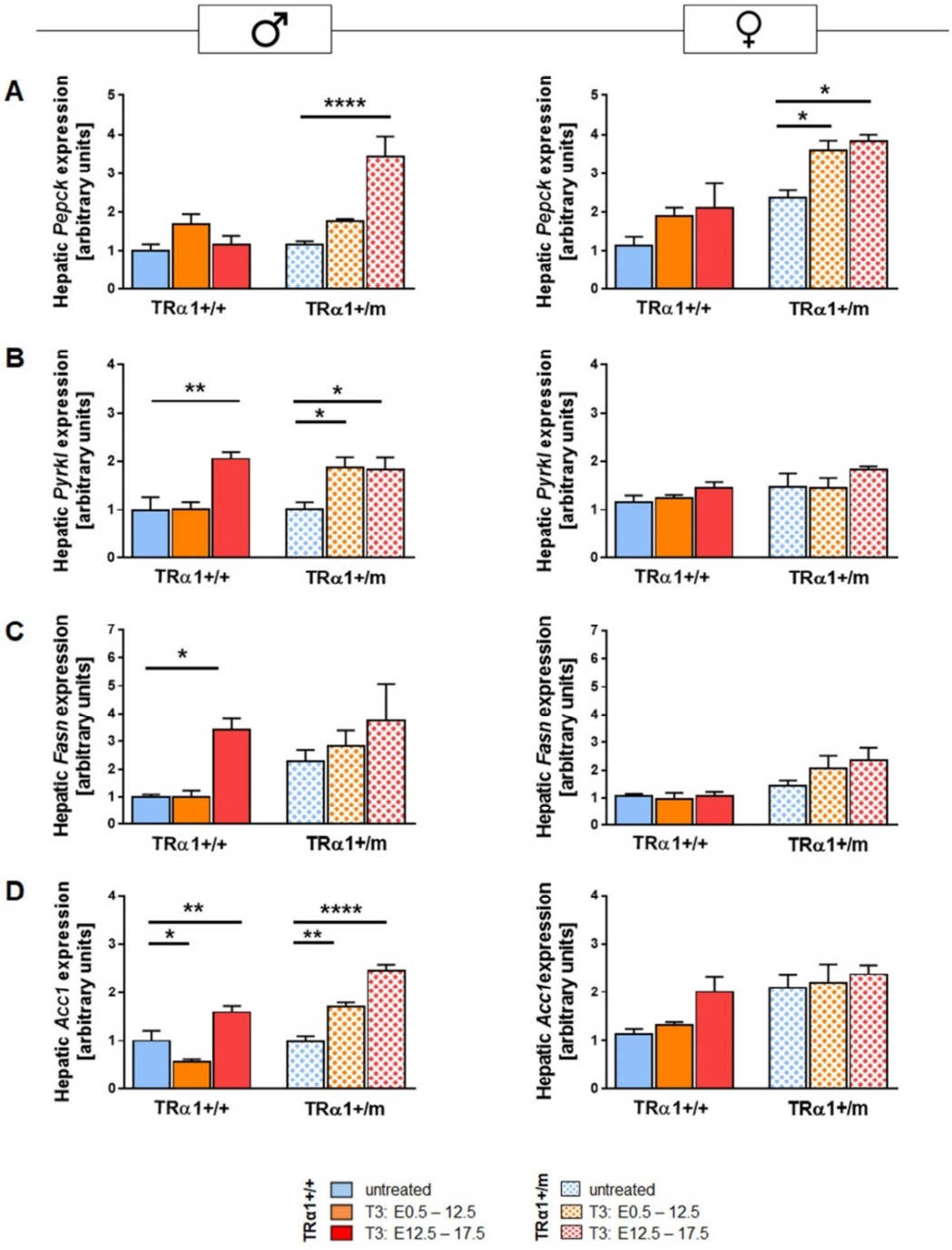

Figure 31: Examination of hepatic gene expression in the offspring. Relative expression of hepatic genes involved in metabolism in offspring whose dams were treated with T3 in either the first (orange) or in the second half of pregnancy (red) compared to untreated dams (blue). Tested genes involved in gluconeogenesis and glycolysis: **A)** *Pepck* (phosphoenolpyruvate carboxykinase) and **B)** *Pyrkl* (Phosphoenolpyruvate Carboxylase). Analyzed genes involved in liponeogenesis and lipolysis: **C)** *Fasn* (fatty acid synthase) and **D)** *Acc1* (acetyl CoA carboxylase 1). All values are expressed as mean ± SEM and were analyzed with two-way ANOVA with Holm-Sidak's multiple comparisons test. $p<0.05$ (*), $p<0.01$ (**) and $p<0.0001$ (****); n=6 for each group.

4. DISCUSSION

During the last decades, several studies have shown that maternal TH dysfunction increases the risk of cognitive impairment and impacts motor development in the offspring. Unfortunately, these focused primarily on the effects of maternal TH on human brain neurocognitive functions. Starting a few years ago, it became immediately relevant to research more about the other effects of maternal TH dysfunction, such as the effects on embryonal development or growth (Eng and Lam 2020; Jansen et al. 2019) and particularly on the cardiovascular system (Cappola et al. 2019; Godoy et al. 2014; Mittag et al. 2013). Nevertheless, the precise consequences of altered maternal TH signaling on offspring growth, cardiovascular function, and metabolism are still not completely understood.

To decipher the effects of altered maternal TH signaling during the first or second half of pregnancy on male and female offspring, corresponding to the first and second trimesters in human (Darby et al. 2019), mice heterozygous for the dominant negative TRα1R384C mutation (TRα1+/m) were used in combination with maternal pharmacological T3 treatments to characterize the temporal role of prenatal TRα1 signaling in fetal programming of offspring properties. Taking advantage of the fact that the mutant TRα1 can be reactivated by elevating T3 levels *in vivo* (Tinnikov et al. 2002), an experimental paradigm was set up in which TRα1 signaling was selectively restored in the TRα1+/m embryo during pregnancy. Treatment started either on the first day after positive plug check and continued until embryonic day E12.5 (first half of pregnancy) or from E12.5 until day E17.5, the day before birth (second half of pregnancy) (Richard and Flamant 2018). The dams received 0.5 µg/mL T3 via drinking water. This treatment duration is known to be sufficient to obtain a stable serum concentration and to reactivate the mutant receptor in the developing embryo (Wallis et al. 2008). The resulting mutant animals (TRα1+/m) were compared to wildtype littermates (TRα1+/+) exposed to high T3 during the same periods and to untreated controls regarding their growth, cardiovascular properties, and metabolic function.

The summary tables in the respective sections simplify understanding of the differentiation between TH effect in the first and second half of pregnancy in male and female offspring of both genotypes.

4.1 Consequence of Maternal T3 Treatment on Early Growth Development

Maternal hypothyroidism is a very common syndrome in pregnant women that compromises the transport of thyroid hormones from mother to fetus and increases the risk of alterations in fetal metabolism and growth (Kiran et al. 2021; Krassas, Karras, and Pontikides 2015).

The first aim of this thesis was to investigate the effects of maternal hypothyroidism and the stage of maternal hypothyroidism after maternal T3 treatment during the first and second half of pregnancy on the growth of male and female adult offspring (Table 22).

Table 22: Summary table of the effects of maternal T3 treatment during pregnancy on offspring growth.

		TRα1+/+			TRα1+/m		
		Control	T3 treatment		Control	T3 treatment	
	Characteristics		1st half	2nd half		1st half	2nd half
Growth	Body weight	m	no effect	no effect	m	no effect	no effect
		f	no effect	no effect	f	no effect	no effect
	Body length	m	no effect	no effect	m	no effect	no effect
		f	no effect	no effect	f	no effect	no effect

***Abbreviations:* no effect**: not significant**, m:** male**, f:** female

Small changes in TH levels throughout pregnancy can affect the body mass and body length of the offspring and persist through a lifetime (Tapia-Martínez et al. 2019). Contrary to published data, body weight and body length were not affected after maternal T3 treatment in this study. The body weight and body length of the offspring were analyzed during the first four months of offspring's life. Gene expression also confirmed that maternal T3 treatment during the different periods of pregnancy did not affect endocrine regulation of growth such as hepatic *Igf1* and pituitary *Gh,* both genes known to be affected by acute TH treatment (Behringer et al. 2018; Gouveia et al. 2018).

A plausible reason for the normal body weight and body length after prenatal T3 treatment might be the shorter duration of treatment, which seems sufficient to induce catabolic condition in utero. In contrast, an effect of TH on offspring body weight and body length could have developed if the dams had been treated with T3 during the entire pregnancy, as reported previously (Zhou et al. 2020).

The mutant TRα1+/m offspring exhibited lower birth weights than their control littermates, which was expected based on previously reported delayed postnatal development, including later eye opening or delayed tooth eruption (Tinnikov et al. 2002; Vennström, Mittag, and Wallis 2008). Thus, the results confirm the well-established importance of TRα1 in postnatal development (van Gucht et al. 2017; Moran et al. 2017; Tylki-Szymańska et al. 2015).

Taken together, these data indicate that maternal T3 treatment in this paradigm has no effect on body weight and body length of offspring of both genders. Therefore, fetal programming effects due to growth retardation in utero can likely be excluded as confounding factors in the analysis of the adult offspring.

4.2 Consequence of Maternal T3 Treatment on Cardiovascular System

Maternal hypothyroidism during pregnancy has profound effects on embryonic and postnatal development, potentially including the cardiovascular system (Ghanbari and Ghasemi 2017; Toloza, Abedzadeh-Anaraki, and Maraka 2019). Therefore, a second aim in this thesis was to investigate the effects of maternal thyroid hormone during different periods of pregnancy on cardiovascular development in the offspring.

4.2.1 Sexual Dimorphism Effects on Cardiac Function after Maternal T3 Treatment

To elucidate the cardiovascular effects of maternal T3 treatment during pregnancy, a detailed cardiovascular analysis of adult offspring was performed (Table 23).

Variations in maternal TH function affect cardiovascular parameters in both humans (Gaillard et al. 2014; Korevaar et al. 2016; Rytter et al. 2016) and mice (Harder et al. 2018; Mittag et al. 2013; Van Tuyl et al. 2004).

In this study, a non-invasive tail-cuff system with a temperature-controlled platform was used to record diastolic, systolic and MAP parameters. Interestingly, and contrary to expectations, blood pressure generally remained unaffected after maternal T3 treatment during pregnancy in both genotypes, suggesting that regulation of this parameter seems flexible enough to escape any effects of fetal programming in this paradigm.

Table 23: Summary table of the effects of maternal T3 treatment during pregnancy on the cardiovascular system of the offspring.

			TRα1+/+			TRα1+/m		
			Control	T3 treatment		Control	T3 treatment	
	Characteristics			1st half	2nd half		1st half	2nd half
Cardiovascular properties	Heart weight		m	∗∗↑	∗∗∗∗↑	m	∗∗↓	∗∗↓
			f	no effect	∗∗ ↑	f	no effect	∗ ↑
	Heart rate		m	no effect	∗∗∗∗↑	m	∗ ↑	∗∗↑
			f	no effect	no effect	f	no effect	∗∗↓
	Blood pressure	Systolic	m	no effect	no effect	m	no effect	no effect
			f	no effect	no effect	f	no effect	∗∗↓
		Diastolic	m	no effect	no effect	m	no effect	no effect
			f	no effect	no effect	f	no effect	∗ ↓
		MAP	m	no effect	∗∗↑	m	no effect	no effect
			f	no effect	∗ ↓	f	no effect	∗∗∗↓

Abbreviations: **MAP:** mean arterial pressure**; no effect:** not significant; **m:** male; **f:** female; **∗ – ∗∗∗∗:** significant alteration (arrow up indicates an increase and arrow down a decrease); $p<0.05$ (∗), $p<0.01$ (∗∗), $p<0.001$ (∗∗∗) and $p<0.0001$ (∗∗∗∗).

TRα1+/+ offspring whose dams were treated with T3 in the second half of pregnancy displayed a significant increase in heart weight. In male TRα1+/m offspring, this effect was not observed, suggesting a protective role of the mutant TRα1. Previous studies consistently showed a reduction in heart weight in offspring of hypothyroid mothers (Korevaar et al. 2016; Medici et al. 2013). Furthermore, the stronger phenotype in offspring treated with T3 in the second half of pregnancy is concordant with the onset of TRα1 expression at E13.5 in mice (Wallis et al. 2010). The actual reason for this hypertrophy is currently not clear. However, it is conceivable that maternal T3 acts either in the developing fetal brain, given that a central mechanism also drives cardiac hypertrophy in adult hyperthyroidism, or directly in the fetal heart to trigger this phenotype (Herrmann et al. 2020; Morte et al. 2021).

Contrary to hypertrophy, which was similar in males and females, a sexual dimorphism was observed in heart rate: male offspring of dams treated with T3 in the second half of pregnancy exhibited increased heart rate in both genotypes, whereas tachycardia was absent in females.

This could be explained by the fact that of fetal programming effects generally affect males more frequently than females (Dasinger and Alexander 2016; Grigore, Ojeda, and Alexander 2008). As expected, heart rate was generally lower in TRα1+/m mice (Mittag, Davis, et al. 2010).

4.2.2 Significantly Altered Gene Expression after Maternal T3 Treatment in the Second Half of Pregnancy in the Offspring

Maternal hypothyroidism is usually associated with a reduction in circulating cardiac T3 levels, leading to downregulation of the adult-to-fetal gene expression program (Cokkinos and Chryssanthopoulos 2016; Forini et al. 2019). Therefore, cardiac gene expression was studied in the offspring to identify possible molecular targets of maternal TH action. Table 24 displays selected cardiac genes that were affected after maternal T3 treatment at various periods of pregnancy compared with the control group.

Table 24: Summary table of the effects of maternal T3 treatment during pregnancy on cardiac mRNA gene expression in offspring.

		TRα1+/+			TRα1+/m		
		Control	T3 treatment		Control	T3 treatment	
	Characteristics		1st half	2nd half		1st half	2nd half
mRNA gene expression	*Serca2*	m	∗↑	∗∗∗∗↑	m	∗∗∗∗↑	∗∗∗∗↑
		f	no effect	∗∗↑	f	∗↑	∗∗∗↑
	α-Mhc	m	∗∗∗∗↑	∗∗∗∗↑	m	∗∗∗∗↑	∗∗∗∗↑
		f	no effect	no effect	f	no effect	no effect
	β-Mhc	m	no effect	∗∗∗↑	m	∗∗∗∗↑	∗∗∗∗↑
		f	no effect	no effect	f	∗∗∗∗↑	∗∗∗∗↑
	Hcn2	m	no effect	∗∗∗∗↑	m	no effect	∗∗∗ ↑
		f	no effect	∗∗↑	f	no effect	∗∗∗∗↑
	Hcn4	m	∗↑	∗∗∗∗↑	m	∗∗∗∗↑	∗∗∗∗↑
		f	no effect	no effect	f	no effect	∗∗∗ ↑

Abbreviations:* *Serca2: Sarcoplasmic/endoplasmic reticulum calcium ATPase 2; **α-*Mhc***: Myosin heavy chain 6; **β-*Mhc*:** Myosin heavy chain 7; ***Hcn2*:** Hyperpolarization activated cyclic nucleotide gated potassium and sodium channel 2; ***Hcn4*:** Hyperpolarization activated cyclic nucleotide gated potassium and sodium channel 4; **no effect**: not significant; **m**: male; **f**: female; **∗ – ∗∗∗∗:** significant alteration (arrow up indicates an increase); $p<0.05$ (∗), $p<0.01$ (∗∗), $p<0.001$ (∗∗∗) and $p<0.0001$ (∗∗∗∗).

Although there were no major differences in blood pressure in male wildtype and mutant offspring after T3 treatment during different periods of pregnancy, and even though there was a reduction in blood pressure in female wildtype and mutant offspring, mRNA levels in both genders and both genotypes revealed significantly elevated *Serca2* levels, which contribute decisively to contractile status through alterations in cytosolic Ca^{2+} levels (Muller et al. 1997). It can be speculated that this alteration may be a compensatory mechanism to stabilize blood pressure that would otherwise be affected by maternal T3 treatment.

It is not uncommon that overlapping regulatory mechanisms exist, which can mask or compensate developmental problems in blood pressure regulation, as seen previously (Mittag et al. 2013).

Interestingly, a significant increase in the expression of α- and β-*Mhc* in the treated offspring was found, although these genes are usually oppositely regulated by T3 (Haddad et al. 2010). Together with the fact that hypertrophy induced by hyperthyroidism is normally reversed after reestablishing euthyroidism (Hoefig et al. 2016), the regulatory mechanism in this animal model, which has normal levels of serum T3 and T4, appears to be different from the classical cardiac T3 signaling cascades.

Remarkably, this effect correlated with the level of expression of the pacemaker genes *Hcn2* and *Hcn4*, as well as HCN2 and HCN4 protein. Given the crucial role of these genes in the regulation of heart rate (Bucchi et al. 2012), it seems reasonable to assume that these genes drive the observed tachycardia (Bai et al. 2021; Gloss et al. 2001; Stieber et al. 2004). However, why this effect was only apparent in males remains unknown. It could be speculated that the previously described crosstalk between TH and sex hormones (B. S. Silva et al. 2019) or the well-known sexual dimorphism in deiodinase regulation may contribute to differences in local TH action during cardiac development (St. Germain and Atasoylu 1988; Köhrle et al. 1995).

4.2.3 Epigenetic Alteration in Pacemaker Genes is Associated with Maternal T3 Treatment

It was observed that T3 treatment during pregnancy resulted in significant upregulation of pacemaker key genes in the heart such as *Hcn2* and *Hcn4,* independent of genotype but with a stronger effect in the second half of pregnancy – both at mRNA and protein level.

To identify an underlying mechanism for the dysregulation of these genes, it was hypothesized that altered fetal programming by DNA methylation might contribute to the observed phenotype (Forini et al. 2019). Table 25 demonstrates the summary of DNA methylation measurement of *Hcn2* and *Hcn4* genes.

Table 25: Summary table of the effects of maternal T3 treatment during pregnancy on DNA methylation in offspring.

		TRα1+/+			TRα1+/m		
		Control	T3 treatment		Control	T3 treatment	
	Characteristics		1st half	2nd half		1st half	2nd half
DNA methylation	***Hcn2*** chr10:79,192,307	m	no effect	***↓	m	no effect	**↓
		f	no effect	**↓	f	no effect	no effect
	Hcn2 chr10:79,192,303	m	no effect	**↓	m	no effect	no effect
		f	no effect	no effect	f	no effect	no effect
	Hcn2 chr10:79,192,274	m	no effect	**↓	m	***↓	***↓
		f	no effect	no effect	f	no effect	no effect
	Hcn4 chr9:58,672,034	m	no effect	*↑	m	no effect	**↑
		f	no effect	*↑	f	no effect	no effect
	Hcn4 chr9:58,672,042	m	no effect	*↑	m	no effect	****↑
		f	no effect	**↑	f	*↑	*↑
	Hcn4 chr9:58,672,044	m	no effect	**↑	m	no effect	no effect
		f	no effect	no effect	f	no effect	no effect

Abbreviations: ***Hcn2*****:** Hyperpolarization activated cyclic nucleotide gated potassium and sodium channel 2; ***Hcn4*****:** Hyperpolarization activated cyclic nucleotide gated potassium and sodium channel 4, **no effect**: not significant**; m:** male; **f:** female; *** – ****:** significant alteration (arrow up indicates an increase and arrow down a decrease); $p<0.05$ (*), $p<0.01$ (**), $p<0.001$ (***) and $p<0.0001$ (****).

A possible interaction between TH and epigenetic programming has been established recently in several studies, which initially demonstrated in humans that the sensitivity to TH action in the offspring is epigenetically controlled (Anselmo et al. 2019; Anselmo and Chaves 2020). Subsequently, it was revealed that alteration in maternal TH can directly affect the DNA methylation pattern of several genes (Martinez et al. 2020). It is therefore not surprising that in this study it observed a similar effect of maternal TH on DNA methylation of *Hcn2* and *Hcn4*, especially since the selected intronic regions are known to be of regulatory importance for the regulation of *Hcn* genes (Kuratomi et al. 2007). While some CpG sites were affected in both genders, others were affected only in males, an effect often observed in fetal programming (Dasinger and Alexander 2016; Grigore, Ojeda, and Alexander 2008; Sah et al. 2013). T3 treatment in the second half of pregnancy had a more pronounced effect on DNA methylation, concurring with the important role of TRα1 in this developmental period of the heart (Mai et al. 2004; Vallortigara et al. 2009).

For a long time, it was claimed that an increase in DNA methylation plays a crucial role in the repression of gene expression by blocking the promoters at which activating should bind. Currently, however, in some cases it has been found that altered binding of transcription factors to CpG regions leads to a decrease in DNA methylation, thereby activating gene

expression in cells (Anastasiadi, Esteve-Codina, and Piferrer 2018; Suzuki and Bird 2008). The extent to which this DNA methylation actually has a causal effect on gene expression in this thesis remains to be elucidated.

4.3 Consequence of Maternal T3 Treatment on Metabolism

4.3.1 Effect on HPT Axis

Maternal TH deficiency, especially during the early critical embryonic stages of development, impacts the molecular and functional pathways of the HPT axis and may impair TH production in the offspring (Anifantaki et al. 2021; Miranda and Sousa 2018; Patel et al. 2011). Interestingly, this effect was not observed in this thesis (Table 26).

After maternal T3 treatment at different periods of pregnancy, no differences were observed in total T3 and T4 in the serum of the offspring.

Likewise, maternal T3 treatment did not affect *Dio1*, which is defined as hepatic T3 marker and increased only in TRα1+/m mice, as observed previously (Vujovic et al. 2009). Interestingly, there was a tendency of elevated *Dio1* mRNA and DIO1 activity despite the slightly reduced serum TH levels in the offspring whose dams were treated with T3. This may suggest that alteration of *Dio1* in the liver may be causally involved in the phenotype, i.e., altered fetal programming in hepatic *Dio1* leads to increased hepatic TH consumption and slightly lower serum TH levels – something that is supported by the reported association between DIO1 polymorphisms and altered serum T3 (De Jong et al. 2007).

More importantly, however, it has recently been demonstrated that perinatal changes in hepatic T3 action do in fact cause a variety of epigenetic modifications in the liver (Fonseca et al. 2015, 2021), supporting this hypothesis.

Unfortunately, however, there were no statistically significant differences in *Dio1* mRNA or DIO1 activity in the posthoc tests following the ANOVA. Therefore, it is assumed that the result of *Dio1* is not robust enough to fully support this hypothesis.

Table 26: Summary table of the effects of maternal T3 treatment during pregnancy on TH metabolism in offspring.

		TRα1+/+			TRα1+/m		
		Control	T3 treatment		Control	T3 treatment	
	Characteristics		1st half	2nd half		1st half	2nd half
T3 metabolism	**Total T3** serum	m	no effect	no effect	m	****↓	no effect
		f	no effect	no effect	f	****↓	no effect
	Total T4 serum	m	no effect	no effect	m	no effect	no effect
		f	no effect	no effect	f	no effect	no effect
	Se level serum	m	***↓	***↓	m	**↓	****↓
		f	no effect	****↓	f	no effect	no effect
	Cu level serum	m	no effect	no effect	m	no effect	no effect
		f	no effect	**↓	f	no effect	no effect
	Tshb pituitary	m	no effect	no effect	m	no effect	no effect
		f	no effect	no effect	f	no effect	no effect
	Dio1 pituitary	m	no effect	no effect	m	no effect	no effect
		f	no effect	no effect	f	no effect	no effect
	Dio1 hepatic	m	no effect	no effect	m	no effect	no effect
		f	no effect	no effect	f	no effect	no effect
	Spot14 hepatic	m	no effect	no effect	m	no effect	**↑
		f	****↓	****↓	f	****↓	****↓
	Se, Cu, GPx1 hepatic	m	no effect	no effect	m	no effect	no effect
		f	no effect	no effect	f	no effect	no effect

Abbreviations: **Se:** Selenium; **Cu:** Copper; ***Tshb***: Thyroid stimulating hormone beta; ***Dio1*****:** Iodothyronine deiodinase type I; ***Spot14:*** Thyroid hormone responsive protein; **GPx1:** Glutathione peroxidase 1; **no effect**: not significant**; m:** male; **f:** female; **** – ****:** significant alteration (arrow up indicates an increase and arrow down a decrease); p<0.01 (**), p<0.001 (***) and p<0.0001 (****).

Additionally, wildtype offspring unexpectedly displayed a reduction in serum selenium levels upon maternal T3 treatment in the second half of pregnancy. It is already known that T3 positively regulates serum selenium levels in mice (Hofstee et al. 2019; Mittag, Behrends, et al. 2010). However, the data in this thesis indicate that maternal T3 treatment may also be epigenetically reprogrammed selenium metabolism, as a similar effect was also found in congenital hypothyroid children (Chanoine et al. 2001; Hofstee et al. 2021). Despite sufficient T4 substitution, their serum selenium levels remained lower compared to the control group. This suggests that even a minor transient developmental hypothyroidism may cause a permanent alteration of selenoprotein physiology in adults. Hepatic selenium levels, DIO1 and GPx1 enzyme activity were not affected. Thus, the liver does not appear to be the origin of the effect and therefore further studies are required for investigation.

4.3.2 Effect on Thermoregulation

It is well established that the thermoregulation in the body is performed mainly through two mechanisms namely obligatory and facultative thermogenesis (J. E. Silva 2006), both of which are regulated by TH (Mittag 2020). The facultative thermogenesis includes shivering and non-shivering thermogenesis (López et al. 2013; J. E. Silva 2011), which is increased through the central control of thermogenesis regulating heat production in response to cold (Iwen, Oelkrug, and Brabant 2018). The obligatory thermogenesis on the other hand is sufficient to maintain the body temperature when the ambient temperature is at thermoneutrality (23°C in humans, 30°C in mice). In this part of the thesis another aspect, namely the effect of maternal TH on thermoregulation in the offspring was tested. Therefore, the temperature of iBAT, inner ear, tail was measured using IR thermography. In addition, the rectal temperature was investigated by inserting a small-diameter temperature probe through the anus (Table 27).

Table 27: Summary table of the effects of maternal T3 treatment effect during pregnancy on thermoregulation in the offspring.

		TRα1+/+			TRα1+/m		
		Control	T3 treatment		Control	T3 treatment	
	Characteristics		1st half	2nd half		1st half	2nd half
Thermoregulation	iBAT	m	no effect	no effect	m	no effect	no effect
		f	no effect	no effect	f	no effect	no effect
	Inner ear	m	no effect	no effect	m	no effect	no effect
		f	no effect	no effect	f	no effect	no effect
	Tail	m	no effect	∗↓	m	no effect	no effect
		f	∗∗↓	∗∗↓	f	no effect	no effect
	Rectal	m	no effect	no effect	m	no effect	no effect
		f	no effect	no effect	f	no effect	no effect

Abbreviations: **iBAT:** intrascapular brown adipose tissue; **no effect**: not significant**; m:** male, **f:** female; **∗ – ∗∗:** significant alteration (arrow down indicates a decrease); $p<0.05$ (∗) and $p<0.01$ (∗∗).

In general, the TRα1+/m mice showed a reduced body temperature of about 0.5°C as compared to the wildtype mice – an effect that has been reported previously (Warner et al. 2013). This difference in body temperature is sustained, even after maternal T3 treatment, suggesting that is not founded prenatally. Unexpectedly, investigation of thermoregulation including iBAT, inner ear and rectum revealed no changes in temperature at the time of measurement, although a higher iBAT temperature was expected in the mutant animals (Warner et al. 2013).

The facultative thermogenesis is generated in specialized tissues, primarily the muscle for more acute and short-term thermogenesis by shivering (Iwen, Oelkrug, and Brabant 2018). A change in facultative thermogenesis via shivering in the muscles was not observed in this thesis and the mRNA gene expression of *Sln* in muscle soleus and gastrocnemius remained unaffected after the maternal T3 treatment during the pregnancy.

On the other hand, brown adipose tissue is essential for classical non-shivering thermogenesis in prolonged periods of cold (Cannon and Nedergaard 2004). In this process the energy metabolism of mitochondria in iBAT is increased by activation of uncoupling protein 1 (UCP1), which dissipates the proton motive force as heat (Oelkrug, Polymeropoulos, and Jastroch 2015). Measurement of the *Ucp1* gene in iBAT revealed that its expression was significantly increased just in male offspring of both genotypes, whereas there was no change in the female offspring. The increased *Ucp1* gene expression may lead to an increase in temperature especially in iBAT, which interestingly was not observed in this thesis. An explanation for this difference between the increase in *Ucp1* gene expression and the unaltered temperature might be the significantly decreased tail temperature in the male offspring, indicating enhanced heat conservation. Recently, TH was shown to be involved in both heat production and dissipation of excess heat through the tail in mice, which is the major hyperthermia control surface in rodents (Warner et al. 2013). Taken together, after considering the results of the thermogenesis study, one might conclude that maternal T3, although necessary for the induction of heat production in the body, is not sufficient by itself to produce permanent changes in the paradigm of this study.

4.3.3 Effect on Energy Homeostasis

To determine the metabolic consequences after maternal T3 treatment during the pregnancy the adult male and female offspring were measured in an indirect calorimetry. Unexpectedly, no significant differences in metabolic parameters such as oxygen consumption, respiratory quotient, daily energy expenditure, resting metabolic rate, and basal metabolic rate were observed in the offspring (Table 28), supporting the finding of a generally unaffected thermoregulation in these animals.

Table 28: Summary table of the effects of maternal T3 treatment during pregnancy on energy homeostasis in the offspring.

		TRα1+/+			TRα1+/m		
		Control	T3 treatment		Control	T3 treatment	
	Characteristics		1st half	2nd half		1st half	2nd half
Energy expenditure	O_2 consumption	m	no effect	no effect	m	no effect	no effect
		f	no effect	no effect	f	no effect	no effect
	RQ	m	no effect	no effect	m	no effect	no effect
		f	no effect	no effect	f	∗↓	∗↓
	DEE	m	no effect	no effect	m	no effect	no effect
		f	no effect	no effect	f	no effect	no effect
	RMR	m	no effect	no effect	m	no effect	no effect
		f	no effect	no effect	f	no effect	no effect
	BMR	m	no effect	no effect	m	no effect	no effect
		f	no effect	no effect	f	no effect	∗↑

Abbreviations: **RQ**: respiratory quotient; **DEE**: daily energy expenditure; **RMR**: resting metabolic rate; **BMR**: basal metabolic rate; **no effect**: not significant**;** **m**: male; **f**: female; **∗:** significant alteration (arrow up indicates an increase and arrow down a decrease); $p<0.05$ (∗).

Several previous studies have already shown that TRα1+/m mice are mainly hypermetabolic, which is caused by the TRα1 aporeceptor activity (transcriptional activity of the TR in its unliganded state) (Capelli et al. 2021; Winter et al. 2006). This high-energy turnover in this mouse model is accompanied by an increase in lipid metabolism, which can be triggered by excess TH (López et al. 2010). Therefore, in this study, the genes responsible for lipolysis and lipogenesis were measured in both genders and genotypes. *Hsl* and *Adrb3* genes in iWAT were analyzed and showed no alteration in gene expression in the offspring. In gWAT, the *Hsl* and *Acc1* genes also did not change. This unaltered lipid metabolism in the offspring is probably a consequence of the unchanged metabolic rate in the offspring. Interestingly, however, iWAT and gWAT tissue weights were significantly decreased in the offspring, which may indicate fetal reprogramming in these tissues after maternal T3 treatment. The molecular mechanisms remain unclear, and further studies are required to determine the cause and consequences of this effect.

4.3.4 Effect on Glucose Tolerance

Next, the effect of maternal hyperthyroidism on fetal programming of glucose tolerance in the offspring was investigated (Table 29). The glucose tolerance test measures the clearance of

a glucose load from the body (Pedro, Tsakmaki, and Bewick 2020), however, no differences were found between treated and untreated animals.

Table 29: Summary table of the effects of maternal T3 treatment effect during pregnancy on glucose tolerance in the offspring.

	TRα1+/+			TRα1+/m		
	Control	T3 treatment		Control	T3 treatment	
Characteristic		1st half	2nd half		1st half	2nd half
Glucose tolerance	m	no effect	no effect	m	no effect	no effect
	f	no effect	no effect	f	no effect	no effect

Abbreviations: **no effect**: not significant; **m**: male; **f**: female

Sjörgen et al. (2007) demonstrated that TRα1+/m mice have enhanced insulin sensitivity, which accelerates glucose clearance in these mice. They also showed that glucose clearance in TRα1+/m mice is not altered by T3 treatment.

In this study, the same result was obtained. No significant changes in basal glucose tolerance were observed in the offspring of T3-treated dams compared to the control group during the different pregnancy periods in both genders and both genotypes. This suggests that maternal T3 treatment has no effect on fetal programming of glucose metabolism in prenatal life.

4.3.5 Effect on Body Composition

THs play a crucial role in the normal development of the body composition of the fetus and thus of the adult offspring. During pregnancy, maternal thyroid hormones are partially permeable through the placenta. This transfer of maternal thyroid hormones to the fetus in combination with fetal production of thyroid hormones is very critical for fetal development and may have implications for body composition in the offspring (Möllers et al. 2021). To investigate the effects of maternal TH during different periods of pregnancy on the offspring in more detail, body composition was measured in this study. In addition, to obtain more precise information about the fat mass, three different adipose tissues of these offspring were weighed and the values were normalized to their body weight (Table 30).

Table 30: Summary table of the effects of maternal T3 treatment during pregnancy on body composition in the offspring.

Characteristics		TRα1+/+			TRα1+/m		
		Control	T3 treatment		Control	T3 treatment	
			1st half	2nd half		1st half	2nd half
Body composition	Lean	m	****↓	****↓	m	**↓	**↓
		f	no effect	no effect	f	no effect	no effect
	Free body fluid	m	****↓	****↓	m	no effect	no effect
		f	no effect	no effect	f	no effect	no effect
	Fat	m	no effect	no effect	m	no effect	no effect
		f	no effect	no effect	f	no effect	no effect
Adipose tissue weight	iWAT	m	no effect	***↓	m	**↓	**↓
		f	no effect	*↓	f	*↓	*↓
	gWAT	m	****↓	****↓	m	no effect	no effect
		f	****↓	****↓	f	*↓	*↓
	iBAT	m	no effect	no effect	m	no effect	no effect
		f	no effect	no effect	f	no effect	no effect

Abbreviations: **iWAT**: intrascapular white adipose tissue; **gWAT**: gonadal white adipose tissue; **iBAT**: intrascapular brown adipose tissue; **no effect**: not significant; **m**: male; **f**: female; *** – ****:** significant alteration (arrow down indicates a decrease); $p<0.05$ (*), $p<0.01$ (**), $p<0.001$ (***) and $p<0.0001$ (****).

It has been published that TRα1+/m mice exhibit a transient growth delay (Bassett and Williams 2009), which is normalized after treatment with 10-fold T3 (Yen 2001). In this study, maternal T3 treatment resulted in hypermetabolism in wildtype and TRα1+/m offspring, including a reduction of lean mass.

Furthermore, a significant reduction in iWAT and gWAT tissue weight was observed in the offspring, while total fat mass was not altered between the genotypes of both genders. The reduction in white fat depots while total fat mass remained unchanged could be related to the different methods used to assess fat composition. Total fat mass includes all fat depots of the body and quantifies just the fat component of the tissue, while tissue weights were measured with a scale and thus are restricted to these tissues and also include non-fat components such as water. Another quite plausible explanation would be that the two main white fat depots were reduced, while other minor fat deposition in the body may have increased. This possible redistribution of fat needs to be further investigated.

4.3.6 Effect on Locomotor Activity

Recently, some studies provided moderate evidence that maternal hypothyroidism during prenatal pregnancy may contribute to the development of attention-deficit hyperactivity disorder (ADHD), particularly characterized by hyperactivity and impulsivity in children. This association should be strongest in boys compared to girls (Drover et al. 2019; Peltier et al. 2021). Moreover, it is known that in the TRα1+/m mouse model, the number of parvalbumin (PV) neurons in the hippocampus is significantly reduced, leading to a massive locomotor deficiency in the mice (Tinnikov et al. 2002; Wallis et al. 2008). Therefore, the next aim in this study was to investigate the effect of maternal T3 treatment on locomotor activity in this offspring.

Impressively, in this study, maternal T3 treatment in the second half of pregnancy was observed to significantly increase locomotor activity in male offspring of both genotypes, while it was significantly reduced in female TRα1+/m offspring (Table 31).

The cause for the difference between the sexes is unclear. Mice are born earlier compared to humans due to the lack of a third trimester in mice. For this reason, it is difficult to explore the reason of this variation. However, the effect of sex hormones on neuronal locomotor function could be related to this difference (Rewal et al. 2003).

Table 31: Summary table of the effects of maternal T3 treatment during pregnancy on locomotor activity in the offspring.

		TRα1+/+			TRα1+/m		
		Control	T3 treatment		Control	T3 treatment	
Characteristic			1st half	2nd half		1st half	2nd half
Locomotor activity	m	no effect	∗∗↑		m	no effect	∗↑
	f	no effect	no effect		f	∗∗↓	∗∗∗∗↓

Abbreviations: **no effect**: not significant; **m**: male; **f**: female; **∗ – ∗∗∗∗:** significant alteration (arrow up indicates an increase and arrow down a decrease); $p<0.05$ (∗), $p<0.01$ (∗∗) and $p<0.0001$ (∗∗∗∗).

Another reason for the increased locomotor activity in the male offspring may be due to a significant increase in muscle mass (muscle soleus and gastrocnemius) in these offspring. The muscle mass of the male offspring increased significantly after maternal T3 treatment in the second half of pregnancy compared to the control group. Meanwhile, the female offspring of both genotypes showed a reduction in locomotor activity, especially in the second half of

pregnancy, although muscle mass increased significantly during this period. These differences should be further investigated in the structure of the muscles of female offspring.

4.3.7 Effect on Glucose and Lipid Utilization

The liver is also a well-known target organ that can be directly and centrally regulated by thyroid hormones (Klieverik et al. 2009; Sentis, Oelkrug, and Mittag 2021).

To address glucose and lipid utilization in the liver after maternal T3 treatment during different periods of pregnancy, some T3-bound thyroid receptors (TRs) that activate genes such as those for phosphoenolpyruvate carboxykinase (*Pepck*), phosphoenolpyruvate carboxylase (*Pyrkl*), and acetyl-CoA carboxylase 1 (*Acc1*) in the liver were measured.

In this study, maternal T3 treatment was found that to increase free-fatty acid (FFA) levels, indicating enhanced lipid mobilization, possibly leading to increased β-oxidation. Furthermore, maternal T3 treatment enhanced gluconeogenesis and glycolysis (Sjögren et al. 2007) (Table 32).

Table 32: Summary table of the effects of maternal T3 treatment during pregnancy on glucose and lipid utilization in the offspring.

		TRα1+/+			TRα1+/m		
		Control	T3 treatment		Control	T3 treatment	
Characteristics			1st half	2nd half		1st half	2nd half
Gluconeogenesis *Pepck*	m	no effect	no effect	m	no effect	****↑
	f	no effect	no effect	f	*↑	*↑
Glycolysis *Pyrkl*	m	no effect	**↑	m	*↑	*↑
	f	no effect	no effect	f	no effect	no effect
Lipogenesis *Fasn*	m	*↓	**↑	m	**↑	****↑
	f	no effect	no effect	f	no effect	no effect
Lipolysis *Acc1*	m	no effect	no effect	m	*↑	no effect
	f	no effect	no effect	f	no effect	no effect

Abbreviations: ***Pepck***: Phosphoenolpyruvate carboxykinase; ***Pyrkl:*** Phosphoenolpyruvate carboxylase; ***Fasn:*** Fatty acid synthesis; ***Acc1:*** Acetyl-coenzyme A carboxylase 1; **no effect**: not significant; **m**: male; **f**: female; *** – ****:** significant alteration (arrow up indicates an increase and arrow down a decrease); $p<0.05$ (*), $p<0.01$ (**) and $p<0.0001$ (****).

Interestingly, the promotion of enhanced glucose and lipid utilization was detected mainly in male TRα1+/m offspring. These results indicate an improvement in glucose and lipid utilization during fetal programming in the TRα1+/m offspring compared with the control

group. In contrast, this improvement in metabolism did not result in a positive effect on DEE, RQ and O_2 consumption. Therefore, these ambiguities require further investigation.

In the metabolic part of this study, a minor metabolic alteration was detected, such as reduced WAT depots, accompanied by changes in gene expression suggesting improved glucose and lipid metabolism. This modification could be triggered by the somewhat increased overall locomotor activity in the offspring treated during the second half of pregnancy; however, the changes were not profound enough to be detected in daily energy expenditure.

5. CONCLUSION AND CLINICAL RELEVANCE

Since there is relatively high incidence of thyroid disorders in pregnant women (Korevaar et al., 2017), the possibly detrimental consequences of alteration in maternal TH signaling on fetal programming and its effects on the offspring should not be neglected. This study for the first time investigated the effect of maternal T3 treatment in wildtype and TRα1+/m mice during different periods of pregnancy on growth, cardiovascular system and metabolic function in male and female offspring.

The main finding of this study was that maternal TH signaling - in particular in the second half of pregnancy - is important for establishing cardiac properties in the adult offspring. These findings are of particular clinical relevance, as cardiovascular disorders are a major health concern in our society; however, there is still a controversial discussion about whether pregnant women should be routinely tested for thyroid disorders (Poppe et al., 2021).

Unfortunately, current arguments against routine testing are largely based on studies with psychological and motoric endpoints, which revealed no major disturbances by subclinical maternal thyroid dysfunctions.

Our study now advocates for the inclusion of cardiovascular endpoints in these human studies, as they seem to be more readily affected, and also underlines the necessity to study endocrine disrupting compounds during pregnancy (Gore et al., 2015).

Furthermore, the data in our study also demonstrate that maternal T3 treatment in the second half of pregnancy also significantly increases locomotor activity in male offspring. This finding serves as an important reminder to avoid maternal TH overtreatment in pregnant women, as it could lead to a hyperactivity disorder in the children resembling attention deficit hyperactivity disorder (ADHD) (Rewal et al., 2003).

.

6. SUPPLEMENTS

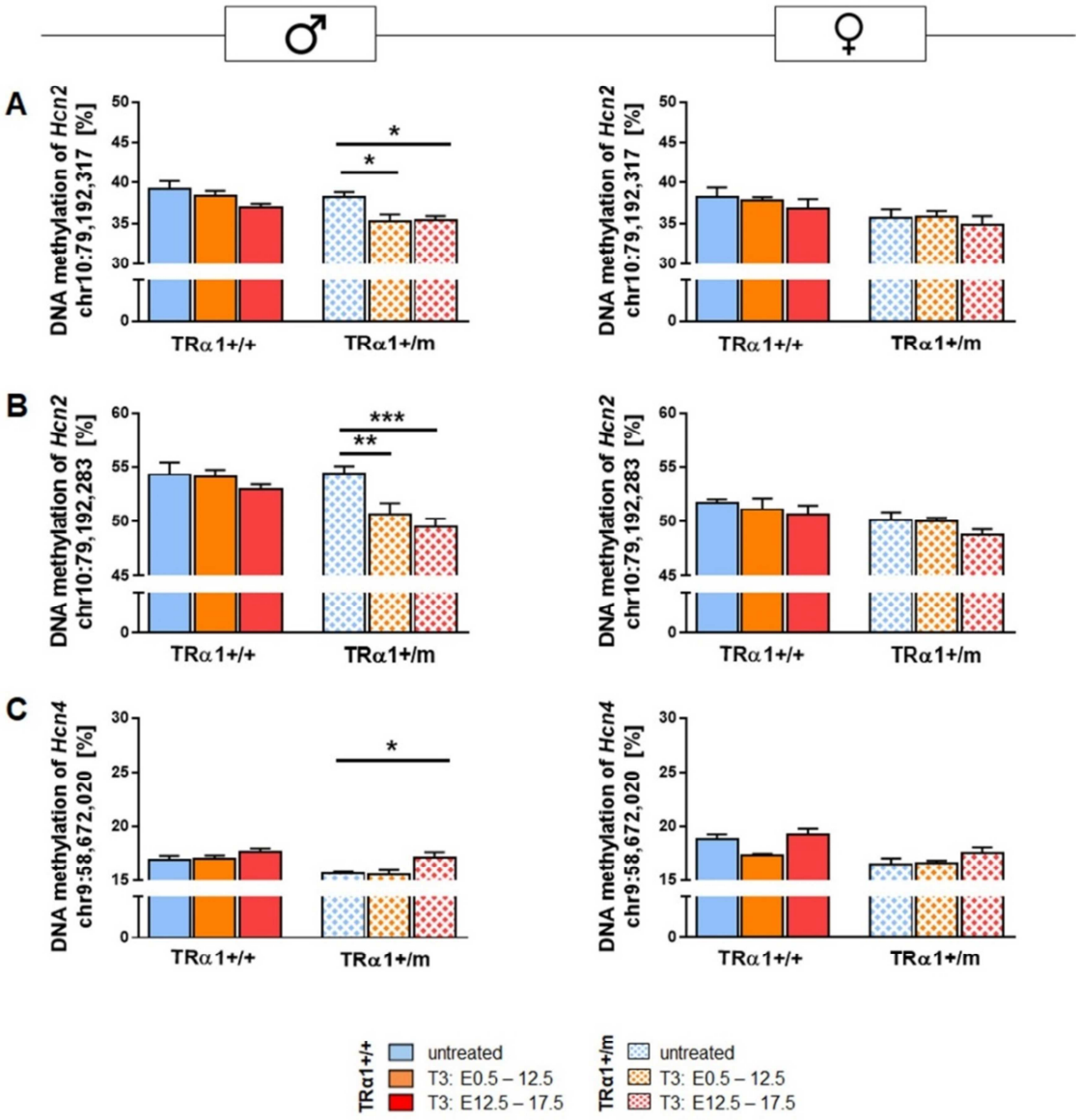

Figure supplement 1: Cytosine-methylation quantification by bisulfite-pyrosequencing. Genomic DNA was extracted from snap-frozen heart of adult male and female offspring, whose dams were treated with T3 either in the first half (orange) or in the second half of pregnancy (red) compared with the control group (blue). DNA methylation of *Hcn2* was measured within the fourth intron. DNA methylation at CpG site **A)** chr10:79,192,317, **B)** chr10: 79,192,283. DNA methylation of *Hcn4* was analyzed within exon 1. DNA methylation in CpG site **C)** chr9:58,672,020. All values are shown as mean ± SEM and were analyzed with two-way ANOVA with Holm-Sidak's multiple comparisons test. $p<0.05$ (*), $p<0.01$ (**) and $p<0.001$ (***); n=6 for each group. The figures were adapted from "Pedaran et al. 2021 Thyroid".

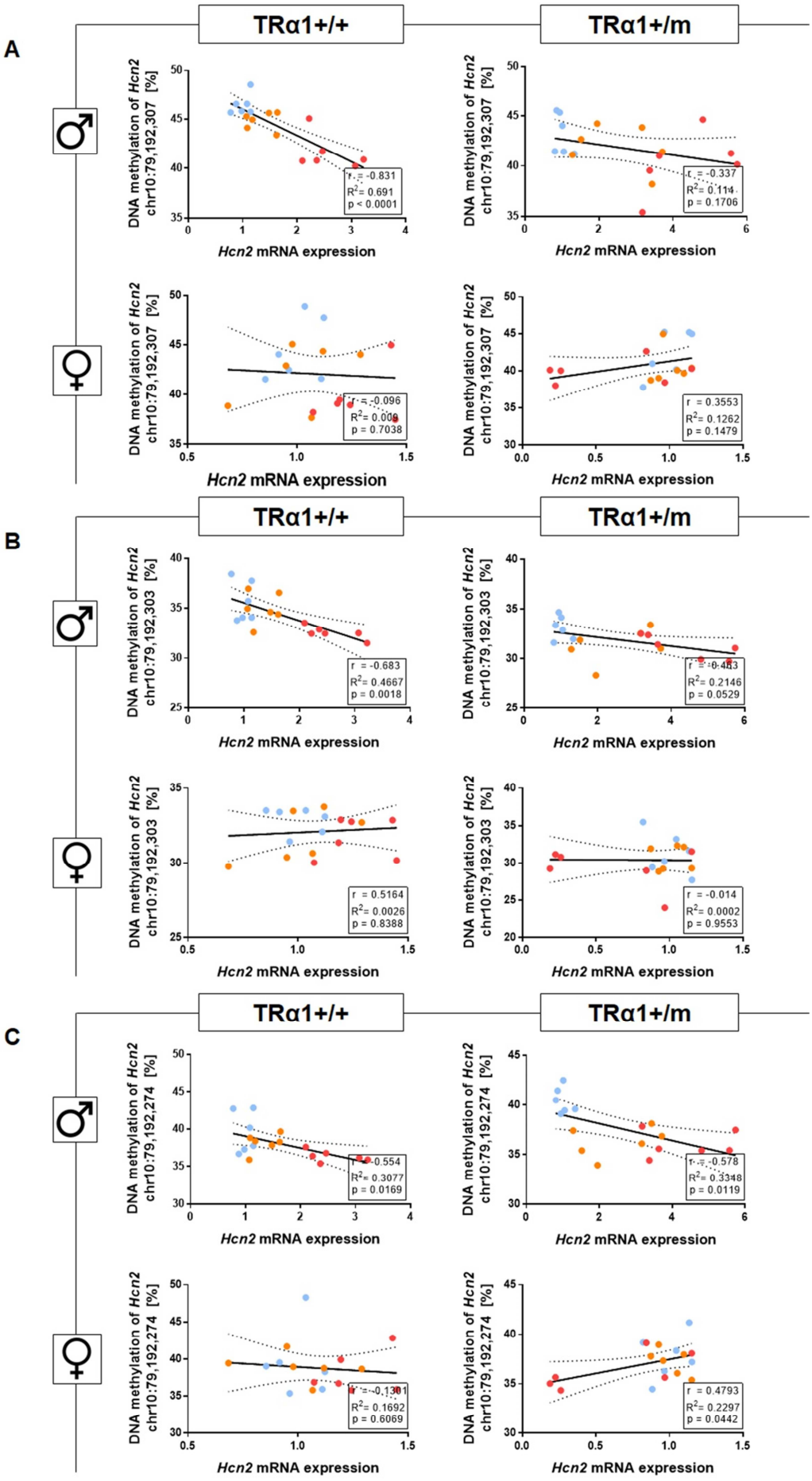
A
TRα1+/+
TRα1+/m
DNA methylation of Hcn2 chr10:79,192,307 [%]
Hcn2 mRNA expression
r = -0.831
R2= 0.691
p < 0.0001
r = -0.337
R2= 0.114
p = 0.1706
r = -0.096
R2= 0.009
p = 0.7038
r = 0.3553
R2= 0.1262
p = 0.1479
B
TRα1+/+
TRα1+/m
DNA methylation of Hcn2 chr10:79,192,303 [%]
Hcn2 mRNA expression
r = -0.683
R2= 0.4667
p = 0.0018
r = -0.463
R2= 0.2146
p = 0.0529
r = 0.5164
R2= 0.0026
p = 0.8388
r = -0.014
R2= 0.0002
p = 0.9553
C
TRα1+/+
TRα1+/m
DNA methylation of Hcn2 chr10:79,192,274 [%]
Hcn2 mRNA expression
r = -0.554
R2= 0.3077
p = 0.0169
r = -0.578
R2= 0.3348
p = 0.0119
r = -0.1301
R2= 0.1692
p = 0.6069
r = 0.4793
R2= 0.2297
p = 0.0442

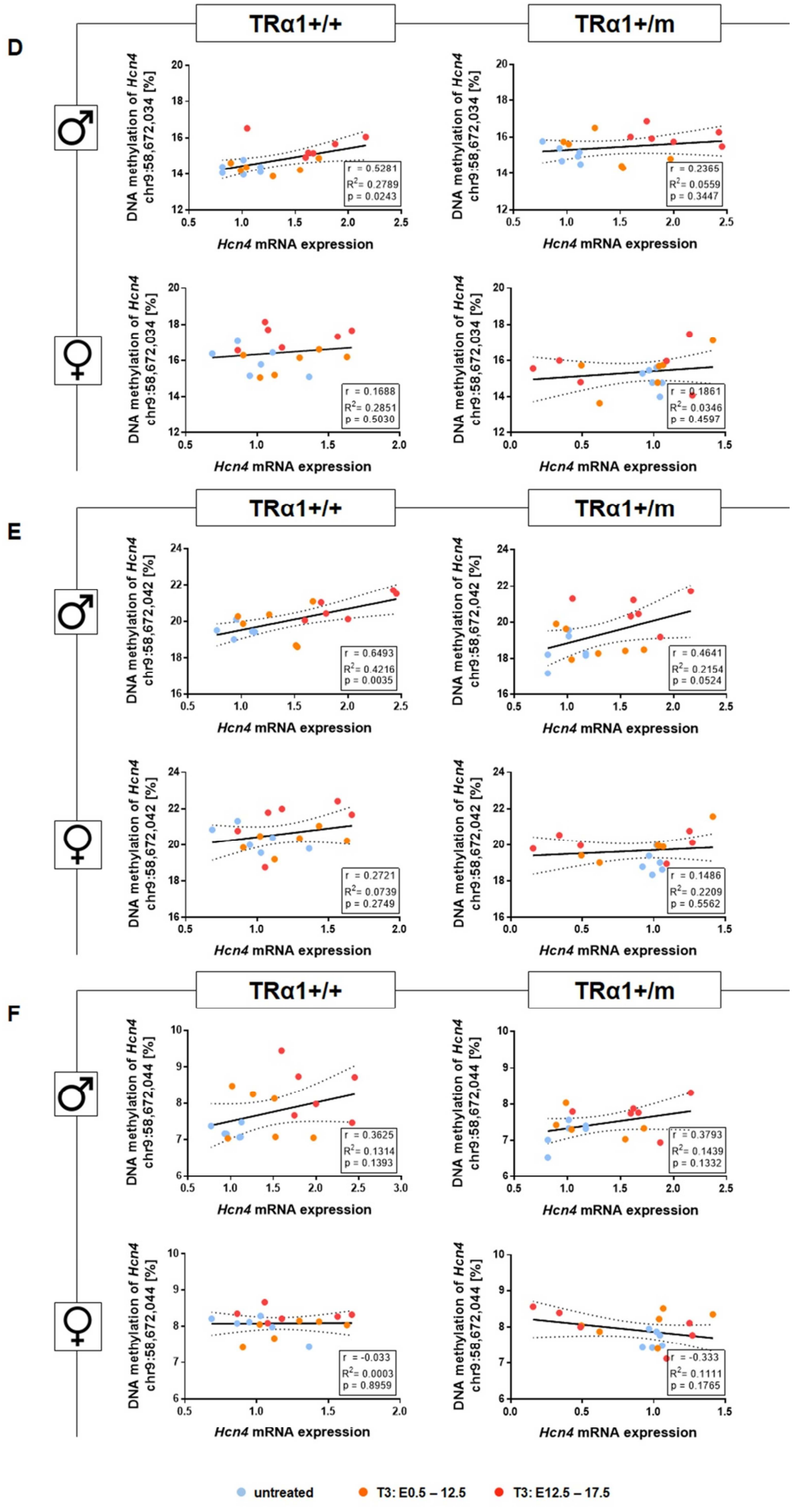
D
TRα1+/+
TRα1+/m
DNA methylation of Hcn4 chr9:58,672,034 [%]
Hcn4 mRNA expression
r = 0.5281
R²= 0.2789
p = 0.0243
r = 0.2365
R²= 0.0559
p = 0.3447
r = 0.1688
R²= 0.2851
p = 0.5030
r = 0.1861
R²= 0.0346
p = 0.4597
E
TRα1+/+
TRα1+/m
DNA methylation of Hcn4 chr9:58,672,042 [%]
Hcn4 mRNA expression
r = 0.6493
R²= 0.4216
p = 0.0035
r = 0.4641
R²= 0.2154
p = 0.0524
r = 0.2721
R²= 0.0739
p = 0.2749
r = 0.1486
R²= 0.2209
p = 0.5562
F
TRα1+/+
TRα1+/m
DNA methylation of Hcn4 chr9:58,672,044 [%]
Hcn4 mRNA expression
r = 0.3625
R²= 0.1314
p = 0.1393
r = 0.3793
R²= 0.1439
p = 0.1332
r = -0.033
R²= 0.0003
p = 0.8959
r = -0.333
R²= 0.1111
p = 0.1765
untreated
T3: E0.5 – 12.5
T3: E12.5 – 17.5

Figure supplement 2: Correlation analysis of pacemaker gene expression with DNA methylation in male and female offspring. Control offspring are shown in blue dots, and the offspring whose dams were treated with T3 in the first half of pregnancy in orange and in the second half in red. The correlation analysis of *Hcn2* gene expression with *Hcn2* DNA methylation in the offspring at CpG site **A)** chr10:79,192,307, **B)** chr10: 79,192,303 and **C)** chr10,79,192,274. The same correlation analysis for *Hcn4* gene expression with *Hcn4* DNA methylation in the offspring at CpG site **D*)*** chr9:58,672,034, **E)** chr9: 58,672,042 and **F)** chr9: 58,672,044. The respective raw p value is given in the figure (r: Pearson correlation coefficient; R^2: coefficient of determination; p: p-value; dashed lines indicate 95% confidence interval); n=6 for each group.

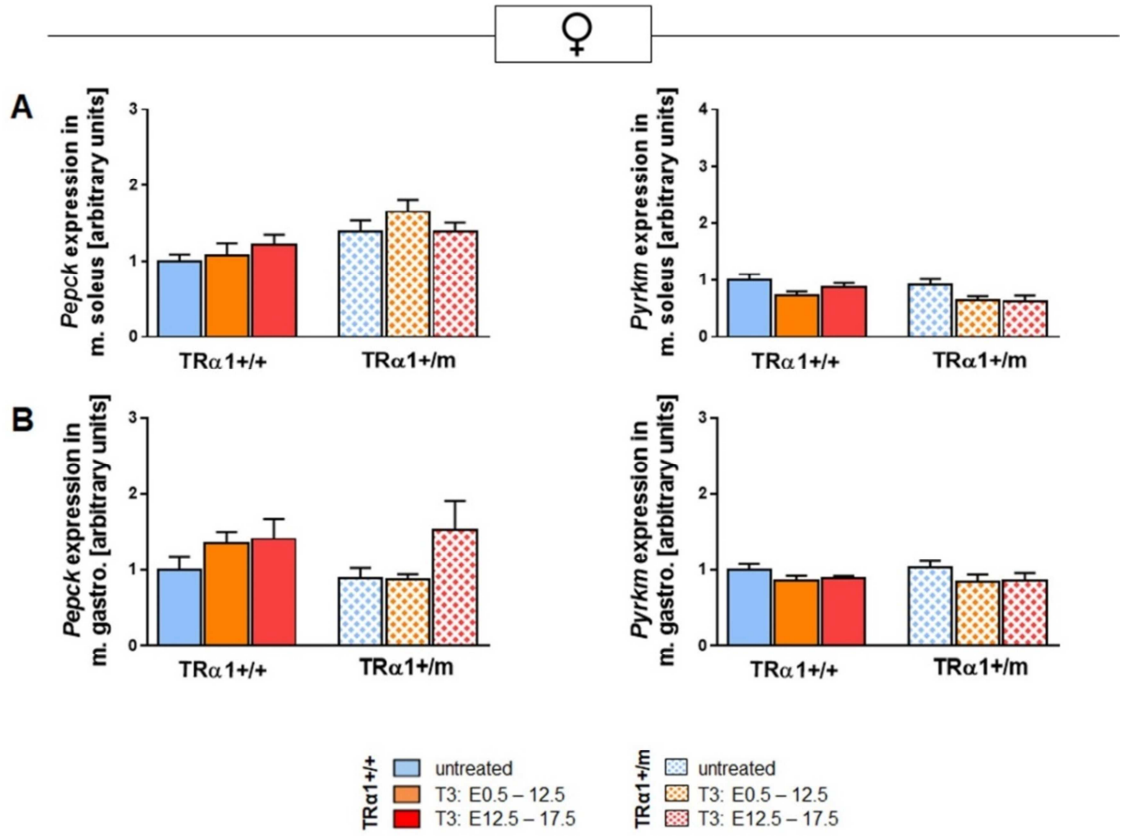

Figure supplement 3: Gene expression of proteins involved in glucose uptake and metabolism in female offspring. Gene expression of proteins involved in glucose metabolism in female offspring whose dams were treated with T3 either in the first half (orange) or in the second half of pregnancy (red) compared to control group (blue). **A)** *Pepck* (phosphoenolpyruvate carboxylase) and *Pyrkm* (Phosphoenolpyruvate Carboxylase for muscle) in muscle soleus and **B)** muscle gastrocnemius. All values are shown as mean ± SEM and were analyzed with two-way ANOVA with Holm-Sidak's multiple comparisons test; n=6 for each group.

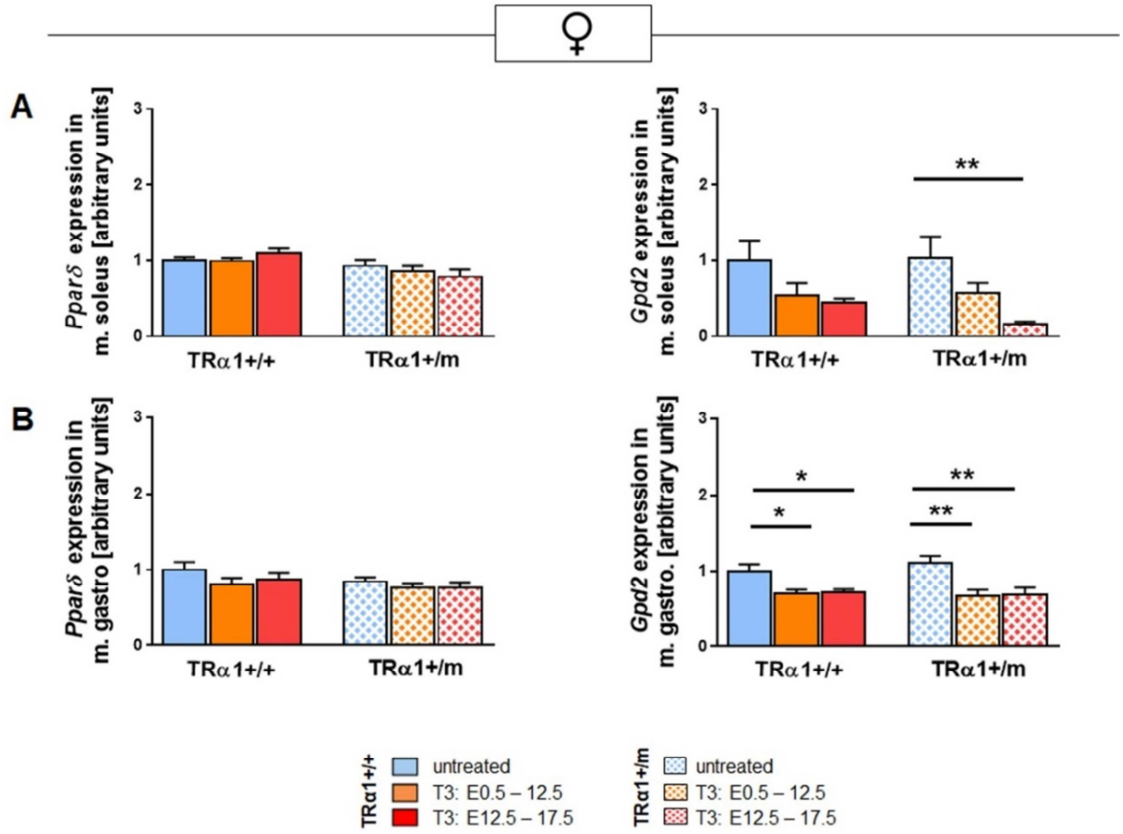

Figure supplement 4: Gene expression of proteins involved in β-oxidation and oxidative phosphorylation in female offspring. Investigation of the gene expression in female offspring whose dams were treated with T3 in either the first half (orange) or in the second half of pregnancy (red) compared to the control group (blue). *Pparδ* (Peroxisome proliferator-activated receptor delta) and *Gpd2* (Glycerol 3-phosphate dehydrogenase) were measured in **A)** muscle soleus and **B)** muscle gastrocnemius of female offspring. All values are shown as mean ± SEM and were analyzed with two-way ANOVA with Holm-Sidak's multiple comparisons test. $p<0.05$ (*) and $p<0.01$ (**); n=6 for each group.

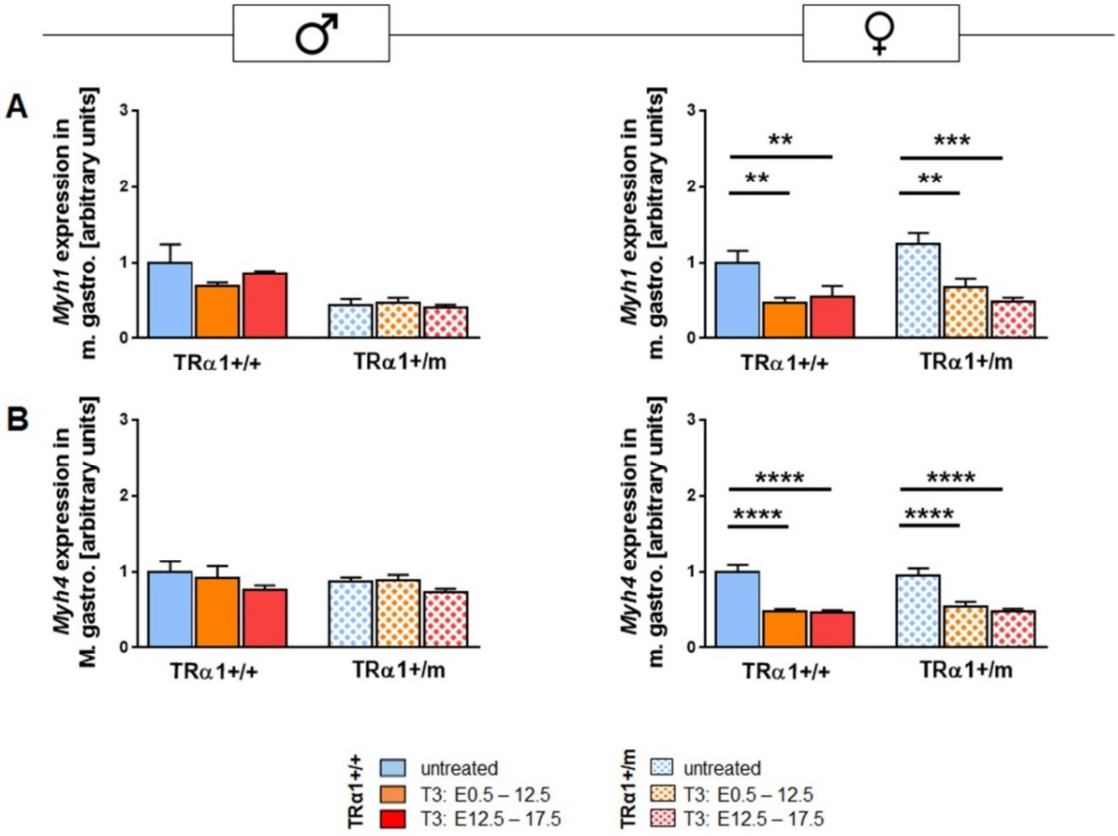

Figure supplement 5: Gene expression of Myh1 and Myh4 in muscle gastrocnemius of offspring. Gene expression in adult male and female offspring of control dams (blue) or dams either treated with T3 in the first (orange) or second half of pregnancy (red) of **A)** *Myh1* (Myosin heavy chain 1) and **B)** *Myh4* (Myosin heavy chain 4) in muscle gastrocnemius. All values are shown as mean ± SEM and were analyzed with two-way ANOVA with Holm-Sidak's multiple comparisons test. $p<0.01$ (**); $p<0.001$ (***) and $p<0.0001$ (****); n=6 for each group.

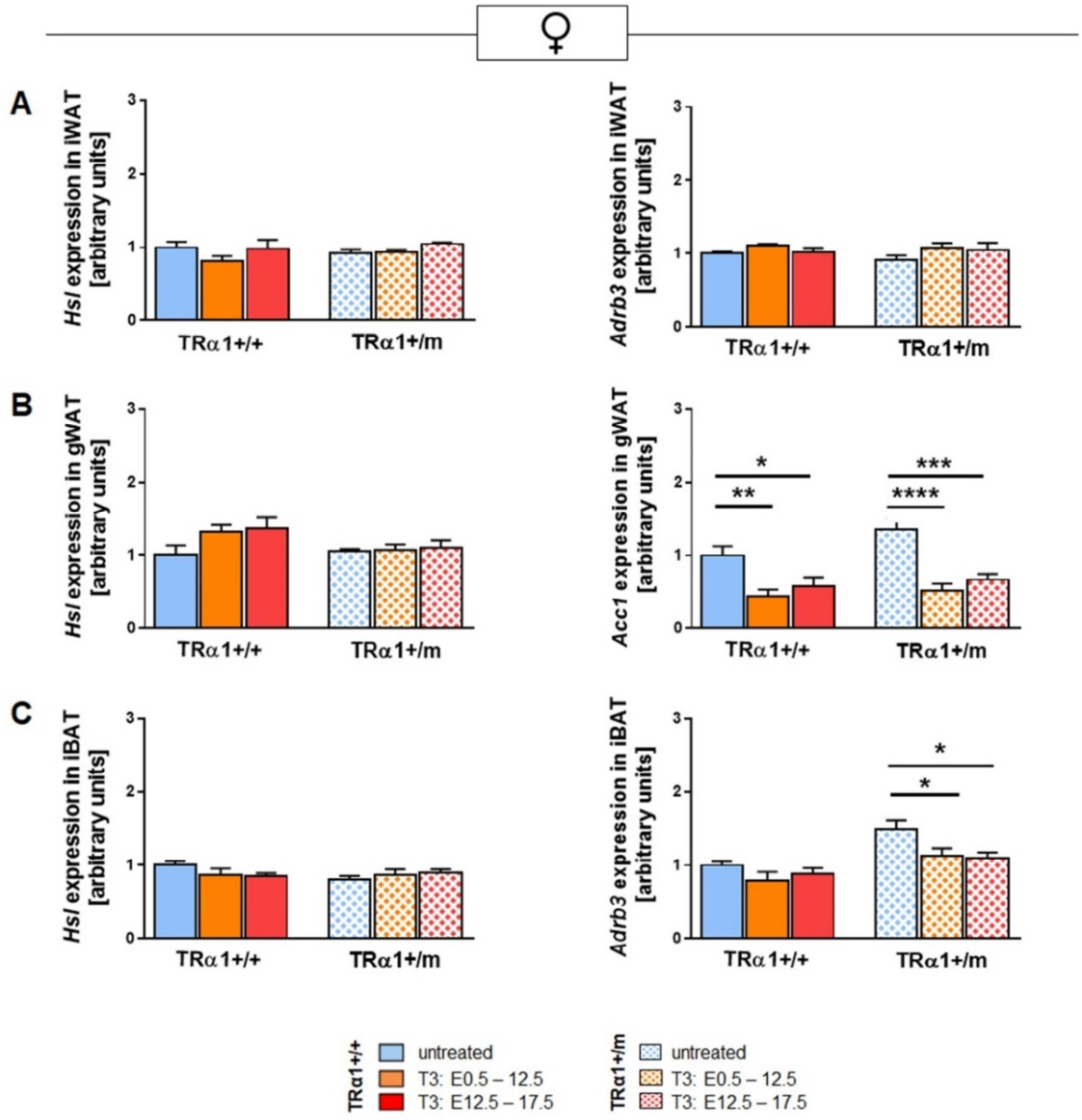

Figure supplement 6: Determination of molecular alterations in iWAT, gWAT and iBAT in female offspring. Gene expression of proteins involved in lipid metabolism in female offspring whose dams were treated with T3 either in the first half (orange) or in the second half of pregnancy (red) compared to the control group (blue). **A)** *Hsl* (hormone sensitive lipase) and *Adrb3* (beta 3-adrenergic receptor) in iWAT, **B)** *Hsl* (hormone sensitive lipase) and *Acc1* (acetyl-Coenzyme A carboxylase 1) in gWAT **C)** *Hsl* (hormone sensitive lipase) and *Adrb3* (beta 3-adrenergic receptor) in iBAT were analyzed. All values are shown as mean ± SEM and were analyzed with two-way ANOVA with Holm-Sidak's multiple comparisons test. $p<0.05$ (*), $p<0.01$ (**), $p<0.001$ (***) and $p<0.0001$ (****); n=6 for each group.

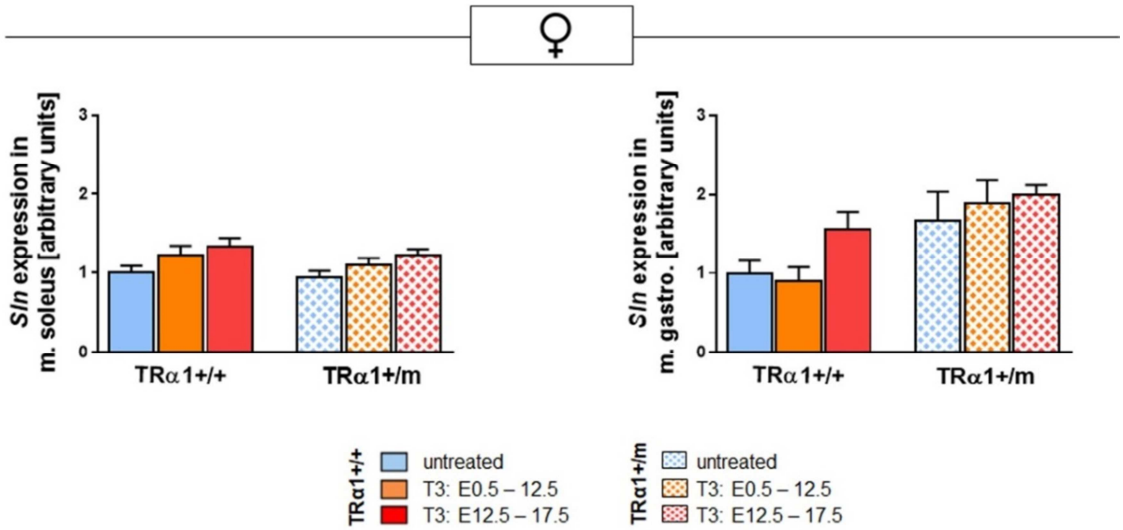

Figure supplement 7: Sln (Sarcolipin) expression in muscle soleus and gastrocnemius of adult female offspring. Dams were treated with T3 either in the first (orange) or second half of pregnancy (red) and compared to the control group (blue). All values are shown as mean ± SEM and were analyzed with two-way ANOVA with Holm-Sidak's multiple comparisons test; n=6 for each group.

7. TABLE OF STATISTICAL ANALYSIS

For statistical analysis, the data were analyzed using two-way ANOVA with post-hoc Holm-Sidak test for differences among genders and genotypes of the offspring to examine the effects of maternal T3 treatment during different periods of pregnancy compared to the control group. Males and females were tested separately. All values are represented as mean ± SEM. Statistical significance was defined as $p < 0.05$ (*), $p < 0.01$ (**), $p < 0.001$ (***) and $p < 0.0001$ (****) (Statistical Analysis Table 1).

Furthermore, the correlation between heart rate and gene expression as well as between gene expression and DNA methylation was analyzed using Pearson correlation coefficient (Pearson r) (Statistical Analysis Table 2).

Statistical Analysis Table 1: Two-way ANOVA with Holm-Sidak post-hoc Test was used for the statistical analysis of the following parameters.

			two-way ANOVA			Holm-Sidak post-hoc Test			
						TRα1+/+		TRα1+/m	
			Interaction	Genotype	Treatment	H_2O vs. T3 1st half	H_2O vs. T3 2nd half	H_2O vs. T3 1st half	H_2O vs. T3 2nd half
Figure 7	Body weight	m	0.107948 ns	000000 ns	0.117454 ns	ns	ns	ns	ns
		f	0.098671 ns	000000 ns	0.756839 ns	ns	ns	ns	ns
Figure 8A	Body length	m	0.9430 ns	<0.0005 ***	>0.9999 ns	ns	ns	ns	ns
		f	0.9045 ns	<0.0001 ****	0.3689 ns	ns	ns	ns	ns
Figure 8B	Hepatic *Igf1*	m	0.6238 ns	0.4173 ns	0.1991 ns	ns	ns	ns	ns
		f	0.7112 ns	0.3148 ns	0.3148 ns	ns	ns	ns	ns
Figure 8C	Pituitary *Gh*	m	0.5253 ns	0.8756 ns	0.4839 ns	ns	ns	ns	ns
		f	0.3935 ns	0.3587 ns	0.2234 ns	ns	ns	ns	ns
Figure 9A	systolic	m	0.5845 ns	0.1107 ns	0.182 ns	ns	ns	ns	ns
		f	0.0965 ns	0.4379 ns	0.0031 **	ns	ns	ns	**

			two-way ANOVA			Holm-Sidak post-hoc Test			
						TRα1+/+		TRα1+/m	
			Interaction	Genotype	Treatment	H_2O vs. T3 1st half	H_2O vs. T3 2nd half	H_2O vs. T3 1st half	H_2O vs. T3 2nd half
Figure 9B	diastolic	m	0.9004 ns	<0.0001 ****	0.4207 ns	ns	ns	ns	ns
		f	0.6066 ns	<0.0001 ****	0.0107 *	ns	ns	ns	*
Figure 9C	MAP	m	0.181 ns	0.2376 ns	0.0161 *	ns	**	ns	ns
		f	0.1077 ns	<0.0001 ****	<0.0001 ****	ns	*	ns	***
Figure 9D	Heart rate	m	0.01 *	<0.0001 ****	<0.0001 ****	ns	****	*	**
		f	0.3605 ns	<0.0001 ****	0.007 **	ns	ns	ns	**
Figure 9E	Heart weight	m	<0.0001 ****	<0.0001 ****	0.092 ns	**	****	**	**
		f	0.7793 ns	<0.0001 ****	0.0004 ***	ns	**	ns	*
Figure 10A	Pulmonary *Ace*	m	0.3529 ns	0.6315 ns	0.0672 ns	ns	*	ns	ns
		f	0.4106 ns	0.0325 *	0.5623 ns	ns	ns	ns	ns
Figure 10B	Hepatic *Agt*	m	0.0002 ***	<0.0001 ****	<0.0001 ****	ns	ns	*	****
		f	0.4616 ns	<0.0001 ****	0.0529 ns	ns	ns	ns	ns
Figure 11A	Cardiac *Serca2*	m	0.0007 ***	0.0002 ***	<0.0001 ****	*	****	****	****
		f	0.7787 ns	0.0126 *	<0.0001 ****	ns	**	*	***
Figure 11B	Cardiac *α-Mhc*	m	<0.0001 ****	0.0030 **	<0.0001 ****	****	****	****	****
		f	0.2510 ns	0.0169 *	0.1107 ns	ns	ns	ns	ns
Figure 11C	Cardiac *β-Mhc*	m	<0.0001 ****	<0.0001 ****	<0.0001 ****	ns	***	****	****
		f	<0.0001 ****	0.0005 ***	<0.0001 ****	ns	ns	****	****
Figure 11D	Cardiac *Hcn2*	m	0.9310 ns	0.0001 ***	<0.0001 ****	ns	***	ns	***
		f	<0.0001 ****	<0.0001 ****	<0.0001 ****	ns	**	ns	****
Figure 11E	Cardiac *Hcn4*	m	0.1161 ns	0.0017 **	<0.0001 ****	*	****	****	****
		f	0.2222 ns	0.0789 ns	0.0005 ***	ns	ns	ns	***

			two-way ANOVA			Holm-Sidak post-hoc Test			
						TRα1+/+		TRα1+/m	
			Interaction	Genotype	Treatment	H_2O vs. T3 1st half	H_2O vs. T3 2nd half	H_2O vs. T3 1st half	H_2O vs. T3 2nd half
Figure 12A	HCN2 Protein level	m	0.3781 ns	0.5760 ns	<0.0001 ****	ns	****	ns	**
		f	0.7706 ns	0.2706 ns	0.0294 *	ns	*	ns	ns
Figure 12B	HCN4 Protein level	m	0.0478 *	<0.0001 ****	<0.0001 ****	**	****	ns	ns
		f	0.3700 ns	0.8067 ns	0.1940 ns	ns	ns	ns	ns
Figure 14A	*Hcn2* DNA methyl.	m	0.6126 ns	<0.0001 ****	<0.0001 ****	ns	***	ns	**
		f	0.5674 ns	0.2236 ns	0.0118 *	ns	*	ns	ns
Figure 14B	*Hcn2* DNA methyl.	m	0.1828 ns	<0.0001 ****	0.0010 **	ns	**	ns	ns
		f	0.7433 ns	0.0161 *	0.1721 ns	ns	ns	ns	ns
Figure 14C	*Hcn2* DNA methyl.	m	0.1368 ns	0.4029 ns	<0.0001 ****	ns	**	**	***
		f	0.8582 ns	0.0227 *	0.1814 ns	ns	ns	ns	ns
Figure 14D	*Hcn4* DNA methyl.	m	0.6386 ns	0.0005 ***	<0.0001 ****	ns	*	ns	**
		f	0.2218 ns	0.0009 ***	0.0170 *	ns	*	ns	ns
Figure 14E	*Hcn4* DNA methyl.	m	0.2717 ns	0.0090 **	<0.0001 ****	ns	*	ns	****
		f	0.0330 *	0.0004 ***	0.0005 ***	ns	**	*	*
Figure 14F	*Hcn4* DNA methyl.	m	0.4248 ns	0.0513 ns	0.0036 **	ns	**	ns	ns
		f	0.1378 ns	0.0956 ns	0.0666 ns	ns	ns	ns	ns
Figure 15A	Serum T3 total	m	0.0006 ***	0.5687 ns	<0.0001 ****	ns	ns	****	****
		f	0.5052 ns	0.6111 ns	0.1035 ns	ns	ns	ns	ns
Figure 15B	Serum T4 total	m	0.6015 ns	0.9427 ns	0.2332 ns	ns	ns	ns	ns
		f	0.9881 ns	<0.0001 ****	0.5462 ns	ns	ns	ns	ns
Figure 15C	Pituitary *Tshb*	m	0.857 ns	0.0006 ***	0.1379 ns	ns	ns	ns	ns
		f	0.4384 ns	<0.0001 ****	0.2558 ns	ns	ns	ns	ns

			two-way ANOVA			Holm-Sidak post-hoc Test			
						TRα1+/+		TRα1+/m	
			Interaction	Genotype	Treatment	H_2O vs. T3 1st half	H_2O vs. T3 2nd half	H_2O vs. T3 1st half	H_2O vs. T3 2nd half
Figure 15D	**Pituitary *Dio2***	**m**	0.1745 ns	0.3835 ns	0.4745 ns	ns	ns	ns	ns
		f	0.0698 ns	0.9917 ns	0.8033 ns	ns	ns	ns	ns
Figure 16A	**Hepatic *Dio1***	**m**	0.9706 ns	<0.0030 **	0.1306 ns	ns	ns	ns	ns
		f	0.8161 ns	0.1579 ns	0.1459 ns	ns	ns	ns	ns
Figure 16B	**Hepatic DIO1 activity**	**m**	0.6852 ns	<0.0001 ****	0.0155 *	ns	ns	ns	ns
		f	0.2521 ns	0.0018 **	0.0473 *	ns	ns	ns	ns
Figure 16C	**Hepatic *Spot14***	m	0.1908 ns	<0.0001 ****	0.0072 **	ns	ns	ns	**
		f	0.0828 ns	0.0297 *	<0.0001 ****	****	****	****	****
Figure 17A	**Hepatic Se levels**	m	0.5202 ns	0.5913 ns	0.1664 ns	ns	ns	ns	ns
		f	0.9771 ns	0.0764 ns	0.9657 ns	ns	ns	ns	ns
Figure 17B	**Hepatic Cu levels**	m	0.7043 ns	0.0073 **	0.0569 ns	ns	ns	ns	ns
		f	0.6623 ns	0.1665 ns	0.4129 ns	ns	ns	ns	ns
Figure 17C	**Hepatic GPx1 activity**	m	0.9234 ns	0.01427 ns	0.1938 ns	ns	ns	ns	ns
		f	0.2156 ns	0.6731 ns	0.3291 ns	ns	ns	ns	ns
Figure 17D	**Serum Se levels**	m	0.0164 *	0.146 *	<0.0001 ****	***	***	**	****
		f	0.0157 *	<0.0001 ****	0.0013 **	ns	****	ns	ns
Figure 17E	**Serum Cu levels**	m	0.4821 ns	0.0906 **	0.4883 ns	ns	ns	ns	ns
		f	0.2576 ns	0.0026 **	0.0113 *	ns	**	ns	ns
Figure 18A/B	**Glucose tolerance**	m	0.5667 ns	<0.0001 ****	0.4839 ns	ns	ns	ns	ns
		f	0.2644 ns	0.0003 ***	0.4385 ns	ns	ns	ns	ns
Figure 19C	**RQ**	m	0.6552 ns	0.1117 ns	0.7955 ns	ns	ns	ns	ns
		f	0.0095 **	0.3896 ns	0.205 *	ns	ns	*	**

			two-way ANOVA			Holm-Sidak post-hoc Test			
						TRα1+/+		TRα1+/m	
			Interaction	Genotype	Treatment	H_2O vs. T3 1st half	H_2O vs. T3 2nd half	H_2O vs. T3 1st half	H_2O vs. T3 2nd half
Figure 19D	**DEE**	m	0.4166 ns	<0.0001 ****	0.1303 ns	ns	ns	ns	ns
		f	0.4958 ns	0.0003 ***	0.1937 ns	ns	ns	ns	ns
Figure 19E	**RMR**	m	0.8522 ns	0.0002 ***	0.8657 ns	ns	ns	ns	ns
		f	0.7242 ns	0.8999 ns	0.0420 *	ns	ns	ns	ns
Figure 19F	**BMR**	m	0.8867 ns	0.0989 ns	0.8643 ns	ns	ns	ns	ns
		f	0.0395 *	0.1638 ns	0.2062 ns	ns	ns	ns	*
Figure 20A	**Locomotor activity**	m	0.9148 ns	0.0065 **	0.0006 ***	ns	**	ns	*
		f	<0.0001 ****	<0.0001 ****	0.0004 ***	ns	ns	**	****
Figure 20B	**Soleus weight**	m	0.7796 ns	0.0005 ***	<0.0001 ****	ns	****	ns	****
		f	0.0363 *	<0.0001 ****	<0.0001 ****	ns	*	**	****
Figure 20C	**Gastro. weight**	m	0.0010 ***	<0.0001 ****	<0.0001 ****	ns	****	ns	*
		f	0.0360 *	<0.0001 ****	<0.0001 ****	****	**	*	***
Figure 21A	***Pepck* in soleus**	m	0.7591 ns	0.1960 ns	0.1400 ns	ns	ns	ns	ns
	Pyrkm in gastro.	m	0.2748 ns	0.0018 **	0.4106 ns	ns	ns	ns	*
Figure 21B	***Pepck* in soleus**	m	0.0028 **	0.7998 ns	0.0001 ***	ns	ns	ns	***
	Pyrkm in gastro.	m	0.3704 ns	0.4938 ns	0.5573 ns	ns	ns	ns	ns
Figure 22A	***Pparδ* in soleus**	m	0.8686 ns	<0.0001 ****	0.0003 ***	ns	****	ns	**
	***Gpd2* in soleus**	m	0.9449 ns	0.3315 ns	0.0038 **	**	**	ns	ns
Figure 22B	***Pparδ in gastro.***	m	0.3418 ns	0.0013 **	0.0055 **	ns	ns	ns	**
	Gpd2 in gastro.	m	0.6308 ns	0.9370 ns	0.1089 ns	ns	ns	ns	ns
Figure 23A	***Myh1* in soleus**	m	0.1209 ns	0.0080 **	0.5643 ns	ns	ns	ns	ns
		f	0.3567 ns	0.2551 ns	0.0004 ***	*	*	ns	**

			two-way ANOVA			Holm-Sidak post-hoc Test			
						TRα1+/+		TRα1+/m	
			Interaction	Genotype	Treatment	H_2O vs. T3 1st half	H_2O vs. T3 2nd half	H_2O vs. T3 1st half	H_2O vs. T3 2nd half
Figure 23B	*Myh4* in soleus	m	0.8326 ns	0.0811 ns	0.8729 ns	ns	ns	ns	ns
		f	0.5380 ns	0.1331 ns	<0.0001 ****	***	**	*	*
Figure 24A	Lean mass	m	0.1321 ns	<0.0001 ****	<0.0001 ****	****	****	**	**
		f	0.6714 ns	0.0082 **	0.1815 ns	ns	ns	ns	ns
Figure 24B	free body fluid	m	<0.0001 ****	0.7030 ns	<0.0001 ****	****	****	ns	ns
		f	0.7624 ns	<0.0001 ****	0.4335 ns	ns	ns	ns	ns
Figure 24C	Fat mass	m	0.7270 ns	<0.0001 ****	0.0981 ns	ns	ns	ns	ns
		f	0.4652 ns	0.0153 *	0.6879 ns	ns	ns	ns	ns
Figure 25A	iWAT weight	m	0.3198 ns	<0.0001 ****	0.0003 ***	ns	***	**	**
		f	0.0794 ns	0.0110 *	0.0032 **	ns	*	*	*
Figure 25B	gWAT wight	m	0.0003 ***	<0.0001 ****	<0.0001 ****	****	****	ns	ns
		f	0.0006 ***	<0.0001 ****	<0.0001 ****	****	****	*	*
Figure 25C	iBAT weight	m	0.2118 ns	0.0155 *	0.5320 ns	ns	ns	ns	ns
		f	0.5593 ns	0.6790 ns	0.0404 *	ns	ns	ns	ns
Figure 26A	*Hsl* in iWAT	m	0.2373 ns	0.5207 ns	0.7448 ns	ns	ns	ns	ns
	Adrb3 in iWAT	m	0.5282 ns	0.1079 ns	0.4153 ns	ns	ns	ns	ns
Figure 26B	*Hsl* in gWAT	m	0.2892 ns	0.0059 **	0.3989 ns	ns	ns	ns	ns
	Acc1 in gWAT	m	0.4983 ns	<0.0001 ****	0.6501 ns	ns	ns	ns	ns
Figure 26C	*Hsl* in iBAT	m	0.4104 ns	0.3575 ns	0.0008 ***	ns	*	*	*
	Adrb3 in iBAT	m	0.4600 ns	0.0209 *	0.0193 *	ns	ns	ns	ns
Figure 28A	iBAT (°C)	m	0.0971 ns	0.1106 ns	0.6485 ns	ns	ns	ns	ns
		f	0.7787 ns	0.0283 *	0.5842 ns	ns	ns	ns	ns

			two-way ANOVA			Holm-Sidak post-hoc Test			
						TRα1+/+		TRα1+/m	
			Interaction	Genotype	Treatment	H_2O vs. T3 1st half	H_2O vs. T3 2nd half	H_2O vs. T3 1st half	H_2O vs. T3 2nd half
Figure 28B	**Ear (°C)**	m	0.0421 *	0.0060 **	0.0331 *	ns	ns	ns	ns
		f	0.8754 ns	0.3698 ns	0.4011 ns	ns	ns	ns	ns
Figure 28C	**Tail (°C)**	m	0.5688 ns	<0.0001 ****	0.0116 *	ns	*	ns	ns
		f	0.0035 **	<0.0001 ****	0.2327 ns	**	**	ns	ns
Figure 28D	**Rectal (°C)**	m	0.6820 ns	0.0007 ***	0.1057 ns	ns	ns	ns	ns
		f	0.8026 ns	0.0509 ns	0.096 ns	ns	ns	ns	ns
Figure 29A	***Ucp1* in iBAT**	m	0.7763 ns	<0.0001 ****	0.0003 ***	*	**	*	*
		f	0.7459 ns	0.3529 ns	0.5328 ns	ns	ns	ns	ns
Figure 29B	***Dio2* in iBAT**	m	0.1411 ns	0.0005 ***	0.0043 **	*	**	ns	ns
		f	0.0026 **	0.6676 ns	0.0259 *	ns	ns	**	**
Figure 30	***Sln* in soleus**	m	0.7817 ns	0.0438 *	0.2690 ns	ns	ns	ns	ns
	***Sln* in gastro.**	m	0.1958 ns	0.0051 **	0.5705 ns	ns	ns	ns	ns
Figure 31A	**Hepatic *Pepck***	m	<0.0001 ****	0.0008 ***	0.0006 ***	ns	ns	ns	****
		f	0.7076 ns	<0.0001 ****	0.0017 **	ns	ns	*	*
Figure 31B	**Hepatic *Pyrkl***	m	0.0200 *	0.0704 ns	<0.0001 ****	ns	**	*	*
		f	0.8596 ns	0.0359 *	0.1248 ns	ns	ns	ns	ns
Figure 31C	**Hepatic *Fasn***	m	0.8462 ns	<0.0001 ****	<0.0001 ****	ns	*	ns	ns
		f	0.3374 ns	0.0001 ***	0.8098 ns	ns	ns	ns	ns
Figure 31D	**Hepatic *Acc1***	m	<0.0001 ****	<0.0001 ****	<0.0001 ****	*	**	**	****
		f	0.4495 ns	0.0010 **	0.0734 ns	ns	ns	ns	ns
Figure S1A	***Hcn2* DNA methyl.**	m	0.3024 ns	0.0029 *	0.0027 **	ns	ns	*	*
		f	0.9452 ns	0.0070 **	0.4551 ns	ns	ns	ns	ns

			two-way ANOVA			Holm-Sidak post-hoc Test			
						TRα1+/+		TRα1+/m	
			Interaction	Genotype	Treatment	H_2O vs. T3 1st half	H_2O vs. T3 2nd half	H_2O vs. T3 1st half	H_2O vs. T3 2nd half
Figure S1B	*Hcn2* DNA methyl.	m	0.0538 ns	0.0012 **	0.0023 **	ns	ns	**	***
		f	0.8164 ns	0.0097 **	0.2058 ns	ns	ns	ns	ns
Figure S1C	*Hcn4* DNA methyl.	m	0.381 ns	0.0009 ***	0.0069 **	ns	ns	ns	*
		f	0.2081 ns	0.0001 ***	0.0099 **	ns	ns	ns	ns
Figure S3A	*Pepck* in soleus	f	0.3618 ns	0.0017 **	0.4518 ns	ns	ns	ns	ns
	Pyrkm in soleus	f	0.5824 ns	0.0499 *	0.0125 *	ns	ns	ns	ns
Figure S3B	*Pepck* in gastro.	f	0.4023 ns	0.3624 ns	0.0682 ns	ns	ns	ns	ns
	Pyrkm in gastro.	f	0.9483 ns	0.9289 ns	0.0965 ns	ns	ns	ns	ns
Figure S4A	*Pparδ* in soleus	f	0.2121 na	0.0045 **	0.8371 ns	ns	ns	ns	ns
	Gpd2 in soleus	f	0.6068 ns	0.6206 ns	0.0016 **	ns	ns	ns	**
Figure S4B	*Pparδ* in gastro.	f	0.7549 ns	0.1186 ns	0.1824 ns	ns	ns	ns	ns
	Gpd2 in gastro.	f	0.6474 ns	0.8450 ns	<0.0001 ****	*	*	**	**
Figure S5A	*Myh1* in gastro.	m	0.2790 ns	<0.0001 ****	0.4185 ns	ns	ns	ns	ns
		f	0.3490 ns	0.1871 ns	<0.0001 ****	**	**	**	***
Figure S5B	*Myh4* in gastro.	m	0.9061 ns	0.3719 ns	0.0254 *	ns	ns	ns	ns
		f	0.6918 ns	0.8622 ns	<0.0001 ****	****	****	****	****
Figure S6A	*Hsl* in iWAT	f	0.3427 ns	0.5397 ns	0.1036 ns	ns	ns	ns	ns
	Adrb3 in iWAT	f	0.5964 ns	0.5800 ns	0.0781 ns	ns	ns	ns	ns
Figure S6B	*Hsl* in gWAT	f	0.2407 ns	0.0831 ns	0.1295 ns	ns	ns	ns	ns
	Acc1 in gWAT	f	0.3722 ns	0.0721 ns	<0.0001 ****	**	*	****	***
Figure S6C	*Hsl* in iBAT	f	0.1565 ns	0.2972 ns	0.8674 ns	ns	ns	ns	ns
	Adrb3 in iBAT	f	0.3509 ns	<0.0001 ****	0.0096 **	ns	ns	*	*

			two-way ANOVA			Holm-Sidak post-hoc Test			
						TRα1+/+		TRα1+/m	
			Interaction	Genotype	Treatment	H_2O vs. T3 1st half	H_2O vs. T3 2nd half	H_2O vs. T3 1st half	H_2O vs. T3 2nd half
Figure S7	*Sln* in soleus	f	0.8488 ns	0.4188 ns	0.0230 *	ns	ns	ns	ns
	Sln in gastro.	f	0.5336 ns	0.0011 **	0.1485 ns	ns	ns	ns	ns

Abbreviations: m: *male;* ***f:*** *female;* ***ns:*** *not significant.*

Statistical Analysis Table 2: Correlation analysis with Pearson correlation coefficient (Pearson r).

			Pearson r							
			TRα1+/+				TRα1+/m			
			r	R^2	p value	p value summary	r	R^2	p value	p value summary
Figure 13A	*Hcn2* vs. heart rate	m	0.740	0.548	0.0004	***	0.581	0.3375	0.0115	*
Figure 13B	*Hcn4* vs. heart rate	m	0.727	0.529	0.0006	***	0.536	0.2873	0.0219	*
Figure 13C	*Hcn2* vs. heart rate	f	-0.172	0.029	0.4934	ns	0.0288	0.0008	0.9095	ns
Figure 13D	*Hcn4* vs. heart rate	f	-0.345	0.119	0.1609	ns	0.0840	0.0070	0.7402	ns
Figure S2A	*Hcn2* vs. *Hcn2* methyl.	m	-0.831	0.691	<0.0001	****	-0.337	0.114	0.1706	ns
		f	-0.963	0.009	0.7038	ns	0.3553	0.1262	0.1479	ns
Figure S2B	*Hcn2* vs. *Hcn2* methyl.	m	-0.683	0.466	0.0018	**	-0.4632	0.2146	0.0529	ns
		f	0.051	0.002	0.8388	ns	-0.014	0.0002	0.9553	ns
Figure S2C	*Hcn2* vs. *Hcn2* methyl.	m	-0.554	0.307	0.0169	*	-0.578	0.3348	0.0119	*
		f	-0.130	0.016	0.6069	ns	0.4793	0.2297	0.0442	*
Figure S2D	*Hcn4* vs. *Hcn4* methyl.	m	0.5281	0.278	0.0243	*	0.2365	0.0559	0.3447	ns
		f	0.168	0.028	0.503	ns	0.1861	0.0346	0.4597	ns

			Pearson r							
			TRα1+/+				TRα1+/m			
			r	R^2	p value	p value summary	r	R^2	p value	p value summary
Figure S2E	*Hcn4* vs. *Hcn4* methyl.	m	0.6493	0.4216	0.0035	**	0.4641	0.2154	0.0524	ns
		f	0.272	0.073	0.2749	ns	0.1486	0.0220	0.5562	ns
Figure S2F	*Hcn4* vs. *Hcn4* methyl.	m	0.0365	0.131	0.1393	ns	0.3793	0.1439	0.1332	ns
		f	0.0175	0.000	0.9449	ns	-0.333	0.1111	0.1765	ns

Abbreviations: m: *male;* ***f:*** *female;* ***ns:*** *not significant.*

8. REFERENCES

Anastasiadi, D., Esteve-Codina, A., & Piferrer, F. (2018). Consistent inverse correlation between DNA methylation of the first intron and gene expression across tissues and species. *Epigenetics and Chromatin*, *11*(1), 1–17. https://doi.org/10.1186/s13072-018-0205-1

Andersen, S. L., Andersen, S., Liew, Z., Vestergaard, P., Lundbye-Christensen, S., Sørensen, T. I. A., & Olsen, J. (2021). Maternal thyroid disease and adiposity in mother and child. *Clinical Endocrinology*, *94*(3), 484–493. https://doi.org/10.1111/cen.14314

Anifantaki, F., Pervanidou, P., Lambrinoudaki, I., Panoulis, K., Vlahos, N., & Eleftheriades, M. (2021). Maternal Prenatal Stress, Thyroid Function and Neurodevelopment of the Offspring: A Mini Review of the Literature. *Frontiers in Neuroscience*, *15*(September), 1–7. https://doi.org/10.3389/fnins.2021.692446

Anselmo, J., & Chaves, C. M. (2020). Physiologic Significance of Epigenetic Regulation of Thyroid Hormone Target Gene Expression. *European Thyroid Journal*, *9*(3), 114–123. https://doi.org/10.1159/000506423

Anselmo, J., Scherberg, N. H., Dumitrescu, A. M., & Refetoff, S. (2019). Reduced Sensitivity to Thyroid Hormone as a Transgenerational Epigenetic Marker Transmitted Along the Human Male Line. *Thyroid*, *29*(6), 778–782. https://doi.org/10.1089/thy.2019.0080

Anyetei-Anum, C. S., Roggero, V. R., & Allison, L. A. (2018). Thyroid hormone receptor localization in target tissues. *Journal of Endocrinology*, *237*(1), R19–R34. https://doi.org/10.1530/JOE-17-0708

Aranda, A., & Pascual, A. (2001). Nuclear hormone receptors and gene expression. *Physiological Reviews*, *81*(3), 1269–1304. https://doi.org/10.1152/physrev.2001.81.3.1269

Astapova, I., Lee, L. J., Morales, C., Tauber, S., Bilban, M., & Hollenberg, A. N. (2008). The nuclear corepressor, NCoR, regulates thyroid hormone action in vivo. *Proceedings of the National Academy of Sciences of the United States of America*, *105*(49), 19544–19549. https://doi.org/10.1073/pnas.0804604105

Badman, M. K., Pissios, P., Kennedy, A. R., Koukos, G., Flier, J. S., & Maratos-Flier, E. (2007). Hepatic Fibroblast Growth Factor 21 Is Regulated by PPARα and Is a Key Mediator of Hepatic Lipid Metabolism in Ketotic States. *Cell Metabolism*, *5*(6), 426–437. https://doi.org/10.1016/j.cmet.2007.05.002

Bai, X., Wang, K., Boyett, M. R., Hancox, J. C., & Zhang, H. (2021). The Functional Role of Hyperpolarization Activated Current (If) on Cardiac Pacemaking in Human vs. in the Rabbit Sinoatrial Node: A Simulation and Theoretical Study. *Frontiers in Physiology*, *12*(August), 1–18. https://doi.org/10.3389/fphys.2021.582037

Barbe, P., Larrouy, D., Boulanger, C., Chevillotte, E., Viguerie, N., Thalamas, C., Oliva Trastoy, M., Roques, M., Vidal, H., & Langin, D. (2001). Triiodothyronine-mediated upregulation of UCP2 and UCP3 mRNA expression in human skeletal muscle without coordinated induction of mitochondrial respiratory chain genes. *The FASEB Journal*, *15*(1), 13–15. https://doi.org/10.1096/fj.00-0502fje

Bassett, J. H. D., & Williams, G. R. (2009). The skeletal phenotypes of TRα and TBβ mutant mice. *Journal of Molecular Endocrinology*, *42*(4), 269–282. https://doi.org/10.1677/JME-08-0142

Behringer, V., Deimel, C., Hohmann, G., Negrey, J., Schaebs, F. S., & Deschner, T. (2018). Applications for non-invasive thyroid hormone measurements in mammalian ecology, growth, and maintenance. *Hormones and Behavior*, *105*(July), 66–85. https://doi.org/10.1016/j.yhbeh.2018.07.011

Benedetti, V., Lavecchia, A. M., Locatelli, M., Brizi, V., Corna, D., Todeschini, M., Novelli, R., Benigni, A., Zoja, C., Remuzzi, G., & Xinaris, C. (2019). Alteration of thyroid hormone signaling triggers the diabetes-induced pathological growth, remodeling, and dedifferentiation of podocytes. *JCI Insight*, *4*(18). https://doi.org/10.1172/jci.insight.130249

Bernal, J. (2017). Thyroid hormone regulated genes in cerebral cortex development. *Journal of Endocrinology*, *232*(2), R83–R97. https://doi.org/10.1530/JOE-16-0424

Bianco, A. C., Anderson, G., Forrest, D., Galton, V. A., Gereben, B., Kim, B. W., Kopp, P. A., Liao, X. H., Obregon, M. J., Peeters, R. P., Refetoff, S., Sharlin, D. S., Simonides, W. S., Weiss, R. E., & Williams, G. R. (2014). American thyroid association guide to investigating thyroid hormone economy and action in rodent and cell models. *Thyroid*, *24*(1), 88–168. https://doi.org/10.1089/thy.2013.0109

Bianco, A. C., & Kim, B. W. (2006). Deiodinases: Implications of the local control of thyroid hormone action. *Journal of Clinical Investigation*, *116*(10), 2571–2579. https://doi.org/10.1172/JCI29812

Boelaert, K., & Franklyn, J. A. (2005). Thyroid hormone in health and disease. *Journal of Endocrinology*, *187*(1), 1–15. https://doi.org/10.1677/joe.1.06131

Brabant, G., Peeters, R. P., Chan, S. Y., Bernal, J., Bouchard, P., Salvatore, D., Boelaert, K., & Laurberg, P. (2015). Management of subclinical hypothyroidism in pregnancy: Are we too simplistic? *European Journal of Endocrinology*, *173*(1), P1–P11. https://doi.org/10.1530/EJE-14-1005

Brent, G. A. (2000). Tissue-Specific Actions of Thyroid Hormone: Insights from Animal Models. *Reviews in Endocrine and Metabolic Disorders*, *1*(1–2), 27–33. https://doi.org/10.1023/A:1010056202122

Brent, G. A. (2012). Mechanisms of thyroid hormone action Find the latest version : Science in medicine Mechanisms of thyroid hormone action. *The Jornal of Clinical Investigation*, *122*(9), 3035–3043. https://doi.org/10.1172/JCI60047.three

Bucchi, A., Barbuti, A., DiFrancesco, D., & Baruscotti, M. (2012). Funny current and cardiac rhythm: Insights from HCN knockout and transgenic mouse models. *Frontiers in Physiology*, *3 JUL*(July), 1–10. https://doi.org/10.3389/fphys.2012.00240

Calsolaro, V., Niccolai, F., Pasqualetti, G., Maria Calabrese, A., Polini, A., Okoye, C., Magno, S., Caraccio, N., & Monzani, F. (2019). Overt and subclinical hypothyroidism in the elderly: When to treat? *Frontiers in Endocrinology*, *10*(MAR), 1–8. https://doi.org/10.3389/fendo.2019.00177

Campanha, F. V. G., Perone, D., de Campos, D. H. S., de Luvizotto, R. A. M., de Síbio, M. T., de Oliveira, M., Olimpio, R. M. C., Moretto, F. C. F., Padovani, C. R., Mazeto, G. M. F. S., Cicogna, A. C., & Nogueira, C. R. (2016). Thyroxine increases Serca2 and Ryr2 gene expression in heart failure rats with euthyroid sick syndrome. *Archives of Endocrinology and Metabolism*, *60*(6), 582–586. https://doi.org/10.1590/2359-3997000000208

Cannon, B., & Nedergaard, J. (2004). Brown Adipose Tissue: Function and Physiological Significance. *Physiological Reviews*, *84*(1), 277–359. https://doi.org/10.1152/physrev.00015.2003

Capelli, V., Diéguez, C., Mittag, J., & López, M. (2021). Thyroid wars: the rise of central actions. *Trends in Endocrinology and Metabolism*, *32*(9), 659–671. https://doi.org/10.1016/j.tem.2021.05.006

Cappola, A. R., Desai, A. S., Medici, M., Cooper, L. S., Egan, D., Sopko, G., Fishman, G. I., Goldman, S., Cooper, D. S., Mora, S., Kudenchuk, P. J., Hollenberg, A. N., McDonald, C. L., & Ladenson, P. W. (2019). Thyroid and Cardiovascular Disease: Research Agenda for Enhancing Knowledge, Prevention, and Treatment. *Thyroid*, *29*(6), 760–777. https://doi.org/10.1089/thy.2018.0416

Chaker, L., Bianco, A. C., Jonklaas, J., & Peeters, R. P. (2017). Hypothyroidism. *Lancet (London, England)*, *390*(10101), 1550–1562. https://doi.org/10.1016/S0140-6736(17)30703-1

Chanoine, J. P., Nève, J., Wu, S., Vanderpas, J., & Bourdoux, P. (2001). Selenium decreases thyroglobulin concentrations but does not affect the increased thyroxine-to-triiodothyronine ratio in children with congenital hypothyroidism. *The Journal of Clinical Endocrinology and Metabolism*, *86*(3), 1160–1163. https://doi.org/10.1210/jcem.86.3.7312

Charles, B. Y., Harington, R., & Barger, G. (1927). The constitution and synthesis of thyroxine. *Nature*, *120*(3013), 170. https://doi.org/10.1038/120170a0

Chatonnet, F., Guyot, R., Benoît, G., & Flamant, F. (2013). Genome-wide analysis of thyroid hormone receptors shared and specific functions in neural cells. *Proceedings of the National Academy of Sciences of the United States of America*, *110*(8). https://doi.org/10.1073/pnas.1210626110

Chen, K. Y., Brychta, R. J., Linderman, J. D., Smith, S., Courville, A., Dieckmann, W., Herscovitch, P., Millo, C. M., Remaley, A., Lee, P., & Celi, F. S. (2013). Brown fat activation mediates cold-induced thermogenesis in adult humans in response to a mild decrease in ambient temperature. *Journal of Clinical Endocrinology and Metabolism*, *98*(7), 1–6. https://doi.org/10.1210/jc.2012-4213

Chen, S. jun, Xu, Y., Liang, Y. mei, Cao, Y., Lv, J. yan, Pang, J. xin, & Zhou, P. zheng. (2018). Identification and characterization of a series of novel HCN channel inhibitors. *Acta Pharmacologica Sinica*, *August 2018*. https://doi.org/10.1038/s41401-018-0162-z

Cheng, S. Y., Leonard, J. L., & Davis, P. J. (2010). Molecular aspects of thyroid hormone actions. *Endocrine Reviews*, *31*(2), 139–170. https://doi.org/10.1210/er.2009-0007

Cini, G., Carpi, A., Mechanick, J., Cini, L., Camici, M., Galetta, F., Giardino, R., Russo, M. A., & Iervasi, G. (2009). Thyroid hormones and the cardiovascular system: Pathophysiology and interventions. *Biomedicine and Pharmacotherapy*, *63*(10), 742–753. https://doi.org/10.1016/j.biopha.2009.08.003

Cokkinos, D. V., & Chryssanthopoulos, S. (2016). Thyroid hormones and cardiac remodeling. *Heart Failure Reviews*, *21*(4), 365–372. https://doi.org/10.1007/s10741-016-9554-7

Cooper, D. S. (2003). Hyperthyroidism. *Lancet*, *362*(9382), 459–468. https://doi.org/10.1016/S0140-6736(03)14073-1

Crunkhorn, S., & Patti, M.-E. (2008). Links between thyroid hormone action, oxidative metabolism, and diabetes risk? *Thyroid : Official Journal of the American Thyroid Association*, *18*(2), 227–237. https://doi.org/10.1089/thy.2007.0249

Danzi, S., & Klein, I. (2002). Thyroid hormone-regulated cardiac gene expression and cardiovascular disease. *Thyroid*, *12*(6), 467–472. https://doi.org/10.1089/105072502760143836

Danzi, S., & Klein, I. (2005). Posttranscriptional regulation of myosin heavy chain expression in the heart by triiodothyronine. *American Journal of Physiology - Heart and Circulatory Physiology*, *288*(2 57-2), 455–460. https://doi.org/10.1152/ajpheart.00896.2004

Danzi, S., & Klein, I. (2012). Thyroid Hormone and the Cardiovascular System. *Medical Clinics of North America*, *96*(2), 257–268. https://doi.org/10.1016/j.mcna.2012.01.006

Danzi, S., & Klein, I. (2014). Thyroid disease and the cardiovascular system. *Endocrinology and Metabolism Clinics of North America*, *43*(2), 517–528. https://doi.org/10.1016/j.ecl.2014.02.005

Danzi, S., & Klein, I. (2020). Thyroid Abnormalities in Heart Failure. *Heart Failure Clinics*, *16*(1), 1–9. https://doi.org/10.1016/j.hfc.2019.08.002

Darby, J. R. T., Mohd Dollah, M. H. B., Regnault, T. R. H., Williams, M. T., & Morrison, J. L. (2019). Systematic review: Impact of resveratrol exposure during pregnancy on maternal and fetal outcomes in animal models of human pregnancy complications—Are we ready for the clinic? *Pharmacological Research*, *144*, 264–278. https://doi.org/10.1016/j.phrs.2019.04.020

Dasinger, J. H., & Alexander, B. T. (2016). Gender differences in developmental programming of cardiovascular diseases. *Clinical Science*, *130*(5), 337–348. https://doi.org/10.1042/CS20150611

Davis, P. J., Leonard, J. L., & Davis, F. B. (2008). Mechanisms of nongenomic actions of thyroid hormone. *Frontiers in Neuroendocrinology*, *29*(2), 211–218. https://doi.org/10.1016/j.yfrne.2007.09.003

De Escobar, G. M., Obregón, M. J., & Del Rey, F. E. (2007). Iodine deficiency and brain development in the first half of pregnancy. *Public Health Nutrition*, *10*(12 A), 1554–1570. https://doi.org/10.1017/S1368980007360928

De Escobar, G. M., Obregón, M. J., & Escobar del Rey, F. (2004). Maternal thyroid hormones early in prenancy and fetal brain development. *Best Practice and Research: Clinical Endocrinology and Metabolism*, *18*(2), 225–248. https://doi.org/10.1016/j.beem.2004.03.012

De Felice, M., & Di Lauro, R. (2004). Thyroid development and its disorders: Genetics and molecular mechanisms. *Endocrine Reviews*, *25*(5), 722–746. https://doi.org/10.1210/er.2003-0028

De Groot, L., Abalovich, M., Alexander, E. K., Amino, N., Barbour, L., Cobin, R. H., Eastman, C. J., Lazarus, J. H., Luton, D., Mandel, S. J., Mestman, J., Rovet, J., & Sullivan, S. (2012). Management of thyroid dysfunction during pregnancy and postpartum: An endocrine society clinical practice guideline. *Journal of Clinical Endocrinology and Metabolism*, *97*(8), 2543–2565. https://doi.org/10.1210/jc.2011-2803

De Jong, F. J., Peeters, R. P., Heijer, T. Den, Van Der Deure, W. M., Hofman, A., Uitterlinden, A. G., Visser, T. J., & Breteler, M. M. B. (2007). The association of polymorphisms in the type 1 and 2 deiodinase genes with circulating thyroid hormone parameters and atrophy of the medial temporal lobe. *Journal of Clinical Endocrinology and Metabolism*, *92*(2), 636–640. https://doi.org/10.1210/jc.2006-1331

Demeneix, B. A. (2019). Evidence for Prenatal Exposure to Thyroid Disruptors and Adverse Effects on Brain Development. *European Thyroid Journal*, *8*(6), 283–292. https://doi.org/10.1159/000504668

Dentice, M., & Salvatore, D. (2011). Local impact of thyroid hormone inactivation. *Journal of Endocrinology*, *209*(3), 273–282. https://doi.org/10.1530/JOE-11-0002

Difrancesco, D. (2010). The role of the funny current in pacemaker activity. *Circulation Research*, *106*(3), 434–446. https://doi.org/10.1161/CIRCRESAHA.109.208041

DiFrancesco, J. C., & DiFrancesco, D. (2015). Dysfunctional HCN ion channels in neurological diseases. *Frontiers in Cellular Neuroscience*, *9*(March), 1–10. https://doi.org/10.3389/fncel.2015.00071

Dillmann, W. H. (2002). Cellular action of thyroid hormone on the heart. *Thyroid : Official Journal of the American Thyroid Association*, *12*(6), 447–452. https://doi.org/10.1089/105072502760143809

Donangelo, I., & Suh, S. Y. (2017). AFP Hyperthyroid. *American Family Physician*, *95*(11), 710–716.

Doubleday, A. R., & Sippel, R. S. (2020). Hyperthyroidism. *Gland Surgery*, *9*(1), 124–135. https://doi.org/10.21037/gs.2019.11.01

Drover, S. S. M., Villanger, G. D., Aase, H., Skogheim, T. S., Longnecker, M. P., Thomas Zoeller, R., Reichborn-Kjennerud, T., Knudsen, G. P., Zeiner, P., & Engel, S. M. (2019). Maternal Thyroid Function during Pregnancy or Neonatal Thyroid Function and Attention Deficit Hyperactivity Disorder: A Systematic Review. *Epidemiology*, *30*(1), 130–144. https://doi.org/10.1097/EDE.0000000000000937

Eerdekens, A., Verhaeghe, J., Darras, V., Naulaers, G., Van den berghe, G., Langouche, L., & Vanhole, C. (2020). The placenta in fetal thyroid hormone delivery: from normal physiology to adaptive mechanisms in complicated pregnancies. *Journal of Maternal-Fetal and Neonatal Medicine*, *33*(22), 3857–3866. https://doi.org/10.1080/14767058.2019.1586875

Eng, L., & Lam, L. (2020). Thyroid function during the fetal and neonatal periods. *NeoReviews*, *21*(1), e30–e36. https://doi.org/10.1542/neo.21-1-e30

Epstein, F. H., & Brent, G. A. (1994). The Molecular Basis of Thyroid Hormone Action. *New England Journal of Medicine*, *331*(13), 847–853. https://doi.org/10.1056/nejm199409293311306

Evans, T. C. (2003). Thyroid disease. *Primary Care - Clinics in Office Practice*, *30*(4), 625–640. https://doi.org/10.1016/S0095-4543(03)00087-3

Fagman, H., Andersson, L., & Nilsson, M. (2006). The developing mouse thyroid: Embryonic vessel contacts and parenchymal growth pattern during specification, budding, migration, and lobulation. *Developmental Dynamics*, *235*(2), 444–455. https://doi.org/10.1002/dvdy.20653

Fagman, H., & Nilsson, M. (2011). Morphogenetics of early thyroid development. *Journal of Molecular Endocrinology*, *46*(1). https://doi.org/10.1677/JME-10-0084

Fekete, C., & Lechan, R. M. (2014). Central regulation of hypothalamic-pituitary-thyroid axis under physiological and pathophysiological conditions. *Endocrine Reviews*, *35*(2), 159–194. https://doi.org/10.1210/er.2013-1087

Feldt-Rasmussen, U., Effraimidis, G., & Klose, M. (2021). The hypothalamus-pituitary-thyroid (HPT)-axis and its role in physiology and pathophysiology of other hypothalamus-pituitary functions. *Molecular and Cellular Endocrinology*, *525*, 111173. https://doi.org/10.1016/j.mce.2021.111173

Fernández, L. P., López-Márquez, A., & Santisteban, P. (2015). Thyroid transcription factors in development, differentiation and disease. *Nature Reviews Endocrinology*, *11*(1), 29–42. https://doi.org/10.1038/nrendo.2014.186

Fisher, D. A., & Polk, D. H. (1989). Development of the thyroid. *Bailliere's Clinical Endocrinology and Metabolism*, *3*(3), 627–657. https://doi.org/10.1016/S0950-351X(89)80046-1

Flamant, F., & Gauthier, K. (2013). Thyroid hormone receptors: The challenge of elucidating isotype-specific functions and cell-specific response. *Biochimica et Biophysica Acta - General Subjects*, *1830*(7), 3900–3907. https://doi.org/10.1016/j.bbagen.2012.06.003

Flamant, F., Gauthier, K., & Richard, S. (2017). Genetic Investigation of Thyroid Hormone Receptor Function in the Developing and Adult Brain. In *Current Topics in Developmental Biology* (1st ed., Vol. 125). Elsevier Inc. https://doi.org/10.1016/bs.ctdb.2017.01.001

Flamant, F., & Samarut, J. (2003). Thyroid hormone receptors: Lessons from knockout and knock-in mutant mice. *Trends in Endocrinology and Metabolism*, *14*(2), 85–90. https://doi.org/10.1016/S1043-2760(02)00043-7

Fliers, E., Boelen, A., & van Trotsenburg, A. S. P. (2014). Central regulation of the hypothalamo-pituitary-thyroid (HPT) axis: Focus on clinical aspects. In *Handbook of Clinical Neurology* (1st ed., Vol. 124). Elsevier B.V. https://doi.org/10.1016/B978-0-444-59602-4.00009-5

Flohé, L., & Günzler, W. A. (1984). Assays of glutathione peroxidase. *Methods in Enzymology*, *105*, 114–121. https://doi.org/10.1016/s0076-6879(84)05015-1

Fonseca, T. L., Fernandes, G. W., McAninch, E. A., Bocco, B. M. L. C., Abdalla, S. M., Ribeiro, M. O., Mohácsik, P., Fekete, C., Li, D., Xing, X., Wang, T., Gereben, B., & Bianco, A. C. (2015). Perinatal deiodinase 2 expression in hepatocytes defines epigenetic susceptibility to liver steatosis and obesity. *Proceedings of the National Academy of Sciences of the United States of America*, *112*(45), 14018–14023. https://doi.org/10.1073/pnas.1508943112

Fonseca, T. L., Garcia, T., Fernandes, G. W., Nair, T. M., & Bianco, A. C. (2021). Neonatal thyroxine activation modifies epigenetic programming of the liver. *Nature Communications*, *12*(1), 1–11. https://doi.org/10.1038/s41467-021-24748-8

Forini, F., Nicolini, G., Pitto, L., & Iervasi, G. (2019). Novel insight into the epigenetic and post-transcriptional control of cardiac gene expression by thyroid hormone. *Frontiers in Endocrinology*, *10*(AUG). https://doi.org/10.3389/fendo.2019.00601

Fox, C. S., Pencina, M. J., D'Agostino, R. B., Murabito, J. M., Seely, E. W., Pearce, E. N., & Vasan, Ramachandran S., M. (2008). Relations of Thyroid Function to Body Weight. *Arch Intern Med*, *168*(6), 587–592. https://jamanetwork-com.rsm.idm.oclc.org/journals/jamainternalmedicine/fullarticle/414105

Friedrichsen, S., Christ, S., Heuer, H., Schäfer, M. K. H., Mansouri, A., Bauer, K., & Visser, T. J. (2003). Regulation of iodothyronine deiodinases in the Pax8-/- mouse model of congenital hypothyroidism. *Endocrinology*, *144*(3), 777–784. https://doi.org/10.1210/en.2002-220715

Gaillard, R., Steegers, E. A. P., Duijts, L., Felix, J. F., Hofman, A., Franco, O. H., & Jaddoe, V. W. V. (2014). Childhood cardiometabolic outcomes of maternal obesity during pregnancy: The generation r study. *Hypertension*, *63*(4), 683–691. https://doi.org/10.1161/HYPERTENSIONAHA.113.02671

Galton, V. A., Larsen, P. R., & Berry, M. J. (2021). The Deiodinases: Their Identification and Cloning of Their Genes. *Endocrinology*, *162*(3). https://doi.org/10.1210/endocr/bqab005

Gereben, B., Zavacki, A. M., Ribich, S., Kim, B. W., Huang, S. A., Simonides, W. S., Zeöld, A., & Bianco, A. C. (2008). Cellular and molecular basis of deiodinase-regulated thyroid hormone signaling. *Endocrine Reviews*, *29*(7), 898–938. https://doi.org/10.1210/er.2008-0019

Gessl, A., Lemmens-Gruber, R., & Kautzky-Willer, A. (2012). Thyroid disorders. *Handbook of Experimental Pharmacology*, *214*, 361–386. https://doi.org/10.1007/978-3-642-30726-3_17

Ghanbari, M., & Ghasemi, A. (2017). Maternal hypothyroidism: An overview of current experimental models. *Life Sciences*, *187*, 1–8. https://doi.org/10.1016/j.lfs.2017.08.012

Gil-Ibañez, P., García-García, F., Dopazo, J., Bernal, J., & Morte, B. (2017). Global transcriptome analysis of primary cerebrocortical cells: Identification of genes regulated by triiodothyronine in specific cell types. *Cerebral Cortex*, *27*(1), 706–717. https://doi.org/10.1093/cercor/bhv273

Gloss, B., Trost, S. U., Bluhm, W. F., Swanson, E. A., Clark, R., Wlnkfein, R., Janzen, K. M., Giles, W., Chassande, O., Samarut, J., & Dillmann, W. H. (2001). Cardiac ion channel expression and contractile function in mice with deletion of thyroid hormone receptor α or β. *Endocrinology*, *142*(2), 544–550. https://doi.org/10.1210/endo.142.2.7935

Godoy, G. A. F., Korevaar, T. I. M., Peeters, R. P., Hofman, A., De Rijke, Y. B., Bongers-Schokking, J. J., Tiemeier, H., Jaddoe, V. W. V., & Gaillard, R. (2014). Maternal thyroid hormones during pregnancy, childhood adiposity and cardiovascular risk factors: The Generation R Study. *Clinical Endocrinology*, *81*(1), 117–125. https://doi.org/10.1111/cen.12399

Goichot, B., Caron, P., Landron, F., & Bouée, S. (2016). Clinical presentation of hyperthyroidism in a large representative sample of outpatients in France: Relationships with age, aetiology and hormonal parameters. *Clinical Endocrinology*, *84*(3), 445–451. https://doi.org/10.1111/cen.12816

Gore, A. C., Chappell, V. A., Fenton, S. E., Flaws, J. A., Nadal, A., Prins, G. S., Toppari, J., & Zoeller, R. T. (2015). EDC-2: The Endocrine Society's Second Scientific Statement on Endocrine-Disrupting Chemicals. *Endocrine Reviews*, *36*(6), 1–150. https://doi.org/10.1210/er.2015-1010

Gouveia, C. H. A., Miranda-Rodrigues, M., Martins, G. M., & Neofiti-Papi, B. (2018). Thyroid Hormone and Skeletal Development. In *Vitamins and Hormones* (1st ed., Vol. 106). Elsevier Inc. https://doi.org/10.1016/bs.vh.2017.06.002

Grigore, D., Ojeda, N. B., & Alexander, B. T. (2008). Sex differences in the fetal programming of cardiovascular disease. *Gend. Med*, *5*(3), S121-132. https://doi.org/10.1016/j.genm.2008.03.012.Sex

Groeneweg, S., Van Geest, F. S., Peeters, R. P., Heuer, H., & Visser, W. E. (2019). Thyroid Hormone Transporters. *Endocrine Reviews*, *41*(2). https://doi.org/10.1210/endrev/bnz008

Haddad, F., Jiang, W., Bodell, P. W., Qin, A. X., & Baldwin, K. M. (2010). Cardiac myosin heavy chain gene regulation by thyroid hormone involves altered histone modifications. *American Journal of Physiology - Heart and Circulatory Physiology*, *299*(6), 1968–1981. https://doi.org/10.1152/ajpheart.00644.2010

Harder, L., Dudazy-Gralla, S., Müller-Fielitz, H., Hjerling Leffler, J., Vennström, B., Heuer, H., & Mittag, J. (2018). Maternal thyroid hormone is required for parvalbumin neurone development in the anterior hypothalamic area. *Journal of Neuroendocrinology*, *30*(3), e12573. https://doi.org/10.1111/jne.12573

He, Y., Hariharan, M., Gorkin, D. U., Dickel, D. E., Luo, C., Castanon, R. G., Nery, J. R., Lee, A. Y., Zhao, Y., Huang, H., Williams, B. A., Trout, D., Amrhein, H., Fang, R., Chen, H., Li, B., Visel, A., Pennacchio, L. A., Ren, B., & Ecker, J. R. (2020). Spatiotemporal DNA methylome dynamics of the developing mouse fetus. *Nature*, *583*(7818), 752–759. https://doi.org/10.1038/s41586-020-2119-x

Heldmaier, G. (1975). The influence of the social thermoregulation on the cold-adaptive growth of BAT in hairless and furred mice. *Pflügers Archiv European Journal of Physiology*, *355*(3), 261–266. https://doi.org/10.1007/BF00583688

Hernandez, A., & Stohn, J. P. (2018). The type 3 deiodinase: Epigenetic control of brain thyroid hormone action and neurological function. *International Journal of Molecular Sciences*, *19*(6). https://doi.org/10.3390/ijms19061804

Herrmann, B., Harder, L., Oelkrug, R., Chen, J., Gachkar, S., Nock, S., Resch, J., Korkowski, M., Heuer, H., & Mittag, J. (2020). Central hypothyroidism impairs heart rate stability and prevents thyroid hormone-induced cardiac hypertrophy and pyrexia. *Thyroid*, *30*(8), 1205–1216. https://doi.org/10.1089/thy.2019.0705

Hoefig, C. S., Harder, L., Oelkrug, R., Meusel, M., Vennström, B., Brabant, G., & Mittag, J. (2016). Thermoregulatory and cardiovascular consequences of a transient thyrotoxicosis and recovery in male mice. *Endocrinology*, *157*(7), 2957–2967. https://doi.org/10.1210/en.2016-1095

Hofstee, P., Bartho, L. A., McKeating, D. R., Radenkovic, F., McEnroe, G., Fisher, J. J., Holland, O. J., Vanderlelie, J. J., Perkins, A. V, & Cuffe, J. S. M. (2019). Maternal selenium deficiency during pregnancy in mice increases thyroid hormone concentrations, alters placental function and reduces fetal growth. *The Journal of Physiology*, *597*(23), 5597–5617. https://doi.org/10.1113/JP278473

Hofstee, P., James-McAlpine, J., McKeating, D. R., Vanderlelie, J. J., Cuffe, J. S. M., & Perkins, A. V. (2021). Low serum selenium in pregnancy is associated with reduced T3 and increased risk of GDM. *The Journal of Endocrinology*, *248*(1), 45–57. https://doi.org/10.1530/JOE-20-0319

Huang, S. A. (2005). Physiology and pathophysiology of type 3 deiodinase in humans. *Thyroid*, *15*(8), 875–881. https://doi.org/10.1089/thy.2005.15.875

Huget-Penner, S., & Feig, D. S. (2020). Maternal thyroid disease and its effects on the fetus and perinatal outcomes. In *Prenatal Diagnosis* (Vol. 40, Issue 9). https://doi.org/10.1002/pd.5684

Hughes, D. J., Fedirko, V., Jenab, M., Schomburg, L., Méplan, C., Freisling, H., Bueno-De-Mesquita, H. B., Hybsier, S., Becker, N. P., Czuban, M., Tjønneland, A., Outzen, M., Boutron-Ruault, M. C., Racine, A., Bastide, N., Kühn, T., Kaaks, R., Trichopoulos, D., Trichopoulou, A., … Hesketh, J. E. (2015). Selenium status is associated with colorectal cancer risk in the European prospective investigation of cancer and nutrition cohort. *International Journal of Cancer*, *136*(5), 1149–1161. https://doi.org/10.1002/ijc.29071

Ishii, S., Amano, I., & Koibuchi, N. (2021). The role of thyroid hormone in the regulation of cerebellar development. *Endocrinology and Metabolism*, *36*(4), 703–716. https://doi.org/10.3803/ENM.2021.1150

Iwen, K. A., Oelkrug, R., & Brabant, G. (2018). Effects of thyroid hormones on thermogenesis and energy partitioning. *Journal of Molecular Endocrinology*, *60*(3), R157–R170. https://doi.org/10.1530/JME-17-0319

Iwen, K. A., Oelkrug, R., Kalscheuer, H., & Brabant, G. (2018). Metabolic syndrome in thyroid disease. *Frontiers of Hormone Research*, *49*, 48–66. https://doi.org/10.1159/000485996

Iwen, K. A., Schröder, E., & Brabant, G. (2013). Thyroid Hormones and the Metabolic Syndrome. *European Thyroid Journal*, *2*(2), 83–92. https://doi.org/10.1159/000351249

Jahnke, G. D., Choksi, N. Y., Moore, J. A., & Shelby, M. D. (2004). Thyroid toxicants: Assessing reproductive health effects. *Environmental Health Perspectives*, *112*(3), 363–368. https://doi.org/10.1289/ehp.6637

Jansen, T. A., Korevaar, T. I. M., Mulder, T. A., White, T., Muetzel, R. L., Peeters, R. P., & Tiemeier, H. (2019). Maternal thyroid function during pregnancy and child brain morphology: a time window-specific analysis of a prospective cohort. *The Lancet Diabetes and Endocrinology*, *7*(8), 629–637. https://doi.org/10.1016/S2213-8587(19)30153-6

Javaid, N., & Choi, S. (2017). Acetylation- and methylation-related epigenetic proteins in the context of their targets. *Genes*, *8*(8). https://doi.org/10.3390/genes8080196

Jones, P. A. (2012). Functions of DNA methylation: Islands, start sites, gene bodies and beyond. *Nature Reviews Genetics*, *13*(7), 484–492. https://doi.org/10.1038/nrg3230

Kalra, B., Sawhney, K., & Kalra, S. (2017). Management of thyroid disorders in pregnancy: Recommendations made simple. *Journal of the Pakistan Medical Association*, *67*(9), 1452–1455.

Kemkem, Y., Nasteska, D., de Bray, A., Bargi-Souza, P., Peliciari-Garcia, R. A., Guillou, A., Mollard, P., Hodson, D. J., & Schaeffer, M. (2020). Maternal hypothyroidism in mice influences glucose metabolism in adult offspring. *Diabetologia*, *63*(9), 1822–1835. https://doi.org/10.1007/s00125-020-05172-x

Khandelwal, D., & Tandon, N. (2012). Overt and subclinical hypothyroidism: Who to treat and how. *Drugs*, *72*(1), 17–33. https://doi.org/10.2165/11598070-000000000-00000

Kiran, Z., Sheikh, A., Humayun, K. N., & Islam, N. (2021). Neonatal outcomes and congenital anomalies in pregnancies affected by hypothyroidism. *Annals of Medicine*, *53*(1), 1560–1568. https://doi.org/10.1080/07853890.2021.1970798

Klieverik, L. P., Janssen, S. F., Van Riel, A., Foppen, E., Bisschop, P. H., Serlie, M. J., Boelen, A., Ackermans, M. T., Sauerwein, H. P., Fliers, E., & Kalsbeek, A. (2009). Thyroid hormone modulates glucose production via a sympathetic pathway from the hypothalamic paraventricular nucleus to the liver. *Proceedings of the National Academy of Sciences of the United States of America*, *106*(14), 5966–5971. https://doi.org/10.1073/pnas.0805355106

Kobori, H., Hayashi, M., & Saruta, T. (2001). Thyroid Hormone Stimulates Renin Gene Expression Through the Thyroid Hormone Response Element. *Hypertension (Dallas, Tex. : 1979)*, *37*(1), 99–104. https://doi.org/10.1161/01.hyp.37.1.99

Köhrle, J. (1994). Thyroid hormone deiodination in target tissues â€" a regulatory role for the trace dement selenium? *Experimental and Clinical Endocrinology and Diabetes*, *102*(2), 63–89. https://doi.org/10.1055/s-0029-1211267

Köhrle, J., Schomburg, L., Drescher, S., Fekete, E., & Bauer, K. (1995). Rapid stimulation of type I 5′-deiodinase in rat pituitaries by 3,3′,5-triiodo-l-thyronine. *Molecular and Cellular Endocrinology*, *108*(1–2), 17–21. https://doi.org/10.1016/0303-7207(95)92574-8

Köhrle, Josef. (2015). Selenium and the thyroid. *Current Opinion in Endocrinology, Diabetes and Obesity*, *22*(5), 392–401. https://doi.org/10.1097/MED.0000000000000190

Köhrle, Josef. (2018). Thyroid hormones and derivatives: Endogenous thyroid hormones and their targets. *Methods in Molecular Biology*, *1801*, 85–104. https://doi.org/10.1007/978-1-4939-7902-8_9

Korevaar, T. I. M., Chaker, L., Jaddoe, V. W. V., Visser, T. J., Medici, M., & Peeters, R. P. (2016). Maternal and birth characteristics are determinants of offspring thyroid function. *Journal of Clinical Endocrinology and Metabolism*, *101*(1), 206–213. https://doi.org/10.1210/jc.2015-3559

Korevaar, T. I. M., Chaker, L., Medici, M., de Rijke, Y. B., Jaddoe, V. W. V., Steegers, E. A. P., Tiemeier, H., Visser, T. J., & Peeters, R. P. (2016). Maternal total T4 during the first half of pregnancy: physiologic aspects and the risk of adverse outcomes in comparison with free T4. *Clinical Endocrinology*, *85*(5), 757–763. https://doi.org/10.1111/cen.13106

Korevaar, T. I. M., Medici, M., De Rijke, Y. B., Visser, W., De Muinck Keizer-Schrama, S. M. P. F., Jaddoe, V. W. V., Hofman, A., Ross, H. A., Visser, W. E., Hooijkaas, H., Steegers, E. A. P., Tiemeier, H., Bongers-Schokking, J. J., Visser, T. J., & Peeters, R. P. (2013). Ethnic differences in maternal thyroid parameters during pregnancy: The generation r study. *Journal of Clinical Endocrinology and Metabolism*, *98*(9), 3678–3686. https://doi.org/10.1210/jc.2013-2005

Korevaar, T. I. M., Medici, M., Visser, T. J., & Peeters, R. P. (2017). Thyroid disease in pregnancy: New insights in diagnosis and clinical management. *Nature Reviews Endocrinology*, *13*(10), 610–622. https://doi.org/10.1038/nrendo.2017.93

Krassas, G., Karras, S. N., & Pontikides, N. (2015). Thyroid diseases during pregnancy: A number of important issues. *Hormones*, *14*(1), 59–69. https://doi.org/10.1007/bf03401381

Kratzsch, J., & Pulzer, F. (2008). Thyroid gland development and defects. *Best Practice and Research in Clinical Endocrinology and Metabolism*, *22*(1), 57–75. https://doi.org/10.1016/j.beem.2007.08.006

Kuratomi, S., Kuratomi, A., Kuwahara, K., Ishii, T. M., Nakao, K., Saito, Y., & Takano, M. (2007). NRSF regulates the developmental and hypertrophic changes of HCN4 transcription in rat cardiac myocytes. *Biochemical and Biophysical Research Communications*, *353*(1), 67–73. https://doi.org/10.1016/j.bbrc.2006.11.119

Ladenson, P. W., Kristensen, J. D., Ridgway, E. C., Olsson, A. G., Carlsson, B., Klein, I., Baxter, J. D., & Angelin, B. (2010). Use of the thyroid hormone analogue eprotirome in statin-treated dyslipidemia. *The New England Journal of Medicine*, *362*(10), 906–916. https://doi.org/10.1056/NEJMoa0905633

Lamberg, B. A. (1991). Endemic goitre - iodine deficiency disorders. *Annals of Medicine*, *23*(4), 367–372. https://doi.org/10.3109/07853899109148075

Lazar, M. A. (1993). Thyroid hormone receptors: multiple forms, multiple possibilities. *Endocrine Reviews*, *14*(2), 184–193. https://doi.org/10.1210/er.14.2.184

Lazarus, J., Brown, R. S., Daumerie, C., Hubalewska-Dydejczyk, A., Negro, R., & Vaidya, B. (2014). 2014 European Thyroid Association Guidelines for the Management of Subclinical Hypothyroidism in Pregnancy and in Children. *European Thyroid Journal*, *3*(2), 76–94. https://doi.org/10.1159/000362597

Leo, S. De, Lee, S. Y., Braverman, L. E., Unit, E., & Sciences, C. (2016). Hyperthyroidism: Lancet review. *Lancet*, *388*(10047), 906–918. https://doi.org/10.1016/S0140-6736(16)00278-6.Hyperthyroidism

Liang, P., Song, F., Ghosh, S., Morien, E., Qin, M., Mahmood, S., Fujiwara, K., Igarashi, J., Nagase, H., & Held, W. A. (2011). Genome-wide survey reveals dynamic widespread tissue-specific changes in DNA methylation during development. *BMC Genomics*, *12*(1), 231. https://doi.org/10.1186/1471-2164-12-231

Licinio, J., & Frost, P. (2000). The neuroimmune-endocrine axis: Pathophysiological implications for the central nervous system cytokines and hypothalamus-pituitary-adrenal hormone dynamics. *Brazilian Journal of Medical and Biological Research*, *33*(10), 1141–1148. https://doi.org/10.1590/S0100-879X2000001000003

Lin, V. H., & Koenig, R. J. (1999). Thyroid hormone receptor coactivators and corepressors. *Current Opinion in Endocrinology and Diabetes*, *6*(4), 287–292. https://doi.org/10.1097/00060793-199912000-00006

Liu, Y.-Y., & Brent, G. A. (2010). Thyroid hormone crosstalk with nuclear receptor signaling in metabolic regulation. *Trends in Endocrinology and Metabolism: TEM*, *21*(3), 166–173. https://doi.org/10.1016/j.tem.2009.11.004

Löf, C., Patyra, K., Kero, A., & Kero, J. (2018). Genetically modified mouse models to investigate thyroid development, function and growth. *Best Practice and Research: Clinical Endocrinology and Metabolism*, *32*(3), 241–256. https://doi.org/10.1016/j.beem.2018.03.007

Lompre, A. M., Nadal-Ginard, B., & Mahdavi, V. (1984). Expression of the cardiac ventricular α- and β-myosin heavy chain genes is developmentally and hormonally regulated. *Journal of Biological Chemistry*, *259*(10), 6437–6446. https://doi.org/10.1016/s0021-9258(20)82162-0

López, M., Alvarez, C. V., Nogueiras, R., & Diéguez, C. (2013). Energy balance regulation by thyroid hormones at central level. *Trends in Molecular Medicine*, *19*(7), 418–427. https://doi.org/10.1016/j.molmed.2013.04.004

López, M., Varela, L., Vázquez, M. J., Rodríguez-Cuenca, S., González, C. R., Velagapudi, V. R., Morgan, D. A., Schoenmakers, E., Agassandian, K., Lage, R., Martínez de Morentin, P. B., Tovar, S., Nogueiras, R., Carling, D., Lelliott, C., Gallego, R., Oresic, M., Chatterjee, K., Saha, A. K., … Vidal-Puig, A. (2010). Hypothalamic AMPK and fatty acid metabolism mediate thyroid regulation of energy balance. *Nature Medicine*, *16*(9), 1001–1008. https://doi.org/10.1038/nm.2207

Lubos, E., Loscalzo, J., & Handy, D. E. (2011). Glutathione peroxidase-1 in health and disease: From molecular mechanisms to therapeutic opportunities. *Antioxidants and Redox Signaling*, *15*(7), 1957–1997. https://doi.org/10.1089/ars.2010.3586

Lucaccioni, L., Ficara, M., Cenciarelli, V., Berardi, A., Predieri, B., & Iughetti, L. (2021). Long term outcomes of infants born by mothers with thyroid dysfunction during pregnancy. *Acta Biomedica*, *92*(1), 1–11. https://doi.org/10.23750/abm.v92i1.9696

Lydiatt, D. D., & Bucher, G. S. (2011). Historical vignettes of the thyroid gland. *Clinical Anatomy*, *24*(1), 1–9. https://doi.org/10.1002/ca.21073

Maenhaut, C., Christophe, D., Vassart, G., Dumont, J., Roger, P. P., & Opitz, R. (2000). *Ontogeny, Anatomy, Metabolism and Physiology of the Thyroid.* (K. R. Feingold, B. Anawalt, A. Boyce, G. Chrousos, W. W. de Herder, K. Dhatariya, K. Dungan, J. M. Hershman, J. Hofland, S. Kalra, G. Kaltsas, C. Koch, P. Kopp, M. Korbonits, C. S. Kovacs, W. Kuohung, B. Laferrère, M. Levy, E. A. McGee, … D. P. Wilson (eds.)).

Mai, W., Janier, M. F., Allioli, N., Quignodon, L., Chuzel, T., Flamant, F., & Samarut, J. (2004). Thyroid hormone receptor α is a molecular switch of cardiac function between fetal and postnatal life. In *Proceedings of the National Academy of Sciences of the United States of America* (Vol. 101, Issue 28, pp. 10332–10337). https://doi.org/10.1073/pnas.0401843101

Malcomson, R. D. G., & Nagy, A. (2015). The endocrine system. *Keeling's Fetal and Neonatal Pathology*, 671–702. https://doi.org/10.1007/978-3-319-19207-9_25

Manolis, A. A., Manolis, T. A., Melita, H., & Manolis, A. S. (2020). Subclinical thyroid dysfunction and cardiovascular consequences: An alarming wake-up call? *Trends in Cardiovascular Medicine*, *30*(2), 57–69. https://doi.org/10.1016/j.tcm.2019.02.011

Martinez, M. E., Duarte, C. W., Stohn, J. P., Karaczyn, A., Wu, Z., DeMambro, V. E., & Hernandez, A. (2020). Thyroid hormone influences brain gene expression programs and behaviors in later generations by altering germ line epigenetic information. *Molecular Psychiatry*, *25*(5), 939–950. https://doi.org/10.1038/s41380-018-0281-4

Medici, M., Timmermans, S., Visser, W., De Muinck Keizer-Schrama, S. M. P. F., Jaddoe, V. W. W., Hofman, A., Hooijkaas, H., De Rijke, Y. B., Tiemeier, H., Bongers-Schokking, J. J., Visser, T. J., Peeters, R. P., & Steegers, E. A. P. (2013). Maternal thyroid hormone parameters during early pregnancy and birth weight: The Generation R Study. *Journal of Clinical Endocrinology and Metabolism*, *98*(1), 59–66. https://doi.org/10.1210/jc.2012-2420

Meyer, C. W., Ootsuka, Y., & Romanovsky, A. A. (2017). Body Temperature Measurements for Metabolic Phenotyping in Mice. *Frontiers in Physiology*, *8*(July), 1–13. https://doi.org/10.3389/fphys.2017.00520

Minakhina, S., De Oliveira, V., Kim, S. Y., Zheng, H., & Wondisford, F. E. (2021). Thyroid hormone receptor phosphorylation regulates acute fasting-induced suppression of the hypothalamic-pituitary-thyroid axis. *Proceedings of the National Academy of Sciences of the United States of America*, *118*(39). https://doi.org/10.1073/pnas.2107943118

Miranda, A., & Sousa, N. (2018). Maternal hormonal milieu influence on fetal brain development. *Brain and Behavior*, *8*(2), 1–23. https://doi.org/10.1002/brb3.920

Mittag, J. (2020). More Than Fever - Novel Concepts in the Regulation of Body Temperature by Thyroid Hormones. *Experimental and Clinical Endocrinology and Diabetes*, *128*(6–7), 428–431. https://doi.org/10.1055/a-1014-2510

Mittag, J., Behrends, T., Hoefig, C. S., Vennström, B., & Schomburg, L. (2010). Thyroid hormones regulate selenoprotein expression and selenium status in mice. *PLoS ONE*, *5*(9), 1–8. https://doi.org/10.1371/journal.pone.0012931

Mittag, J., Behrends, T., Nordström, K., Anselmo, J., Vennström, B., & Schomburg, L. (2012). Serum copper as a novel biomarker for resistance to thyroid hormone. *Biochemical Journal*, *443*(1), 103–109. https://doi.org/10.1042/BJ20111817

Mittag, J., Davis, B., Vujovic, M., Arner, A., & Vennström, B. (2010). Adaptations of the autonomous nervous system controlling heart rate are impaired by a mutant thyroid hormone receptor-α1. *Endocrinology*, *151*(5), 2388–2395. https://doi.org/10.1210/en.2009-1201

Mittag, J., Lyons, D. J., Sällström, J., Vujovic, M., Dudazy-Gralla, S., Warner, A., Wallis, K., Alkemade, A., Nordström, K., Monyer, H., Broberger, C., Arner, A., & Vennström, B. (2013). Thyroid hormone is required for hypothalamic neurons regulating cardiovascular functions. *Journal of Clinical Investigation*, *123*(1), 509–516. https://doi.org/10.1172/JCI65252

Mittag, J., Wallis, K., & Vennström, B. (2010). Physiological consequences of the TRa1 aporeceptor state. *Heart Failure Reviews*, *15*(2), 111–115. https://doi.org/10.1007/s10741-008-9119-5

Moleti, M., Trimarchi, F., & Vermiglio, F. (2014). Thyroid physiology in pregnancy. *Endocrine Practice*, *20*(6), 589–596. https://doi.org/10.4158/EP13341.RA

Möllers, L. S., Yousuf, E. I., Hamatschek, C., Morrison, K. M., Hermanussen, M., Fusch, C., & Rochow, N. (2021). Metabolic-endocrine disruption due to preterm birth impacts growth, body composition, and neonatal outcome. *Pediatric Research*, *April*. https://doi.org/10.1038/s41390-021-01566-8

Moran, C., Agostini, M., McGowan, A., Schoenmakers, E., Fairall, L., Lyons, G., Rajanayagam, O., Watson, L., Offiah, A., Barton, J., Price, S., Schwabe, J., & Chatterjee, K. (2017). Contrasting Phenotypes in Resistance to Thyroid Hormone Alpha Correlate with Divergent Properties of Thyroid Hormone Receptor α1 Mutant Proteins. *Thyroid*, *27*(7), 973–982. https://doi.org/10.1089/thy.2017.0157

Moreno, M., Giacco, A., Di Munno, C., & Goglia, F. (2017). Direct and rapid effects of 3,5-diiodo-L-thyronine (T2). *Molecular and Cellular Endocrinology*, *458*, 121–126. https://doi.org/10.1016/j.mce.2017.02.012

Morkin, E. (2000). Control of cardiac myosin heavy chain gene expression. *Microscopy Research and Technique*, *50*(6), 522–531. https://doi.org/10.1002/1097-0029(20000915)50:6<522::AID-JEMT9>3.0.CO;2-U

Morte, B., Gil-Ibañez, P., Heuer, H., & Bernal, J. (2021). Brain gene expression in systemic hypothyroidism and mouse models of MCT8 deficiency: The Mct8-Oatp1c1-Dio2 triad. *Thyroid*, *31*(6), 922–932. https://doi.org/10.1089/thy.2020.0649

Mottis, A., Mouchiroud, L., & Auwerx, J. (2013). Emerging roles of the corepressors NCoR1 and SMRT in homeostasis. *Genes and Development*, *27*(8), 819–835. https://doi.org/10.1101/gad.214023.113

Muller, A., Zuidwijk, M. J., Simonides, W. S., & Van Hardeveld, C. (1997). Modulation of SERCA2 expression by thyroid hormone and norepinephrine in cardiocytes: Role of contractility. *American Journal of Physiology*, *272*(4 PART 2).

Mullur, R., Liu, Y.-Y., & Brent, G. A. (2014). Thyroid hormone regulation of metabolism. *Physiological Reviews*, *94*(2), 355–382. https://doi.org/10.1152/physrev.00030.2013

Nilsson, M., & Fagman, H. (2017). Development of the thyroid gland. *Development (Cambridge)*, *144*(12), 2123–2140. https://doi.org/10.1242/dev.145615

Oelkrug, R., Polymeropoulos, E. T., & Jastroch, M. (2015). Brown adipose tissue: physiological function and evolutionary significance. *Journal of Comparative Physiology B: Biochemical, Systemic, and Environmental Physiology*, *185*(6), 587–606. https://doi.org/10.1007/s00360-015-0907-7

Oelkrug, Rebecca, Krause, C., Herrmann, B., Resch, J., Gachkar, S., El Gammal, A. T., Wolter, S., Mann, O., Oster, H., Kirchner, H., & Mittag, J. (2020). Maternal Brown Fat Thermogenesis Programs Glucose Tolerance in the Male Offspring. *Cell Reports*, *33*(5), 108351. https://doi.org/10.1016/j.celrep.2020.108351

Oelkrug, Rebecca, & Mittag, J. (2021). An improved method for the precise unravelment of non-shivering brown fat thermokinetics. *Scientific Reports*, *11*(1), 1–9. https://doi.org/10.1038/s41598-021-84200-1

Okosieme, O. E., Khan, I., & Taylor, P. N. (2018). Preconception management of thyroid dysfunction. In *Clinical Endocrinology* (Vol. 89, Issue 3). https://doi.org/10.1111/cen.13731

Ortiga-Carvalho, T. M., Sidhaye, A. R., & Wondisford, F. E. (2014). Thyroid hormone receptors and resistance to thyroid hormone disorders. *Nature Reviews. Endocrinology*, *10*(10), 582–591. https://doi.org/10.1038/nrendo.2014.143

Pachucki, J., Burmeister, L. A., & Larsen, P. R. (1999). Thyroid hormone regulates hyperpolarization-activated cyclic nucleotide-gated channel (HCN2) mRNA in the rat heart. *Circulation Research*, *85*(6), 498–503. https://doi.org/10.1161/01.res.85.6.498

Paisdzior, S., Knierim, E., Kleinau, G., Biebermann, H., Krude, H., Straussberg, R., & Schuelke, M. (2021). A new mechanism in thra resistance: the first disease-associated variant leading to an increased inhibitory function of thra2. *International Journal of Molecular Sciences*, *22*(10), 1–19. https://doi.org/10.3390/ijms22105338

Papaleontiou, M., & Haymart, M. R. (2012). Approach to and treatment of thyroid disorders in the elderly. *The Medical Clinics of North America*, *96*(2), 297–310. https://doi.org/10.1016/j.mcna.2012.01.013

Pascual, A., & Aranda, A. (2013). Thyroid hormone receptors, cell growth and differentiation. *Biochimica et Biophysica Acta - General Subjects*, *1830*(7), 3908–3916. https://doi.org/10.1016/j.bbagen.2012.03.012

Patel, J., Landers, K., Li, H., Mortimer, R. H., & Richard, K. (2011). Delivery of maternal thyroid hormones to the fetus. *Trends in Endocrinology and Metabolism*, *22*(5), 164–170. https://doi.org/10.1016/j.tem.2011.02.002

Pedro, P. F., Tsakmaki, A., & Bewick, G. A. (2020). The Glucose Tolerance Test in Mice. *Methods in Molecular Biology (Clifton, N.J.)*, *2128*, 207–216. https://doi.org/10.1007/978-1-0716-0385-7_14

Peltier, M. R., Fassett, M. J., Chiu, V. Y., & Getahun, D. (2021). Maternal Hypothyroidism Increases the Risk of Attention-Deficit Hyperactivity Disorder in the Offspring. *American Journal of Perinatology*, *38*(2), 191–201. https://doi.org/10.1055/s-0040-1717073

Perkins, A. V., & Vanderlelie, J. J. (2016). Multiple micronutrient supplementation and birth outcomes: The potential importance of selenium. *Placenta*, *48*, S61–S65. https://doi.org/10.1016/j.placenta.2016.02.007

Picou, F., Fauquier, T., Chatonnet, F., Richard, S., & Flamant, F. (2014). Minireview: Deciphering direct and indirect influence of thyroid hormone with mouse genetics. *Molecular Endocrinology*, *28*(4), 429–441. https://doi.org/10.1210/me.2013-1414

Pilo, A., Iervasi, G., Vitek, F., Ferdeghini, M., Cazzuola, F., & Bianchi, R. (1990). Thyroidal and peripheral production of 3,5,3'-triiodothyronine in humans by multicompartmental analysis. *The American Journal of Physiology*, *258*(4 Pt 1), E715-26. https://doi.org/10.1152/ajpendo.1990.258.4.E715

Pirahanchi, Y., Tariq, M. A., & Jialal, I. (2021). *Physiology, Thyroid.*

Poppe, K., Bisschop, P., Fugazzola, L., Minziori, G., Unuane, D., & Weghofer, A. (2021). 2021 European Thyroid Association Guideline on Thyroid Disorders prior to and during Assisted Reproduction. *European Thyroid Journal*, *9*(6), 281–295. https://doi.org/10.1159/000512790

Porst, T., Johannes, J., Gluschke, H., Köhler, R., Mehl, S., Kühnen, P., Renko, K., Minich, W. B., Wiegand, S., & Schomburg, L. (2021). Natural autoimmunity to the thyroid hormone monocarboxylate transporters mct8 and mct10. *Biomedicines*, *9*(5), 1–12. https://doi.org/10.3390/biomedicines9050496

Prummel, M. F., Brokken, L. J. S., & Wiersinga, W. M. (2004). Ultra short-loop feedback control of thyrotropin secretion. *Thyroid*, *14*(10), 825–829. https://doi.org/10.1089/thy.2004.14.825

Pucci, E., Chiovato, L., & Pinchera, A. (2000). Thyroid and lipid metabolism. *International Journal of Obesity*, *24*, S109–S112. https://doi.org/10.1038/sj.ijo.0801292

Ramadoss, P., Abraham, B. J., Tsai, L., Zhou, Y., Costa-E-Sousa, R. H., Ye, F., Bilban, M., Zhao, K., & Hollenberg, A. N. (2014). Novel mechanism of positive versus negative regulation by thyroid hormone receptor β1 (TRβ1) identified by genome-wide profiling of binding sites in mouse liver. *Journal of Biological Chemistry*, *289*(3), 1313–1328. https://doi.org/10.1074/jbc.M113.521450

Receptor, T. H., & Development, A. (2018). *Chapter 20 Development*. *1801*, 247–263.

Renko, K., Hoefig, C. S., Hiller, F., Schomburg, L., & Köhrle, J. (2012). Identification of iopanoic acid as substrate of type 1 deiodinase by a novel nonradioactive iodide-release assay. *Endocrinology*, *153*(5), 2506–2513. https://doi.org/10.1210/en.2011-1863

Rewal, M., Jung, M. E., Wen, Y., Brun-Zinkernagel, A. M., & Simpkins, J. W. (2003). Role of the GABAA system in behavioral, motoric, and cerebellar protection by estrogen during ethanol withdrawal. *Alcohol*, *31*(1–2), 49–61. https://doi.org/10.1016/j.alcohol.2003.07.005

Richard, S., & Flamant, F. (2018). Regulation of T3 availability in the developing brain: The mouse genetics contribution. *Frontiers in Endocrinology*, *9*(MAY), 1–11. https://doi.org/10.3389/fendo.2018.00265

Rivolta, I., Binda, A., Masi, A., & DiFrancesco, J. C. (2020). Cardiac and neuronal HCN channelopathies. *Pflugers Archiv European Journal of Physiology*, *472*(7), 931–951. https://doi.org/10.1007/s00424-020-02384-3

Ruiz-Llorente, L., Ardila-González, S., Fanjul, L. F., Martínez-Iglesias, O., & Aranda, A. (2014). microRNAs 424 and 503 are mediators of the anti-proliferative and anti-invasive action of the thyroid hormone receptor beta. *Oncotarget*, *5*(10), 2918–2933. https://doi.org/10.18632/oncotarget.1577

Rytter, D., Andersen, S. L., Bech, B. H., Halldorsson, T. I., Henriksen, T. B., Laurberg, P., & Olsen, S. F. (2016). Maternal thyroid function in pregnancy may program offspring blood pressure, but not adiposity at 20 y of age. *Pediatric Research*, *80*(1), 7–13. https://doi.org/10.1038/pr.2016.56

Sadakierska-Chudy, A., & Filip, M. (2015). A Comprehensive View of the Epigenetic Landscape. Part II: Histone Post-translational Modification, Nucleosome Level, and Chromatin Regulation by ncRNAs. *Neurotoxicity Research*, *27*(2), 172–197. https://doi.org/10.1007/s12640-014-9508-6

Safayee, S., Karbalaei, N., Noorafshan, A., & Nadimi, E. (2016). Induction of oxidative stress, suppression of glucose-induced insulin release, ATP production, glucokinase activity, and histomorphometric changes in pancreatic islets of hypothyroid rat. *European Journal of Pharmacology*, *791*, 147–156. https://doi.org/10.1016/j.ejphar.2016.08.024

Sah, R., Mesirca, P., Mason, X., Gibson, W., Bates-Withers, C., Van Den Boogert, M., Chaudhuri, D., Pu, W. T., Mangoni, M. E., & Clapham, D. E. (2013). Timing of myocardial TRPM7 deletion during cardiogenesis variably disrupts adult ventricular function, conduction, and repolarization. *Circulation*, *128*(2), 101–114. https://doi.org/10.1161/CIRCULATIONAHA.112.000768

Sap, J., Muñoz, A., Damm, K., Goldberg, Y., Ghysdael, J., Leutz, A., Beug, H., & Vennström, B. (1986). The c-erb-A protein is a high-affinity receptor for thyroid hormone. *Nature*, *324*(6098), 635–640. https://doi.org/10.1038/324635a0

Schaffner, M., Rochau, U., Mühlberger, N., Conrads-Frank, A., Rushaj, V. Q., Sroczynski, G., Koukkou, E., Thuesen, B. H., Völzke, H., Oberaigner, W., & Siebert, U. (2021). The economic impact of prevention, monitoring and treatment strategies for iodine deficiency disorders in Germany. *Endocrine Connections*, *10*(1), 1–12. https://doi.org/10.1530/EC-20-0384

Schomburg, L. (2010). Genetics and phenomics of selenoenzymes-How to identify an impaired biosynthesis? *Molecular and Cellular Endocrinology*, *322*(1–2), 114–124. https://doi.org/10.1016/j.mce.2010.01.011

Schussler, G. C. (2000). *Thyroxine-Binding*. *10*(2), 141–149.

Schweizer, U., Towell, H., Vit, A., Rodriguez-Ruiz, A., & Steegborn, C. (2017). Structural aspects of thyroid hormone binding to proteins and competitive interactions with natural and synthetic compounds. *Molecular and Cellular Endocrinology*, *458*, 57–67. https://doi.org/10.1016/j.mce.2017.01.026

Sentis, S. C., Oelkrug, R., & Mittag, J. (2021). Thyroid hormones in the regulation of brown adipose tissue thermogenesis. *Endocrine Connections*, *10*(2), R106–R115. https://doi.org/10.1530/EC-20-0562

Silva, B. S., Bertasso, I. M., Pietrobon, C. B., Lopes, B. P., Santos, T. R., Peixoto-Silva, N., Carvalho, J. C., Claudio-Neto, S., Manhães, A. C., Cabral, S. S., Kluck, G. E. G., Atella, G. C., Oliveira, E., Moura, E. G., & Lisboa, P. C. (2019). Effects of maternal bisphenol A on behavior, sex steroid and thyroid hormones levels in the adult rat offspring. *Life Sciences*, *218*, 253–264. https://doi.org/10.1016/j.lfs.2018.12.039

Silva, J. E. (2005). Thyroid hormone and the energetic cost of keeping body temperature. *Bioscience Reports*, *25*(3–4), 129–148. https://doi.org/10.1007/s10540-005-2882-9

Silva, J. E. (2006). Thermogenic mechanisms and their hormonal regulation. *Physiological Reviews*, *86*(2), 435–464. https://doi.org/10.1152/physrev.00009.2005

Silva, J. E. (2011a). [Frontiers in Bioscience S3, 352-371, January 1, 2011] Physiological importance and control of non-shivering facultative thermogenesis J. Enrique Silva. 2, 352–371.

Silva, J. E. (2011b). Physiological importance and control of non-shivering facultative thermogenesis. *Frontiers in Bioscience (Scholar Edition)*, *3*, 352–371. https://doi.org/10.2741/s156

Silva, J. E., & Bianco, S. D. C. (2008). Thyroid-adrenergic interactions: Physiological and clinical implications. *Thyroid*, *18*(2), 157–165. https://doi.org/10.1089/thy.2007.0252

Sinclair, D. (2015). *Review Article Clinical and laboratory aspects of thyroid autoantibodies*. 173–183.

Sjögren, M., Alkemade, A., Mittag, J., Nordström, K., Katz, A., Rozell, B., Westerblad, H., Arner, A., & Vennström, B. (2007). Hypermetabolism in mice caused by the central action of an unliganded thyroid hormone receptor α1. *EMBO Journal*, *26*(21), 4535–4545. https://doi.org/10.1038/sj.emboj.7601882

Slater, S. (2011). The discovery of thyroid replacement therapy. Part 3: A complete transformation. *Journal of the Royal Society of Medicine*, *104*(3), 100–106. https://doi.org/10.1258/jrsm.2010.10k052

Small, E. M., & Krieg, P. A. (2004). Molecular Regulation of Cardiac Chamber-Specific Gene Expression. *Trends in Cardiovascular Medicine*, *14*(1), 13–18. https://doi.org/10.1016/j.tcm.2003.09.005

St. Germain, D. L., & Atasoylu, A. (1988). Dual mechanisms of regulation of type I iodothyronine 5'-deiodinase in the rat kidney, liver, and thyroid gland. Implications for the treatment of hyperthyroidism with radiographic contrast agents. *Journal of Clinical Investigation*, *81*(5), 1476–1484. https://doi.org/10.1172/JCI113479

St Germain, D. L., Galton, V. A., & Hernandez, A. (2009). Miniereview: Defining the roles of the lodothyronine deiodinases: Current concepts and challenges. *Endocrinology*, *150*(3), 1097–1107. https://doi.org/10.1210/en.2008-1588

Stagnaro-Green, A., Abalovich, M., Alexander, E., Azizi, F., Mestman, J., Negro, R., Nixon, A., Pearce, E. N., Soldin, O. P., Sullivan, S., & Wiersinga, W. (2011). Guidelines of the American Thyroid Association for the diagnosis and management of thyroid disease during pregnancy and postpartum. *Thyroid*, *21*(10), 1081–1125. https://doi.org/10.1089/thy.2011.0087

Stepien, B. K., & Huttner, W. B. (2019). Transport, metabolism, and function of thyroid hormones in the developing mammalian brain. *Frontiers in Endocrinology*, *10*(APR), 1–16. https://doi.org/10.3389/fendo.2019.00209

Sterrett, M. (2019). Maternal and Fetal Thyroid Physiology. *Clinical Obstetrics and Gynecology*, *62*(2), 302–307. https://doi.org/10.1097/GRF.0000000000000439

Stieber, J., Hofmann, F., Ludwig, A., & Viswanathan, P. C. (2004). Pacemaker Channels and Sinus Node Arrhythmia. *Trends in Cardiovascular Medicine*, *14*(1), 23–28. https://doi.org/10.1016/j.tcm.2003.09.006

Sullivan, S. A. (2019). Hypothyroidism in Pregnancy. *Clinical Obstetrics and Gynecology*, *62*(2), 308–319. https://doi.org/10.1097/GRF.0000000000000432

Suzuki, M. M., & Bird, A. (2008). DNA methylation landscapes: Provocative insights from epigenomics. *Nature Reviews Genetics*, *9*(6), 465–476. https://doi.org/10.1038/nrg2341

Tagami, T., Kopp, P., Johnson, W., Arseven, O. K., & Jameson, J. L. (1998). The thyroid hormone receptor variant α2 is a weak antagonist because it is deficient in interactions with nuclear receptor corepressors. *Endocrinology*, *139*(5), 2535–2544. https://doi.org/10.1210/endo.139.5.6011

Tapia-Martínez, J., Franco-Colín, M., Ortiz-Butron, R., Pineda-Reynoso, M., & Cano-Europa, E. (2019). Hypothyroid offspring replacement with euthyroid wet nurses during lactation improves thyroid programming without modifying metabolic programming. *Archives of Endocrinology and Metabolism*, *63*(3), 199–207. https://doi.org/10.20945/2359-3997000000132

Tapia-Martínez, J., Torres-Manzo, A. P., Franco-Colín, M., Pineda-Reynoso, M., & Cano-Europa, E. (2019). Maternal Thyroid Hormone Deficiency during Gestation and Lactation Alters Metabolic and Thyroid Programming of the Offspring in the Adult Stage. *Hormone and Metabolic Research*, *51*(6), 381–388. https://doi.org/10.1055/a-0896-0968

Taylor, P. N., & Lazarus, J. H. (2019). Hypothyroidism in Pregnancy. *Endocrinology and Metabolism Clinics of North America*, *48*(3), 547–556. https://doi.org/10.1016/j.ecl.2019.05.010

Taylor, P. N., Zouras, S., Min, T., Nagarahaj, K., Lazarus, J. H., & Okosieme, O. (2018). Thyroid screening in early pregnancy: Pros and cons. *Frontiers in Endocrinology*, *9*(OCT), 1–7. https://doi.org/10.3389/fendo.2018.00626

Teixeira, P. de F. D. S., Dos Santos, P. B., & Pazos-Moura, C. C. (2020). The role of thyroid hormone in metabolism and metabolic syndrome. *Therapeutic Advances in Endocrinology and Metabolism*, *11*, 2042018820917869. https://doi.org/10.1177/2042018820917869

Teng, W., Shan, Z., Patil-Sisodia, K., & Cooper, D. S. (2013). Hypothyroidism in pregnancy. *The Lancet Diabetes and Endocrinology*, *1*(3), 228–237. https://doi.org/10.1016/S2213-8587(13)70109-8

ThyagaRajan, S., & Priyanka, H. P. (2012). Bidirectional communication between the neuroendocrine system and the immune system: Relevance to health and diseases. *Annals of Neurosciences*, *19*(1), 40–46. https://doi.org/10.5214/ans.0972.7531.180410

Tinnikov, A., Nordström, K., Thorén, P., Kindblom, J. M., Malin, S., Rozell, B., Adams, M., Rajanayagam, O., Pettersson, S., Ohlsson, C., Chatterjee, K., & Vennström, B. (2002). Retardation of post-natal development caused by a negatively acting thyroid hormone receptor α1. *EMBO Journal*, *21*(19), 5079–5087. https://doi.org/10.1093/emboj/cdf523

Toloza, F. J. K., Abedzadeh-Anaraki, S., & Maraka, S. (2019). Subclinical hypothyroidism in pregnancy. *Current Opinion in Endocrinology, Diabetes and Obesity*, *26*(5), 225–231. https://doi.org/10.1097/MED.0000000000000491

Trueba, S. S., Augé, J., Mattei, G., Etchevers, H., Martinovic, J., Czernichow, P., Vekemans, M., Polak, M., & Attié-Bitach, T. (2005). PAX8, TITF1, and FOXE1 gene expression patterns during human development: New insights into human thyroid development and thyroid dysgenesis-associated malformations. *Journal of Clinical Endocrinology and Metabolism*, *90*(1), 455–462. https://doi.org/10.1210/jc.2004-1358

Tschöp, M. H., Speakman, J. R., Arch, J. R. S., Auwerx, J., Brüning, J. C., Chan, L., Eckel, R. H., Farese, R. V., Galgani, J. E., Hambly, C., Herman, M. A., Horvath, T. L., Kahn, B. B., Kozma, S. C., Maratos-Flier, E., Müller, T. D., Münzberg, H., Pfluger, P. T., Plum, L., … Ravussin, E. (2012). A guide to analysis of mouse energy metabolism. *Nature Methods*, *9*(1), 57–63. https://doi.org/10.1038/nmeth.1806

Tylki-Szymańska, A., Acuna-Hidalgo, R., Krajewska-Walasek, M., Lecka-Ambroziak, A., Steehouwer, M., Gilissen, C., Brunner, H. G., Jurecka, A., Rózdzyńska-Świątkowska, A., Hoischen, A., & Chrzanowska, K. H. (2015). Thyroid hormone resistance syndrome due to mutations in the thyroid hormone receptor α gene (THRA). *Journal of Medical Genetics*, *52*(5), 312–316. https://doi.org/10.1136/jmedgenet-2014-102936

Vaidya, B., Hubalewska-Dydejczyk, A., Laurberg, P., Negro, R., Vermiglio, F., & Poppe, K. (2012). Treatment and screening of hypothyroidism in pregnancy: Results of a European survey. *European Journal of Endocrinology*, *166*(1), 49–54. https://doi.org/10.1530/EJE-11-0729

Vallortigara, J., Chassande, O., Higueret, P., & Enderlin, V. (2009). Thyroid hormone receptor alpha plays an essential role in the normalisation of adult-onset hypothyroidism-related hypoexpression of synaptic plasticity target genes in striatum. *Journal of Neuroendocrinology*, *21*(1), 49–56. https://doi.org/10.1111/j.1365-2826.2008.01802.x

van der Spek, A. H., Fliers, E., & Boelen, A. (2017). The classic pathways of thyroid hormone metabolism. *Molecular and Cellular Endocrinology*, *458*, 29–38. https://doi.org/10.1016/j.mce.2017.01.025

van Gucht, A. L. M., Moran, C., Meima, M. E., Visser, W. E., Chatterjee, K., Visser, T. J., & Peeters, R. P. (2017). Resistance to Thyroid Hormone due to Heterozygous Mutations in Thyroid Hormone Receptor Alpha. In *Current Topics in Developmental Biology* (1st ed., Vol. 125). Elsevier Inc. https://doi.org/10.1016/bs.ctdb.2017.02.001

Van Tuyl, M., Blommaart, P. E., De Boer, P. A. J., Wert, S. E., Ruijter, J. M., Islam, S., Schnitzer, J., Ellison, A. R., Tibboel, D., Moorman, A. F. M., & Lamers, W. H. (2004). Prenatal exposure to thyroid hormone is necessary for normal postnatal development of murine heart and lungs. *Developmental Biology*, *272*(1), 104–117. https://doi.org/10.1016/j.ydbio.2004.03.042

Van Vliet, G. (2003). Development of the thyroid gland: lessons from congenitally hypothyroid mice and men. *Clinical Genetics*, *63*(6), 445–455. https://doi.org/10.1034/j.1399-0004.2003.00107.x

Vargas, F., Rodríguez-Gómez, I., Vargas-Tendero, P., Jimenez, E., & Montiel, M. (2012). The renin-angiotensin system in thyroid disorders and its role in cardiovascular and renal manifestations. *The Journal of Endocrinology*, *213*(1), 25–36. https://doi.org/10.1530/JOE-11-0349

Venero, C., Guadaño-Ferraz, A., Herrero, A. I., Nordström, K., Manzano, J., De Escobar, G. M., Bernal, J., & Vennström, B. (2005). Anxiety, memory impairment, and locomotor dysfunction caused by a mutant thyroid hormone receptor α1 can be ameliorated by T3 treatment. *Genes and Development*, *19*(18), 2152–2163. https://doi.org/10.1101/gad.346105

Vennström, B., Mittag, J., & Wallis, K. (2008). Severe psychomotor and metabolic damages caused by a mutant thyroid hormone receptor alpha 1 in mice: Can patients with a similar mutation be found and treated? *Acta Paediatrica, International Journal of Paediatrics*, *97*(12), 1605–1610. https://doi.org/10.1111/j.1651-2227.2008.01031.x

Visser, W. E., Friesema, E. C. H., & Visser, T. J. (2011). Minireview: Thyroid hormone transporters: The knowns and the unknowns. *Molecular Endocrinology*, *25*(1), 1–14. https://doi.org/10.1210/me.2010-0095

Visser, W. E., & Peeters, R. P. (2020). Interpretation of thyroid function tests during pregnancy. *Best Practice and Research: Clinical Endocrinology and Metabolism*, *34*(4), 101431. https://doi.org/10.1016/j.beem.2020.101431

Vujovic, M., Nordström, K., Gauthier, K., Flamant, F., Visser, T. J., Vennström, B., & Mittag, J. (2009). Interference of a mutant thyroid hormone receptor α1 with hepatic glucose metabolism. *Endocrinology*, *150*(6), 2940–2947. https://doi.org/10.1210/en.2008-1085

Wallis, K., Dudazy, S., Van Hogerlinden, M., Nordström, K., Mittag, J., & Vennström, B. (2010). The thyroid hormone receptor α1 protein is expressed in embryonic postmitotic neurons and persists in most adult neurons. *Molecular Endocrinology*, *24*(10), 1904–1916. https://doi.org/10.1210/me.2010-0175

Wallis, K., Sjögren, M., Van Hogerlinden, M., Silberberg, G., Fisahn, A., Nordström, K., Larsson, L., Westerblad, H., De Escobar, G. M., Shupliakov, O., & Vennström, B. (2008). Locomotor deficiencies and aberrant development of subtype-specific GABAergic interneurons caused by an unliganded thyroid hormone receptor α1. *Journal of Neuroscience*, *28*(8), 1904–1915. https://doi.org/10.1523/JNEUROSCI.5163-07.2008

Warner, A., Rahman, A., Solsjö, P., Gottschling, K., Davis, B., Vennström, B., Arner, A., & Mittag, J. (2013). Inappropriate heat dissipation ignites brown fat thermogenesis in mice with a mutant thyroid hormone receptor α1. In *Proceedings of the National Academy of Sciences of the United States of America* (Vol. 110, Issue 40, pp. 16241–16246). https://doi.org/10.1073/pnas.1310300110

Wartofsky, L., Nostrand, D. Van, & Burman, K. D. (2006). *Cme reviewarticle 23*. *61*(8).

Webb, P. (2010). Thyroid hormone receptor and lipid regulation. *Current Opinion in Investigational Drugs (London, England : 2000)*, *11*(10), 1135–1142.

Westerlund, J., Andersson, L., Carlsson, T., Zoppoli, P., Fagman, H., & Nilsson, M. (2008). Expression of islet1 in thyroid development related to budding, migration, and fusion of primordia. *Developmental Dynamics*, *237*(12), 3820–3829. https://doi.org/10.1002/dvdy.21772

Winter, H., Braig, C., Zimmermann, U., Geisler, H. S., Fränzer, J. T., Weber, T., Ley, M., Engel, J., Knirsch, M., Bauer, K., Christ, S., Walsh, E. J., McGee, J. A., Köpschall, I., Rohbock, K., & Knipper, M. (2006). Thyroid hormone receptors TRα1 and TRβ differentially regulate gene expression of Kcnq4 and prestin during final differentiation of outer hair cells. *Journal of Cell Science*, *119*(14), 2975–2984. https://doi.org/10.1242/jcs.03013

Wondisford, F. E. (2018). Evaluating the Hypothalamic-Pituitary-Thyroid (HPT) Axis in Mice. *Methods in Molecular Biology (Clifton, N.J.)*, *1801*, 155–161. https://doi.org/10.1007/978-1-4939-7902-8_13

Yalamanchi, S., & Cooper, D. S. (2015). Thyroid disorders in pregnancy. *Current Opinion in Obstetrics and Gynecology*, *27*(6), 406–415. https://doi.org/10.1097/GCO.0000000000000226

Yelon, D., Weinstein, B. M., & Fishman, M. C. (2002). Cardiovascular system. *Results and Problems in Cell Differentiation*, *40*, 298–321. https://doi.org/10.1007/978-3-540-46041-1_15

Yen, P. M. (2001). Physiological and molecular basis of Thyroid hormone action. *Physiological Reviews*, *81*(3), 1097–1142. https://doi.org/10.1152/physrev.2001.81.3.1097

Yen, P. M., Ando, S., Feng, X., Liu, Y., Maruvada, P., & Xia, X. (2006). Thyroid hormone action at the cellular, genomic and target gene levels. *Molecular and Cellular Endocrinology*, *246*(1–2), 121–127. https://doi.org/10.1016/j.mce.2005.11.030

Zhou, B., Chen, Y., Cai, W. Q., Liu, L., & Hu, X. J. (2020). Effect of Gestational Weight Gain on Associations Between Maternal Thyroid Hormones and Birth Outcomes. *Frontiers in Endocrinology*, *11*(September), 1–9. https://doi.org/10.3389/fendo.2020.00610

LIST OF TABLES

LIST OF FIGURES

NON- STANDARD ABBREVIATIONS

°C	Degree Celsius
µg	Microgram
µL	Microliter
µM	Micromolar
ABCA1	ATP-binding cassette transporter A1
ACC	Acetyl-CoA-carboxylase
ADP	Adenosine diphosphate
Adrb3	β_3-adrenergic receptor
AF	Activation function
AHA	Anterior hypothalamic area
AHDS	Allan-Herndon-Dudley syndrome
ANOVA	Analysis of variance
ATP	Adenosine triphosphate
AU	Arbitrary units
AUC	Area under the curve
BAT	Brown adipose tissue
BC	Before christ
BCA	Bicinchoninic acid
BMR	Basal metabolic rate
bpm	Beats per minute
BSA	Bovine serum albumin
Ca^{2+}	Calcium
cDNA	Complementary DNA
CNS	Central nervous system
CPT1α	Carnitine palmitoyl transferase 1α
Ct	Treshold cycle
Cu	Copper
CV	Cardiovascular system
D	Day after fertilization
DBD	DNA binding domain
DEE	Daily energy expenditure
DEPC	Diethylpyrocarbonate
Dio1	Iodothyronine deiodinase 1
Dio2	Iodothyronine deiodinase 2

Dio3	Iodothyronine deiodinase 3
DMSO	Dimethyl sulfoxide
DNA	Deoxyribonucleic acid
dNTP	Deoxynucleotide triphosphate
E	Embryonic day
EDTA	Ethylenediaminetetraacetic acid
ELISA	Enzyme-linked immunosorbent assay
Fasn	Fatty acid synthase
FFA	Free fatty acids
fT3	Free 3,3',5-Triiodothyronine
fT4	Free 3,3',5,5'-Tetraiodothyronine
g	Gram
Gpd2	Mitochondrial glycerol-3-phosphate dehydrogenase 2
GPx1	Glutathione peroxidase 1
GTH	Core animal facility
gWAT	Gonadal white adipose tissue
HCN channel	Hyperpolarization activated cyclic nucleotide gated channel
HDAC	Histone deacethylase
Hprt	Hypoxanthine phosphoribosyltransferase
HPT axis	Hypothalamus-pituitary-thyroid axis
i.p.	Intraperitoneal injection
iBAT	Intrascapular brown adipose tissue
I_f	Funny current
ipGTT	Intraperitoneal glucose tolerance test
IR	Infrared
iWAT	Inguinal white adipose tissue
kg	Kilogram
KH_2PO_4	Potassium dihydrogenphosphate
ko	Knockout
L	Liter
LBD	Ligand-binding domain
LDL-R	Low-density lipoprotein receptor
M	Molar
MAP	Mean arterial pressure
Mct8/10	Monocarboxylate transport protein 8/10
mg	Milligram
$MgCl_2$	Magnesium chloride
min	Minute

MHC	Myosin heavy chain
mL	Milliliter
mM	Millimolar
mmHg	Millimeter of mercury
mRNA	Messenger ribonucleic acid
Na_3VO_4	Sodium orthovandate
Na_2HPO_4	Disodium phosphate
NaCl	Sodium chloride
NCoA	Nuclear receptor coactivator
NCoR	Nuclear receptor corepressor
ng	Nanogram
nM	Nanomolar
NMR	Nuclear magnetic resonance
ns	No significant
Oatp1c1	Organic anion transporting peptides 1c1
PBS	Phosphate buffered saline
PCR	Polymerase chain reaction
PEPCK	Phosphoenolpyruvate carboxykinase
PFA	Paraformaldehyde
pM	Picomolar
Pparα	Peroxisome proliferator activated receptor alpha
Pparγ	Peroxisome proliferator activated receptor gamma
Pparδ	Peroxisome proliferator activated receptor delta
Prdm16	PR domain containing 16
PTU	Propylthiouracil
PV	Parvalbumin
PVDF	Polyvinylidene difluoride
PVN	Paraventricular nucleus
qPCR	Quantitative polymerase chain reaction
RNA	Ribonucleic acid
RQ	Respiratory quotient
RT	Room temperature
rT3	3,3',5'-Triiodothyronine
RXR	Retinoid X receptor
Ryr2	Ryanodine receptor 2
SDS	Sodium dodecyl sulfate
Se	Selenium
SERCA	Sarcoendoplasmic reticulum Ca^{2+} adenosine triphosphatase

Sln	Sarcolipin
SMRT	Silencing mediator of retinoic and thyroid receptor
SNS	Sympathetic nervous system
SRC-1	Steroid receptor coactivator 1
T2	3,5-Diiodothyronine
T3	3,3',5-triiodo-L-thyronine
T4	3,3',5,5'-tetraiodo-L-thyronine, thyroxine
TBG	Thyroxine-binding globulin
TBS	Tris-buffered saline
TG	Thyroglobulin
TH	Thyroid hormone
TIF-2	Transcriptional intermediary factor
TN	Thermoneutrality
TR	Thyroid hormone receptor
TRE	TR response element
TRH	Thyrotropin-releasing hormone
TRIS	Tris(hydroxymethyl)-aminomethane
TRα	Thyroid hormone receptor alpha
TRβ	Thyroid hormone receptor beta
TSH	Thyroid stimulating hormone
tT3	Total 3,3',5-Triiodothyronine
tT4	Total 3,3',5,5'-Tetraiodothyronine
Ucp1	Uncoupling protein 1
V	Volt
VO_2	Oxygen consumption
WT	Wildtype